ASHOK ASPATWAR

# Distribution and Function of Carbonic Anhydrase Related Proteins (CARPs) VIII, X and XI

■

ACADEMIC DISSERTATION
To be presented, with the permission of
the Board of the BioMediTech of the University of Tampere,
for public discussion in the Main Auditorium of Building B,
School of Medicine of the University of Tampere,
Medisiinarinkatu 3, Tampere, on October 31st, 2014, at 12 o'clock.

UNIVERSITY OF TAMPERE

ASHOK ASPATWAR

# Distribution and Function of Carbonic Anhydrase Related Proteins (CARPs) VIII, X and XI

*Acta Universitatis Tamperensis 1981*
*Tampere University Press*
*Tampere 2014*

UNIVERSITY
OF TAMPERE

ACADEMIC DISSERTATION
University of Tampere, BioMediTech
Finland

*Supervised by*
Professor Mauno Vihinen
University of Lund
Sweden
Professor Seppo Parkkila
University of Tampere
Finland

*Reviewed by*
Professor Matti Airaksinen
University of Helsinki
Finland
Professor Todd Alexander
University of Alberta
Canada

The originality of this thesis has been checked using the Turnitin OriginalityCheck service in accordance with the quality management system of the University of Tampere.



Cover design by
Mikko Reinikka

Distributor:
kirjamyynti@juvenes.fi
http://granum.uta.fi

Acta Universitatis Tamperensis 1981
ISBN 978-951-44-9594-6 (print)
ISSN-L 1455-1616
ISSN 1455-1616

Acta Electronica Universitatis Tamperensis 1468
ISBN 978-951-44-9595-3 (pdf)
ISSN 1456-954X
http://tampub.uta.fi

Suomen Yliopistopaino Oy – Juvenes Print
Tampere 2014

# Contents

# List of original communications

This thesis is based on the following original communications, which are referred to in the text by their Roman numerals (**I-IV**)

I. **Aspatwar A,** Tolvanen ME, Parkkila S. 2010. Phylogeny and expression of carbonic anhydrase-related proteins. BMC Mol Biol. 11:25.

II. **Aspatwar A,** Tolvanen M, Ortutay C, Parkkila S. 2010. Carbonic anhydrase related protein VIII and its role in neurodegeneration and cancer. Curr Pharm Des. 16:3264-76.

III. **Aspatwar A,** Tolvanen MEE, Jokitalo E, Parikka M, Ortutay C, Rämet M, Vihinen M, Parkkila S. 2013. Abnormal cerebellar development and ataxia in CARP VIII morphant zebrafish. Hum Mol Genet. 22:417-32.

IV. **Aspatwar A,** Tolvanen MEE, Barker H, Ortutay C, Pan P, Kuuslahti M, Parikka M, Rämet M, Parkkila S. 2014. Abnormal embryonic development and movement pattern in *ca10a* and *ca10b* morphant zebrafish. *Submitted.*

# Abbreviations

| | |
|---|---|
| aa | amino acid |
| bp | base pair |
| BSA | bovine serum albumin |
| BLAST | Basic Local Alignment Search Tool |
| BLAT | Blast-Like Alignment Tool |
| BMD | bone mineral density |
| CA | carbonic anhydrase |
| *CA8* | carbonic anhydrase 8 gene (human) |
| *CA10* | carbonic anhydrase 10 gene (human) |
| *CA11* | carbonic anhydrase 11 gene (human) |
| *ca8* | carbonic anhydrase 8 gene (zebrafish) |
| *ca10a* | carbonic anhydrase 10a gene (zebrafish) |
| *ca10b* | carbonic anhydrase 10b gene (zebrafish) |
| *cah-1* | carbonic anhydrase 1 gene (*Cenorhabditis elegans*) |
| *cah-2* | carbonic anhydrase 2 gene (*Cenorhabditis elegans*) |
| *Car8* | carbonic anhydrase 8 gene (mouse) |
| *Car10* | carbonic anhydrase 10 gene *(*mouse) |
| *Car11* | carbonic anhydrase 11 gene (mouse) |
| CARP VIII | carbonic anhydrase related protein VIII |
| CARP X | carbonic anhydrase related protein X |
| CARP XI | carbonic anhydrase related protein XI |
| CARP-A | carbonic anhydrase related proteins (fruit fly) |
| CARP-B | carbonic anhydrase related proteins (fruit fly) |
| cDNA | complementary deoxyribonucleic acid |
| CNS | central nervous system |
| DAB | 3, 3'-diaminobenzidine tetrahydrochloride |
| dpf | day post fertilized |
| EDTA | ethylene-diamine-tetra-acetic acid |
| EST | expressed sequence tags |
| GPI | glycosylphoshpatidylinositol |
| hpf | hours post fertilized |
| HRP | horseradish peroxidase |
| IP3 | inositol trisphosphate-3 |
| ITPR1 | inositol trisphosphate receptor1 protein |
| *itpr 1a* | inositol trisphosphate receptor 1a gene (zebrafish) |
| *itpr 1b* | inositol trisphosphate receptor 1b gene (zebrafish) |

| | |
|---|---|
| kb | kilo base |
| MJD | Machado-Joseph Disease |
| kDa | kilo Dalton |
| LB | Luria-Bertani |
| mRNA | messenger ribonucleic acid |
| MEGA | molecular and evolutionary genetic analysis |
| MO | Morpholino oligonucleotide |
| MSA | multiple sequence alignment |
| NB | Northern blot |
| PBS | phosphate buffered saline |
| PCs | Purkinje cells |
| PCR | polymerase chain reaction |
| *p53* | gene for Tumor protein p53 |
| RC | random control |
| RT-PCR | reverse transcriptase-polymerase chain reaction |
| RT-qPCR | real-time quantitative polymerase chain reaction |
| SNP | single nucleotide polymorphism |
| SCA | spinocerebellar ataxia |
| SDS | sodium dodecyl sulfate |
| TUNEL | terminal deoxynucleotidyl transferase dUTP nick end labeling |
| UCSC | University of California Santa Cruz |
| WB | Western blotting |
| *wdl* | waddles |
| *wd* | waddler |
| WT | wild type |

# Abstract

The α-carbonic anhydrases (CAs) are zinc containing metalloenzymes whose primary role is to catalyze the reversible hydration of carbon dioxide to bicarbonate and a hydrogen ion. The α-CAs are found abundantly in nature and participate in many biologically important processes apart from reversible hydration of carbon dioxide. Among the α-CA gene family, there are three homologues that have no catalytic activity due to lack of one or more of the three functionally important histidine residues and are named as carbonic anhydrase related proteins (CARPs) VIII, X and XI. Interestingly, the CARPs VIII, X, and XI are predominantly expressed in all parts of the brain in humans and mice. However, the precise physiological roles of these proteins are poorly understood.

The main aim of the present work was to perform a systematic analysis of CARPs in order to elucidate their phylogenesis, distribution, and functional role. Among the three CARPs, CARP VIII was first to be reported from the mouse complementary DNA (cDNA) library. Mutations in *CA8* gene have been linked to ataxia and mental retardation in humans and mice. CARP VIII interacts with inositol tris-phosphate receptor1 (ITPR1) and might be involved in intracellular $Ca^{2+}$ signaling. Some studies have suggested that CARP X is expressed in mouse and human brain. CARP XI is also predominantly expressed in the central nervous system (CNS) and upregulation of CARP XI has been reported in some cancers.

Database searches and phylogenetic analyses showed a nearly universal distribution for CARP X-like sequences in vertebrates and invertebrates, whereas CARP VIII was limited to chordates and a few invertebrates (deuterostomes). In contrast, CARP XI is limited to vertebrates, and was found to be missing in fish and bird lineages. Surprisingly, many fish species exhibited independent duplication of CARP X sequences. Expression of CARP proteins and their messenger ribonucleic acids (mRNAs) were studied using immunohistochemistry and real-time quantitative polymerase chain reaction (RT-qPCR), respectively. At the protein level CARP VIII demonstrated very strong expression in the cerebellum and cerebrum; moderate expression in the lung, liver, salivary gland, and stomach; and low expression in the colon and kidney. CARP X was expressed in the lung and a weak signal was observed in the kidney. Low levels of CARP XI expression was seen in the cerebellum, cerebrum, stomach, kidney, liver, and small intestine, and weak staining was also seen in the colon. RT-qPCR analyses confirmed the results of the immunohistochemical staining, showing wide distribution of *Car8* and *Car11* mRNAs in different tissues, whereas the expression of *Car10* mRNA was restricted to the frontal cortex, parietal cortex, cerebellum, midbrain, and eye. CARPs are widely distributed with a very high

sequence similarity among the organisms analyzed in the study. Distribution of CARPs and *Car* mRNAs suggests that these proteins may play role in brain development and motor coordination function in the cerebellum, and that they might also play some physiological role in other tissues.

The comparative analysis of human CARP VIII structure with catalytically active human CA II indicated that the surface of the CARP VIII protein molecule is highly conserved. Whether or not the conserved surface of CARP VIII is involved in interaction with ITPR1 remains to be studied in the future. The structural basis of the misfolding of the S100P mutant protein associated with ataxia can be suggested based on the crystal structure of the wild-type CARP VIII. Substitution of Ser to Pro will cause a rigid bend in the peptide backbone, which might prevent the β6 and/or the β6/β7 loop from assuming the conformations they have in the wild-type protein. Having a shorter, more constrained loop between strands β5 and β6 may amplify the problem in folding of the S100P mutant protein even further.

The presence of CARP orthologs in zebrafish led us to investigate their role by knocking down the CARP genes using antisense morpholino oligonucleotides (MOs). The expression analysis of CARP VIII in zebrafish showed that CARP VIII is expressed in the cerebellar Purkinje cells (PCs) similar to the distribution in humans. Bioinformatic analysis revealed that the CARP VIII and ITPR1 sequences are coevolved. Knockdown of *CA8* gene in 0-5 day post fertilized (dpf) zebrafish embryos led to abnormal cerebellar development and ataxia in 5 dpf *ca8* morphants similar to human patients with a mutation in the *CA8* gene. Similarly, developmental expression of *ca10a* and *ca10b* genes suggested that these genes are required for the embryonic development in 1-5 dpf embryos. Expression studies on *ca10a* and *ca10b* genes in adult tissues suggested that these genes are highly expressed in the brain, similar to the expression pattern in human and mouse. Bioinformatic analysis revealed conserved signal peptides, N-glycosylation sites and potential disulfides, suggesting that CARP Xa and Xb proteins are secretory and potentially dimeric. Knockdown of these genes using antisense MOs led to phenotypic abnormalities in 5 dpf morphant zebrafish with gross morphological changes in the brain and ataxic movement. Our studies introduced novel zebrafish models to further investigate the mechanisms of CARP functions in vertebrates.

# 1 Introduction

The α-carbonic anhydrases (α-CAs) are $Zn^{2+}$ containing enzymes that catalyze the reversible hydration of $CO_2$ (Sly and Hu, 1995). There are 17 α-CAs in vertebrates, of which 14 isozymes (CA I, II, III, IV, VA, VB, VI, VII, IX, XII, XIII, XIV, XV, and XVII) are catalytically active (Tolvanen et al., 2013). Three of the isoforms, namely, CARPs VIII, X, and XI, represent inactive isoforms due to lack of one or more of the three His residues required for binding to the $Zn^{2+}$ atom essential for CA activity (Hewett-Emmett and Tashian, 1996).

Among the inactive CA isoforms, the CARP VIII gene was the first to be reported from the mouse brain cDNA library (Kato, 1990a). The catalytic inactivity of CARP VIII is due to the lack of one of the three His residues essential for zinc binding. CARP VIII has been well studied compared to CARP X and CARP XI (Lakkis et al., 1997a; Taniuchi et al., 2002a; Taniuchi et al., 2002b). CARP VIII is primarily expressed in cerebellar PCs, and its expression has also been reported in several other normal and cancer tissues (Akisawa et al., 2003; Kato, 1990b; Miyaji et al., 2003; Taniuchi et al., 2002b). CARP VIII interacts with ITPR1, a $Ca^{2+}$ channel protein (Hirota et al., 2003). The crystal structure of human CARP VIII has been resolved and the structural basis of its inactivity has been reported (Picaud et al., 2009). CARP VIII protein deficit is also associated with ataxia and mental retardation both in mouse and human (Jiao et al., 2005; Kaya et al., 2011; Turkmen et al., 2009).

Similar to CARP VIII, both CARP X and CARP XI are catalytically inactive owing to the absence of two and three histidine residues, respectively, which are required for CA activity. Unlike CARP VIII, so far, very few studies have been reported on CARP X and CARP XI. Most of the studies have been mainly related to their expression in human and mouse (Taniuchi et al., 2002a; Taniuchi et al., 2002b). Similar to CARP VIII, both CARP X and CARP XI are predominantly expressed in the CNS and CARP XI is also upregulated in gastrointestinal tumors (Morimoto et al., 2005). Apart from the few expression related studies very little is known about CARP X and CARP XI proteins.

The purpose of the present work is to study the distribution of CARP sequences across the species and to study the expression pattern of CARPs at both gene and protein levels in mouse tissues. In addition, analysis of databases revealed the presence of CARP orthologs in zebrafish, and therefore we used zebrafish as a vertebrate model to study the expression pattern during embryonic development and in adult tissues. Furthermore, we knocked down the CARP genes in zebrafish using antisense morpholinos to study their role in the zebrafish model.

# 2 Review of the literature

## 2.1 Carbonic anhydrases

### 2.1.1 Historical aspects of carbonic anhydrase isozymes

The carbonic anhydrases (CAs, EC 4.2.1.1) are ubiquitous metalloenzymes and their basic function is to catalyze the reversible hydration of $CO_2$ in the reaction: $CO_2+H_2O \Leftrightarrow H^++HCO_3^-$, which is important for many biological processes, such as photosynthesis, respiration, renal tubular acidification, and bone resorption (Sly and Hu, 1995). The CAs have been found in almost every living organism, and are encoded by five distinct evolutionarily unrelated gene families denoted as α, β, γ, δ and ζ CAs (Hewett-Emmett and Tashian, 1996). These gene families do not share any structural similarity between each other, and indeed, they are good examples of convergent evolution of catalytic function (Hewett-Emmett and Tashian, 1996).

The CAs of various animal species belong to the α-CA gene family and contain $Zn^{2+}$ in the active site. In mammals, only 13 enzymatically active α-CAs have been identified, (CA I, II, III, IV, VA, VB, VI, VII, IX, XII, XIII, XIV, and XV). The 13 active CA isozymes have different subcellular localizations such that CAs I, II, III, VII, and XIII are all cytosolic, CAs IV, IX, XII, XIV, and XV are all membrane-associated, CAs VA and VB are mitochondrial, and CA VI is a secreted protein (Hewett-Emmett, 2000; Hewett-Emmett and Tashian, 1996; Sly and Hu, 1995).

In addition to the active CAs, there are CA isoforms which have sequence and structural similarity with active CAs but do not possess any CA catalytic activity. In mammals, the catalytically inactive CA isoforms occur either independently, and are named as carbonic anhydrase related proteins (CARPs), or they exist as domains of other proteins. The catalytic inactivity of these CA isoforms is due to the absence of one or more of the three histidine residues required for the classical enzymatic activity (Sly and Hu, 1995; Tashian et al., 2000).

## 2.2 Carbonic anhydrase related proteins

The catalytically inactive CAs and CA domains of other proteins lacking CA activity were discovered in the 1990s (Kato, 1990b; Maa et al., 1990). There are three CARPs which exist in all vertebrates and two CARPs which are part of other proteins occurring as domains of protein tyrosine phosphate receptor (PTPR) ζ or β and γ

(Ohradanova et al., 2007). In addition to the presence of CARPs and CARP domains in the vertebrates, the D8 transmembrane protein in the vaccinia virus contains an N-terminal CA domain (Maa et al., 1990) (Table 1).

**Table 1**. Molecular properties of CARPs

| CARPs | Accession No[a]. | Amino acids (aa) | MW (kDa) | Chromosomal localization |
|---|---|---|---|---|
| VIII[c] | AK090655 | 290 | 33 | 8q11-q12 |
| X[c] | AF288385 | 328 | 37.6 | 17q24 |
| XI[c] | AF067662 | 328 | 36.2 | 19q13.3 |
| PTPRζ[c] | NP_002842 | 280[b] | - | 7q31-33 |
| PTPRγ[c] | NP_002832 | 266[b] | - | 3pl4.2-p2l |
| CA in D8[d] | J05190 | 236[b] | 32 | - |

[a]The accession numbers represent the longest cDNA sequences deposited in the GenBank. [b]The length of CA domain. [c]Human and [d]Vaccinia virus CARPs (Ohradanova et al., 2007; Supuran, 2004).

The CARPs VIII, X, and XI were discovered based on the sequence homology with the catalytic CA isozymes (Tashian et al., 2000). The *Car8* gene was first reported by Kato from the mouse brain cDNA library (Kato, 1990a). The presence of *CA10* was mentioned by Hewett and Tashian based on the expressed sequence tags (ESTs) which showed very high homology to CA isozymes, and the predicted protein was devoid of the histidine residues essential for CA catalytic activity (Hewett-Emmett and Tashian, 1996). CARP XI was accidentally found in 1998 and reported as CARP-2 (Bellingham et al., 1998). The sequences of CARP VIII, X and XI are highly conserved and represent a sub-class of the α-CA gene family. Importantly, they lack one or more of the three histidine residues which are essential for coordinating the zinc atom at the active site and therefore, they lack the CA enzymatic activity (Hewett-Emmett and Tashian, 1996). In CARP VIII, one of the His is replaced by Arg and in CARP X two of the His residues are replaced by Arg and Gln. In CARP XI, all the three important histidines are replaced by Arg, Leu, and Gln (Fig 1) (Bellingham et al., 1998; Fujikawa-Adachi et al., 1999; Lovejoy et al., 1998; Okamoto et al., 2001; Skaggs et al., 1993). Based on the phylogenetic analysis of the human α-CAs, the fourteen CA isozymes are grouped into extracellular and intracellular CAs (Okamoto et al., 2001). The phylogenetic analysis indicated that three CARPs are grouped together forming a single divergent branch that shares the same branch as intracellular CA isozymes, suggesting that CARPs are intracellular.

The protein tyrosine phosphatases (PTPs) regulate cell proliferation, differentiation, communication and adhesion by dephosphorylating tyrosine residues of proteins (Andersen et al., 2004). The PTPRs are integral cell surface proteins which have PTP activity. There are eight subfamilies (R1/R6, R2A, R2B, R3, R4, R5, R7 and R8) of PTPRs based on the structure of their extracellular domains (Andersen et al., 2004) ). The PTPRs ζ and γ, which belong to the R5 subfamily, are known to contain N-terminal CARP domains and lack enzymatic activity due to the absence of two of the three His residues required for binding to the zinc atom (Barnea et al., 1993; Gavrieli et al., 1992; Levy et al., 1993). The CARP

domains of PTPRs ζ and γ genes are made up of seven exons and six introns which are similar to the introns of mammalian *CA1*,*2*,*3*,*5* and *7* genes (Kastury et al., 1996). The CARP domains of these receptor proteins have close to 50% aa similarity with mammalian CAs (Barnea et al., 1993; Levy et al., 1993).

In PTPR ζ two of the three His residues required for the co-ordination of $Zn^{2+}$ at the active site are replaced by Thr at position His-94 and Gln at position His-119 (Fig 1). Similarly, in PTPRs γ two His obligatory for binding to the $Zn^{2+}$ at the active site are replaced by Glu at position His-94 and Gln at position His-119 (Fig 1) making the proteins catalytically inactive (Ohradanova et al., 2007). The PTPR ζ is present on the surface of glial cells where it interacts with contactin, a cell recognition molecule, via CA domain and thus plays a role in neuronal cell adhesion and neurite outgrowth (Peles et al., 1995). The PTPR γ protein is expressed in several different tissues and is associated with many diseases including renal and lung cancers in humans and motor coordination function in mice (LaForgia et al., 1991; Lamprianou et al., 2006).


**Figure 1.** Alignment of aa residues 64–128 (CA II numbering, relevant for the catalytic activity) of hCARPs, hCAs I–XIV, hRPTPβ/ζ, γ and vaccinia virus CA. The $Zn^{2+}$ binding His of CAs and corresponding residues in the CARPs are in red and indicated with arrow. Modified from (Ohradanova et al., 2007).

The presence of the CA domain in the D8 transmembrane protein at the N-terminal region was reported in 1990 (Maa et al., 1990). The N-terminal domain of D8 protein contains 236 aa residues which are homologous to the catalytic domain of the mammalian CAs. In CA domain of D8 protein the His residues at positions 69 and 92 which correspond to positions 96 and 119 in CAII, are replaced by Tyr and Asn, respectively, making it catalytically inactive (Fig 1) (Ohradanova et al., 2007). Phylogenetic analysis revealed that the viral CA domain is related to CARP X and XI, indicating that the vaccinia virus might have obtained the CA domain from humans via horizontal transfer of the gene (Ohradanova et al., 2007). The molecular weight (MW) of the CA domain of D8 protein was 32 kDa (kilo Dalton) with a pI of ~ 8.7. The mutated protein with a replacement of Tyr and Asn (vaccCA

N92H/Y69H) with His residues showing catalytic activity similar to the catalytic activity of human CA VA and CA XII (Ohradanova et al., 2007).

Apart from the CARPs and CARP domains found in vertebrate species, the invertebrates were found to contain CARP X like sequences, unlike CARP VIII orthologs which are found only in deuterostome invertebrates, with the exception of single protostome species (Miyamoto, 2012). Many protostome species, such as *C. elegans,* a nematode and insects like *D. melanogaster* contain more than one copy of CARP X like sequences (Ortutay et al., 2010). Interestingly, these CAX-like sequences are expressed in the neuronal cells of insects and nematodes (Tolvanen et al unpublished result).

## 2.3 General properties of CARP VIII

CARP VIII was discovered from mouse cDNA clones with a specific expression pattern in the brain (Kato, 1990a). The nucleotide sequence analysis of these clones exhibited a strong homology with α-CAs (Kato, 1990b). CARP VIII showed replacement of His and Glu residues by Arg and Gln at positions 124 and 122. His 124 is one of the three histidines essential for the co-ordination of the $Zn^{2+}$ at the active site and Gln residue at position 122 forms a hydrogen bond network to the zinc bound solvent molecule (Tashian, 1989). In addition to high homology with CAs, CARP VIII had a Glu stretch at the N-terminal end and it was only expressed in cerebellar PCs (Kato, 1990b). CARP VIII is well characterized inactive isoform and many studies have been done related to its expression (Hirota et al., 2003; Lakkis et al., 1997a; Taniuchi et al., 2002a; Taniuchi et al., 2002b) and the role of *CA8* in lung and colon cancer (Akisawa et al., 2003; Lu et al., 2004; Miyaji E et al., 2003; Miyaji et al., 2003; Nishikata et al., 2007). In the past, the association of CARP VIII mutation with ataxia has been reported in mouse (Jiao et al., 2005). Recent studies revealed a mutation in the *CA8* gene which leads to ataxia in humans (Kaya et al., 2011; Turkmen et al., 2009). The crystal structure of CARP VIII has been resolved and its structural basis of inactivity has also been studied (Picaud et al., 2009). In addition to the above studies CARP VIII has been implicated in several other diseases (Bataller et al., 2004; Miyaji et al., 2003; Mori et al., 2009).

### 2.3.1 Expression of CARP VIII in animal models

The expression of the *Car8* gene was originally studied in mouse using Northern blot (NB) and *in-situ* hybridization (Kato, 1990a). The mRNA exhibited a unique distribution in neuronal PCs of the cerebellum (Kato, 1990b; Lakkis et al., 1997b). Subsequently, several studies were carried out related to CARP VIII gene expression in both mouse and human tissues. *In-situ* hybridization suggested that the *Car8* gene

is expressed at 9.5 days of gestation in several organs in the developing mouse. The high level of expression was seen between 10.5 to 12.5 days of development in the brain, liver, lung, heart, gut, thymus and epithelium covering the head and oronasal cavity (Lakkis et al., 1997a). *In-situ* hybridization and immunohistochemistry revealed the presence of CARP VIII mRNA and its protein product in the PCs of 9-day-old mouse (Nogradi et al., 1997). Reverse transcriptase (RT) PCR and NB of whole mouse embryos at 7, 11, 15 and 17 gestational days showed strong signals for the *Car8* gene in 11, 15 and 17 days of gestation, supporting the earlier findings that the *Car8* gene appears after 7 days during development of the embryo (Lakkis et al., 1997a; Taniuchi et al., 2002b).

In adult mouse tissues, *Car 8* mRNA was predominantly found in the brain and the expression was also seen in the lung, liver, heart, skeletal muscle and kidney (Taniuchi et al., 2002b). Western blot of CARP VIII protein in a panel of mouse tissues revealed that it is predominantly expressed in the cerebellum similar to the expression of *Car8* mRNA. In addition, low expression was also seen in the cerebrum, olfactory bulb, olfactory epithelium, vomeronasal organ, lung, submandibular gland, liver, adrenal gland, stomach, small intestine and large intestine (Hirota et al., 2003). However, there was no signal for the presence of CARP VIII protein in the heart, thymus, spleen, pancreas, ovary, uterus, testis or muscle (Hirota et al., 2003). The microarray analysis of single rod bipolar cells indicated the enrichment of the *Car8* gene in these cells, and the expression of *Car8* gene was subsequently confirmed by *in-situ* hybridization using RNA probes (Kim et al., 2008). Recently, the localization pattern of CARP VIII was studied in retinal sections of mice that were heterozygous or homozygous for a mutation in waddles *(wdl)* gene (Puthussery et al., 2011). Immunohistochemistry showed CARP VIII protein in the inner retina of the heterozygous mouse, but the retina of the homozygous mouse for *wdl* mutation exhibited no signal. The pattern of CARP VIII localization was similar in the retina of rat and macaque, suggesting conservation of CARP VIII expression in mammals (Puthussery et al., 2011).

### 2.3.2 Expression of CARP VIII in humans and human cell line

The polymerase chain reaction (PCR) amplification of human *CA8* gene from cDNA libraries of human tissues revealed the presence of *CA8* in placenta, salivary gland and testis (Skaggs et al., 1993). The regional and cellular distribution of CARP VIII protein was analyzed in the sections of adult and fetal brains at five different gestational periods (Taniuchi et al., 2002a). In the fetal brain the signal for CARP VIII protein was seen in neuroprogenitor cells and sub-ventricular zone at 84 days of gestation, while the distribution was more widespread in the adult brain (Taniuchi et al., 2002a). The expression analysis using microarray suggested that the *CA8* gene is predominantly expressed in the cerebellum, and high levels of *CA8* gene was also seen in several other tissues (Kilpinen et al., 2008; Wu et al., 2009).

The gene expression profile of the human neuroblastoma cell line exhibited a 9 fold increase in the expression of *CA8* gene when mutant ataxin 3 was present in the cells compared to the cells containing wild type (WT) ataxin 3 (Wen et al., 2003). Recent studies on the distribution of CARP VIII protein displayed a significant increase of CARP VIII protein in the neuroblastoma cells (SK-N-SH) expressing mutant ataxin 3 protein (Hsieh et al., 2013). Immunochemical analysis showed that the CARP VIII protein was evenly distributed in the perinuclear and cytoplasmic regions. Interestingly, ITPR1, which is expressed in the endoplasmic reticulum co-localizes with CARP VIII in the perinuclear region (Hirota et al., 2003). Studies done earlier suggested that the mutant ataxin 3 disrupts $Ca^{2+}$ signaling in the neurons by interacting with ITPR1 on the surface of the endoplasmic reticulum (Chen et al., 2008). Studies in the cultured cells also suggested that the binding of mutant ataxin 3 to ITPR1 increases its sensitivity to inositol tris-phosphate-3 (IP3), leading to alteration in $Ca^{2+}$ signaling. Therefore, it appears that the presence of mutant ataxin 3 in the neuronal cells changes the localization of CARP VIII, along with its increased expression and leads to disruption of ITPR1-mediated calcium signaling in the neurons (Hsieh et al., 2013).

### 2.3.3 Crystal structure of CARP VIII and its interaction with ITPR1

The crystal structure of human CARP VIII (hCARP VIII) has been determined at 1.6 Å resolution (2W2J in PDB) (Picaud et al., 2009). The 3-dimentional structure of hCARP VIII (Fig 2) has a Glu stretch at the N-terminal end from aa 24 to 36 (E loop). CARP VIII has the central core domain (aa 37 to aa 290) which is similar to the mammalian CA enzymes. The core domain consists of 10-stranded central β-sheets surrounded by several α-helices and β-strands. The crystal structure of CARP VIII has similarity with cytosolic human CA XIII (hCA XIII) (41% sequence identity) and has several differences in two loop regions (Fig 3 II). In hCARP VIII, the E loop protrudes into the exterior and packs against the α3-β15 loop, which incorporates a five-residue insertion compared with other isozymes.

Compared with hCA II the hCARP VIII cavity is spatially narrower due to replacement of H94, which is essential for binding to the zinc in the active site. Other residues in the active site essential for CA enzymatic activity in CAII, such as T200, V121, and V143 in CAII were substituted by I224, I143 and I165, respectively. The replaced aa are bulkier, reduced the pocket size in hCARP VIII, and obstruct the binding of $CO_2$ in the active site. The crystal structure showed that the central core domain allows the CARP VIII protein to adopt the classic CA fold but the replacement of aa residues, which play a key role in CA enzymatic activity, rendered the CARP VIII catalytically inactive. Interestingly, replacement of R116, E114, and I224 with H117, Q115, and T225 makes the CA VIII enzymatically active (Elleby et al., 2000; Sjoblom et al., 1996). However the sequence and structural similarity of hCARP VIII with active CAs suggest that over the course of evolution CARPs have

gained new functions possibly to control the function of other proteins through the protein-protein interactions.

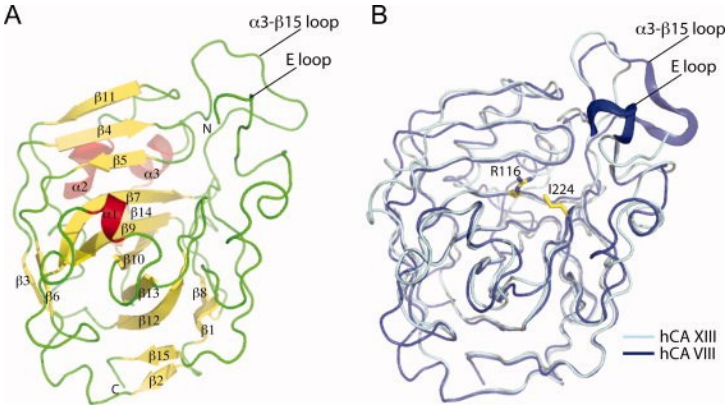


**Figure 2.** Crystal structure of hCARP VIII. (A) Ribbon diagram exhibiting the secondary structure elements: α-helices (red) and β-strands (yellow). (B) $C_\alpha$-superposition of hCARP VIII (blue) and hCA XIII structures (cyan, PDB code 3DA2). The two loop regions that are unique in hCARP VIII are shown in thick ribbons. **Source:** (Picaud et al., 2009).

It has been reported that ITPR1, which interacts with CARP VIII, has an electropositive $IP_3$ binding site (Bosanac et al., 2002; Hirota et al., 2003). The unique electronegative surface in CARP VIII could form a charge-complementary binding site for ITPR1 and might be involved in the release of $Ca^{2+}$ from endoplasmic reticulum (Jiao et al., 2005). ITPR1, which is expressed in the PCs of cerebellum similar to CARP VIII, has been identified as a binding partner for CARP VIII (Hirota et al., 2003). The deletion mutation analysis of CARP VIII revealed that the aa region from 45 to 291 interacts with the regulatory domain of ITPR1, which is located between aa 1387-1647 (Fig 3). It is suggested that CARP VIII reduces the sensitivity of ITPR1 to $IP_3$ and thereby controlled release of $Ca^{2+}$ in the PCs. This finding suggests that the co-expression of CARP VIII with ITPR1 in PCs has an inhibitory effect on $IP_3$ binding (Hirota et al., 2003).

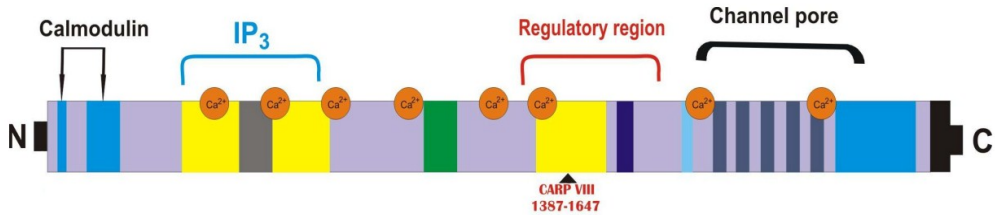


**Figure 3:** Schematic presentation of ITPR1 presenting the binding regions for calmodulin, IP3 at N-terminal end and a channel pore at C-terminal region. The regulatory region of ITPR1 shows the region of aa 1387-1647 which interacts with CARP VIII protein. Modified from (Mikoshiba, 2007).

### 2.3.4 Role of *Car8* gene in gait disorder in mouse

The association of *Car8* gene mutation with ataxia was first reported from studies on *wdl* mice (Jiao et al., 2005). The mice which had a spontaneously occurring mutation in *Car8* gene were characterized by wobbly side-to-side ataxic movement when the mice reached two weeks of age, and the disorder persisted throughout their life span. Further studies on these mice revealed a 19 base pair (bp) deletion in exon 8 of the *Car8* gene responsible for waddled phenotype. The *Car8* gene was located in the genetic region of *wdl* and the deletion of *Car8* was the only defect found among the genes and ESTs within the *wdl* locus of *wdl* mice. Similarly, the *wdl* mice had no detectable CARP VIII protein. The *Car8* (*wdl)* mutation was autosomal recessive and it was located close to the waddler (*wd*) locus on mouse chromosome 4 (Yoon 1959). The sequence analysis of the affected gene showed a deletion of 19 bp, in the exon 8 of *Car8* gene and caused a shifting of the reading frame. The shifting of the reading frame inserted a stop codon in the gene which eliminated 50 aa in the protein leading to a non-functional protein (Jiao et al., 2005). Further, structural level studies in these mice exhibited functional abnormalities of excitatory synapses of PCs. The functional abnormalities of excitatory synapses of PCs might be responsible for motor coordination defects in these mice (Hirasawa et al., 2007). These studies suggest the importance of CARP VIII in the development and/or maintenance of the proper morphology and function of PC synapses (Hirasawa et al., 2007).

### 2.3.5 Association of *CA8* gene with ataxia in humans

The involvement of *CA8* gene in human neurodevelopmental disorder was suggested based on the studies in members of Iraqi and Saudi Arabian families (Kaya et al., 2011; Turkmen et al., 2009). In the first study, the genetic analysis of members of the Iraqi family showed a homozygous missense mutation, where serine 100 was replaced by proline (S100P) in the CARP VIII protein (Turkmen et al., 2009). The affected members exhibited a mild mental retardation and congenital ataxia accompanied by a quadrupedal gait (Fig 4) (Turkmen et al., 2009). *In-vitro* studies suggest that the change produced by the S100P change leads to proteasome-mediated elimination of CARP VIII protein due to misfolding. This is a common mechanism in cases of loss of function mutations which are associated with various human genetic diseases (Lukacs and Verkman, 2012; Wang and Moult, 2001). The affected members of the Iraqi family had a phenotype similar to *wdl* mice (Jiao et al., 2005). In this study, the clinical features of the patients included cerebellar ataxia, dysarthria, mild mental retardation and tremor (Turkmen et al., 2009).

**Figure 4.** Members of the Iraqi family with a quadrupedal gait. With permission (Turkmen et al., 2009).

In the second study, all the seven affected members of Saudi Arabian family had cerebellar ataxia, mental retardation, and disequilibrium syndrome type 3 (Kaya et al., 2011). Sequencing of exons revealed a novel homozygous variation (484G>A) in exon 4 of *CA8* gene of all the affected members and the parents of the affected members showed heterozygous variation (484G>A) in exon 4 of *CA8* gene. Homozygosity for the variation cosegregated with the disease phenotype and the substitution was not present in 200 unrelated healthy controls of the same ethnic origin, indicating that the G162R (484G>A) variation in CARP VIII protein is very likely to be pathogenic. The clinical features in the patients included variable cerebellar ataxia and mild cognitive impairment and interestingly none of the patients had a quadrupedal gait. The affected patients showed loss in the cerebellar volume (Fig 5) and ill-defined peritrigonal white matter abnormalities along with hypometabolic cerebellar hemispheres, temporal lobes, and mesial cortex. The common clinical features between affected members of the present study and the members of Iraqi family were mild cognitive impairment, variable cerebellar ataxia, absence of seizures, and lack of dysmorphism. In this study the absence of a quadrupedal gait could probably be associated with the environmental factors rather than genuine phenotypic change due to the disease (Kaya et al., 2011).

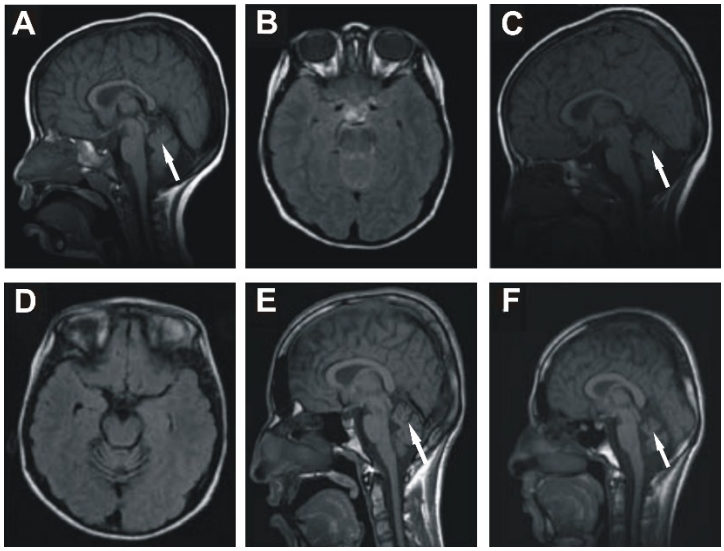


**Figure 5.** The cerebellar volumes of Saudi Arabian patients. The progressive cerebellar loss (arrows) in patient 1 between the sagittal T1 (A and C) and axial flair images (B and D) at 4 (A, B) and 8 years of age (C, D), respectively. Sagittal T1 images indicate reduction in cerebellar volume more prominent in patient 3 (E) than in patient 2 (F). Modified with permission (Kaya et al., 2011).

The phenotypic changes observed in mice and humans could be due to altered $Ca^{2+}$ signaling because of the mutation in CARP VIII gene which increased the sensitivity of ITPR1 to $IP_3$ (Jiao et al., 2005; Kaya et al., 2011; Turkmen et al., 2009). The release of intracellular $Ca^{2+}$ ions from endoplasmic reticulum is responsible for several cellular activities which include: synaptic recycling, proliferation, fertilization, learning and memory, long-term potentiation, depression, apoptosis, contraction, metabolism, and the control of other signaling systems. In fact, the cerebellar gene expression profile of *wdl* mouse revealed that many genes involved in synaptogenesis, synaptic vesicle formation and transport, cellular proliferation and differentiation, and signal transduction were dysregulated (Yan et al., 2007). These findings suggest that ultrastructural abnormalities of specific neuronal elements may be present in *wdl* cerebellar cortex. Similarly, dysregulation of many genes in *wdl* mouse suggests that the *Car8* gene may be playing a role in the cerebellar cortex (Yan et al., 2007).

### 2.3.6 Role of CARP VIII in cancer and other diseases

The potential role of CARP VIII was investigated in human colorectal epithelial carcinomas by immunohistochemistry (Miyaji et al., 2003). Expression of CARP VIII and Ki-67, a marker for cell proliferation, was studied in 60 human adenocarcinomas and 13 human adenoma samples. The expression of CARP VIII

was found in 78% of colorectal carcinomas, whereas only 5% of the 73 normal colon samples were positive for CARP VIII. The signal for CARP VIII was observed more frequently at the tumor invasion front compared with Ki-67 antigen. CARP VIII staining for colorectal adenoma was significantly lower in comparison with adenocarcinomas (Miyaji et al., 2003). The selective expression of CARP VIII at the tumor invasion front suggests that it plays a role in invasion of colorectal cancer. Further the role of CARP VIII was explored using colon cancer cell lines (LoVo-CA8) (Nishikata et al., 2007). The studies on LoVo-CA8 and the control cell line (LoVo-pCIneo) suggested that the LoVo-CA8 cell line expressed high levels of *CA8* mRNA and the corresponding CARP VIII protein. The LoVo-CA8 cell line showed higher cell proliferation and cell invasion abilities compared to the parental LoVo and LoVo-pCIneo cells . The tumor growth in mice transplanted with LoVo-CA8 cells was higher than the parental LoVo cells. The knockdown of *CA8* using small interfering RNA in another cell line (HCT116), expressing high level of endogenous CARP VIII, efficiently inhibited cell proliferation and colony formation. This result also suggested that the CARP VIII plays a role in colon cancer.

Comparative expression studies of CARP VIII in mouse and human tissues exhibited a very faint signal for *CA8* in adult human lung compared with the signal for *Car8* in mouse lung (Akisawa et al., 2003). However, the expression analysis in human fetal lung indicated a very strong signal for *CA8* both at protein and mRNA level. Further analysis of expression by immunohistochemistry showed a signal for CARP VIII in non-tumorous lung tissues in adults. The signals for CARP VIII protein were restricted to bronchial ciliated cells, chondrocytes of bronchial cartilage, and smooth muscle cells. However, developing pulmonary epithelium showed abundant CARP VIII. This pattern of CARP VIII presence led to the study, whether CARP VIII is an oncofetal antigen in human lungs. The immunochemical staining of pulmonary non-small cell carcinoma specimens exhibited a very strong signal for CARP VIII in 54 out of 55 cases. The staining was strong at the front of the tumor progression and a weak staining was observed in the center of the carcinomas. These findings suggested that CARP VIII is strongly expressed in highly proliferative lung cancer cells (Akisawa et al., 2003).

CARP VIII expression studies were done in human lung adenocarcinoma cell line (PC-9), where the exogenous CARP VIII expression leads to intracytoplasmic vacuole formation (Ishihara et al., 2006). Similarly, signet ring cells, which are seen in several carcinomas and contain intracytoplasmic mucin were observed among CARP VIII expressing PC-9 cells compared to control PC-9 cells. Expression of CARP VIII in adenomatous hyperplasia and early-stage lung adenocarcinoma suggested an abundant presence of CARP VIII in invasive lung adenocarcinoma compared with noninvasive adenocarcinoma. Matrigel invasion assay revealed invasiveness by PC-9 cells expressing CARP VIII but not by control PC-9 cells, suggesting that CARP VIII expression in lung cancer is involved in cancer cell invasion (Ishihara et al., 2006).

The expression of CARP VIII was studied in gastrointestinal stromal tumors (GIST) and in gastric tissues of a patient with von Recklinghausen disease (the disease causing tumors called neurofibromas in the tissues and organs of the body) by immunohistochemistry. The expression analysis of 22 GIST samples indicated high levels of CARP VIII in 13 samples (59%) and an intense signal for CARP VIII was also seen in neural cell bodies of a patient with von Recklinghausen disease. In the same study, expression of CARP VIII was analyzed in GIST-T1 cells and the same cells transfected with *CA11* expression vector (GIST-T1-CA11). There was no change in the expression level of CARP VIII in these cells, but surprisingly, there was a change in the subcellular localization of CARP VIII. The immunohistochemistry suggested localization of CARP VIII in the perinuclear region of GIST-T1 cells, whereas CARP VIII was localized in the whole cell body in GIST-T1-CA11 cells. The expression pattern of CARP VIII in these studies suggested that CARP VIII might play a role in the development of GIST and may also indirectly, or directly, interplay with CARP XI (Morimoto et al., 2005). The CARP VIII protein may also act as an autoantigen, which is associated with the pathogenesis of melanoma-associated Paraneoplastic cerebellar degeneration (PCD). Even though it is a single observation, serum of a patient with PCD and malignant melanoma had reactivity with PCs, and the autoantibody showed reactivity against CARP VIII protein (Bataller et al., 2004).

Association of single nucleotide polymorphisms (SNPs) in *CA8* with femoral and lumbar bone mineral density (BMD) was studied in 337 women suffering from osteoporosis. The study presented a significant correlation between *CA8* SNP rs6984526 and femoral BMD, and the BMD of homozygous carriers of major (C) allele was higher compared with heterozygous carriers. Similarly, *CA8* SNP also suggested a very strong association with lumbar BMD. The variations of *CA8* loci could be an important determinant of osteoporosis and the *CA8* gene seem to have an additional role in the process of bone resorption (Mori et al., 2009).

### 2.3.7 Catalytic activity and inhibition of mutant CARP VIII

The restoration of two aa residues (Arg117 to His and Glu115 to Gln) required for the $Zn^{2+}$ co-ordination converts the inactive mouse CARP VIII to an active enzyme (Sjoblom et al., 1996). The enzymatic activity of the mutated CARP VIII was significantly higher in comparison with the mammalian CA III and the activity could be strongly inhibited by acetazolamide (Sjoblom et al., 1996). In fact, the same authors showed that a single mutation to restore the $Zn^{2+}$ binding His residue at position 117 in place of Arg is sufficient for the catalytic activity of CARP VIII but the catalytic activity was half of the double mutated CARP VIII enzyme (Elleby et al., 2000). The replacement of Gln92 to Glu in CA II showed a slight effect on its enzymatic activity, suggesting that the replacement of Glu115 with Gln in CARP VIII might lead to an increase in enzymatic activity (Elleby et al., 2000; Kiefer, 1995;

Sjoblom et al., 1996). In the same study, the authors replaced three more residues in mouse CARP VIII, namely Ile225 to Thr and two isoleucines at positions 144 and 166 to Val. The replacement of these residues was done based on the information that the Thr at that position is not required for the catalytic activity but it has a significant effect on the catalytic activity (Behravan et al., 1991; Elleby et al., 1999). Similarly, occurrences of two Val residues, which are bulky, make the active site region too small for optimal catalytic activity (Elleby et al., 2000; Kato, 1990b). Indeed, the mouse CARP VIII with an additional three mutations revealed a significantly increased activity (Elleby et al., 2000).

In a recent study, the catalytic activity of hCARP VIII was restored. The mutated CARP VIII had a very high catalytic activity with a kcat/km of 67.3% of hCA II, which is one of the highly active enzymes. The mutated CARP VIII could be effectively inhibited by acetazolamide. The catalytic activity of the mutated hCARP VIII was higher than the mutated mouse CARP VIII, although there is only a difference of three aa between the mouse and human CARP VIII (Nishimori et al., 2013).

## 2.4 General properties of CARP X

CARP X was discovered in 1996 based on expressed sequence tags (ESTs), which displayed significant homology with catalytically active CAs (Hewett-Emmett and Tashian, 1996). Further analysis of EST's revealed that these sequences lacked two of the three His essential for binding to a $Zn^{2+}$ and were named as *CA10* (Hewett-Emmett and Tashian, 1996). Later on, Kleiderlein and coworkers found a cDNA homologue showing 61% identity (accession No. AF064854) with *CA11* sequence while screening human cDNA libraries for the CCG repeats (Kleiderlein et al., 1998). Subsequently, a 2720 bp full length cDNA clone was obtained encoding 328 aa protein with a predicated molecular mass of 37.6 kDa. The aa sequence deduced from 2720 bp cDNA showed 25-57% similarity with catalytically active CAs and exhibited highest identity with CARP XI (Okamoto et al., 2001). The *CA10* sequence is known to contain seven CCG repeats at the 5'-untranslated region followed by two CCG repeats at 16 bp downstream region and the polymorphism of its repeat number has been reported in normal humans (Kleiderlein et al., 1998).

### 2.4.1 Expression of CARP X in human and mouse tissues

After the discovery of *CA10* in mid 90s the expression of its mRNA was studied in the human brain and in several other tissues (Okamoto et al., 2001). The NB analysis revealed the presence of 2.8 kilo base (kb) band which corresponded to a full length *CA10* sequence. The Dot blot (DB) analysis of *CA10* mRNA exhibited a low but

significant signal in the whole brain and in all parts of the CNS, including the amygdala, cerebellum, cerebral cortex, frontal lobe, hippocampus, medulla oblongata, occipital lobe, putamen, substantia nigra, temporal lobe, thalamus, nucleus accumbens, and spinal cord. The DB technique could not detect any signal for *CA10* in the human fetal brain. However, a more detailed analysis indicated the appearance of CARP X protein in the neural cells of the cortex at day 141 of fetal brain development (Taniuchi et al., 2002a). Expression analysis of *CA10* was also done using RT-PCR in a panel of human tissues displaying a very strong expression in the brain, kidney and salivary gland and a weak expression in the pancreas, liver, mammary gland and testis (Okamoto et al., 2001). Tashian´s group has reported the presence of many ESTs for *CA10* in the human placenta (Tashian et al., 2000). Immunohistochemical staining of CARP X showed a positive signal in both the medulla and cortex of the cerebrum. A very strong signal for CARP X was seen in the myelin sheath and weak signals were also seen in the cerebellar PCs and medullar olivary nuclei (Taniuchi et al., 2002a).

The tissue distribution of CARP X in the adult mouse and its developmental expression in the brain showed interesting findings (Taniuchi et al., 2002b). The NB and RT-PCR analysis exhibited a signal only in the brain for the presence of *CA10*. Expression analysis was done in whole mouse embryos at four different stages (E7, E11, E15 and E17) of development. The signal for *CA10* was seen at E11, E15 and E17 during the development by RT-PCR and the NB displayed a significant signal only at E11 during the development. The cellular distribution of CARP X by immunohistochemistry showed moderate expression in neural cells of the cerebrum and midbrain. In the cerebellum, both PCs and dental nuclei exhibited moderate signals for CARP X and weak expression was also seen in the molecular layer, ependymal cells and choroid plexus. The RNA *in-situ* localization studies revealed that *Car10* is mainly expressed in the cone bipolar cells of the mouse retina and weak expression was also seen in the amacrine cells and ganglion cell layer of the retina (Kim et al., 2008).

### 2.4.2 Expression of CARP X in pathological conditions

The cellular distribution of CARP XI in human brain showed a very strong signal in the linear structures which were assumed to represent the axons or myelin sheaths in the cerebellar medulla and the brain stem (Taniuchi et al., 2002a). These findings prompted the authors to study in more detail whether CARP X is localized in the axon or myelin sheath. The brain sections of a patient with acute disseminated encephalomyelitis were stained with CARP X antibodies and there was no signal for CARP X in the demyelinated axons. Further, CARP X was located to the cytoplasm of neuroblastoma cells (NH12). Similar staining was done in shiverer mouse which had a defective myelin basic protein, and as a result the myelinization was incomplete

(Mikoshiba et al., 1995). The immunohistochemical staining of the shiverer mouse brain showed a complete absence of CARP X in the myelin sheath. The results of the above studies indicate that the CARP X protein is expressed in the myelin sheath. The expression of CARP X in the myelin sheath in the normal human and mouse brain and the loss of expression in the disease suggests the involvement of CARP X in myelin sheath organization (Taniuchi et al., 2002a).

The 5'-untranslated region of *CA10* gene contains a CCG trinucleotide repeat in normal humans. The presence CCG repeats in *CA10* gene and its specific expression in the myelin sheath tends to indicated that the CARP X could be involved in demyelination disorders (Kleiderlein et al., 1998). The microarray expression analysis shows the up-regulation of *CA10* mRNA in several cancers suggesting its involvement in the development of neuroblastoma and in several other cancers in humans and other pathological conditions (Kilpinen et al., 2008).

### 2.4.3 Catalytic activity and inhibition of mutant CARP X

hCARP X lacks the two His at positions 94 and 119 which are essential for binding of a zinc atom. Recently, the His were restored making the CARP X active (Nishimori et al., 2013). The mutated CARP X had 92% of the catalytic activity of hCA II. The enzymatic activity of the mutant CARP X protein was effectively inhibited by acetazolamide with the inhibition constant ($K_I$) of 16 nM.

## 2.5 General properties of CARP XI

The human *CA11* gene was discovered accidentally during the construction of a physical map for cone-rod retinal dystrophy. The identified EST D19S799E mapped close to the distal flanking polymorphic marker D19S412 and was reported as CARP-2 (Bellingham et al., 1998). The EST coded for a novel CARP with 328 aa. The catalytic domain of the predicted protein had a substitution of four aa critical for the catalytic activity of the protein (His94Arg, His96Leu, His119Gln, and Thr199Ser). Simultaneously, the existence of the CARP XI sequence was also reported by two other groups from sheep and human (Fujikawa-Adachi et al., 1999; Lovejoy et al., 1998).

The first group unexpectedly identified a 1331 bp cDNA while screening a sheep brain cDNA library for frog corticotropin-releasing factor-like peptide sauvagine (Lovejoy et al., 1998). The predicted protein of 328 aa had a theoretical mass of 36 kDa with a signal sequence, suggesting that this protein was secreted. The protein had seven aa residues that are found in sauvagine, but the primary structure of this novel protein was similar to α-CAs and was named as CARP XI. The second group obtained a full length *CA 11* cDNA from the human pancreas based on the existence

of partial cDNA sequence from dbEST (accession Nos. AA297055 and AA297730) (Fujikawa-Adachi et al., 1999). The cDNA clone was sequenced containing 1475 bp and predicted to encode 328 aa with a mass of 36,200 Da. The deduced aa sequence showed 42-53% similarity to the active CAs and was devoid of catalytically important His residues. Genetic analysis revealed that the *CA11* gene was located on chromosome 19q13.2-3. The 3'-UTR had a putative polyA cleavage signal (ATTAAA). NB exhibited a signal for 1.5 kb transcript in the brain, particularly in the cerebellum, cerebral cortex, and putamen.

### 2.5.1 Expression of CARP XI in normal tissues

An expression pattern of CARP XI was first completed in a panel of human tissues using NB (Bellingham et al., 1998). A strong signal for the *CA11* gene product was seen in brain in the region of 1.6 kb in addition to the less intense transcripts of 2.6 and 3.5 kb. The 1.6 kb transcript was the expected size of *CA11* cDNA. The analysis also displayed lower intensity bands in the spinal cord and thyroid gland and faint signals were seen in the heart, skeletal muscle, kidney, pancreas, ovary, small intestine, mucosal lining of the colon, peripheral blood leukocyte, stomach, lymph node, trachea and adrenal gland (Bellingham, et al. 1998). In another study, NB analysis showed a presence of 1.5 kb *CA11* transcript in the human brain including the cerebellum, cerebral cortex, medulla, spinal cord, occipital pole, frontal lobe, temporal lobe and putamen (Fujikawa-Adachi et al., 1999). No signal for *CA11* was detected in heart, placenta, lung, liver, skeletal muscle, kidney and pancreas. However, RT-PCR analysis indicated the expression of *CA11* mRNA in the pancreas, liver and kidney, suggesting low levels of expression in these organs.

The expression pattern of CARP XI using immunohistochemistry has been studied in the fetal brain at five different gestational periods (Days 84, 95, 121, 141 and 222) and in different parts of the adult brain (Taniuchi et al., 2002a). The presence of CARP XI was seen in neuroprogenitor cells in the subventricular area at day 84 of gestation and in neural cells and choroid plexus at day 95. In the adult brain, a strong signal for CARP XI was seen in the choroid plexus and pia arachnoid. Neurons and astrocytes exhibited a moderate expression of CARP XI. Although the exact function of CARP XI in the brain and especially in the developing brain is uncertain, the expression pattern suggests certain roles in the early development of the brain or differentiation of neuroprogenitor cells.

The cellular distribution of *CA11* has been analyzed in both adult mouse tissues and embryos of different developmental stages (Taniuchi et al., 2002b). NB analysis revealed the presence of six different bands (1.4, 1.6, 2.4, 3.4, 3.8, and 4.9 kb) in the brain, lung and liver. Among the six bands observed, the 1.5 kb band was the strongest one in the brain. A moderate signal for a 2.4 kb transcript was seen in the heart, skeletal muscle and kidney. The developmental expression of *CA11* mRNA was studied in whole mouse embryos at four different gestational periods (E7, E11,

E15, and E17) using RT-PCR and NB. The RT-PCR results suggested the presence of *CA11* mRNA at all the stages of development. NB showed the appearance of *CA11* mRNA at E7 stage of development and the *CA11* signal level decreased as the development progressed. In mouse brain, moderate signals for CARP XI protein were seen in neural cells of the cerebrum, Ammon's horn and midbrain as well as in the molecular layer, PCs and dental nuclei of the cerebellum, ependymal cells and choroid plexus(Taniuchi et al., 2002b).

### 2.5.2 Expression of CARP XI in pathological conditions

The expression analysis of CARPs in cancer tissues and in cultured cells has been reported previously (Akisawa et al., 2003; Miyaji et al., 2003). These studies suggested that CARP VIII plays some role in the lung and colorectal cancers. As a continuation to previous studies, the authors studied the expression pattern of all the CARPs in gastrointestinal stromal tumors (GISTs) and *in-vitro* in cultured GIST-T1 cells (Morimoto et al., 2005). The immunohistochemical analysis of 22 GIST samples presented a very strong signal for CARP XI in 20 (91%) GIST specimens. To understand the role of CARP XI in the GISTs, further studies were performed in GIST-T1 cultured cells transfected with *CA11* cDNA (GIST-T1-*CA11*). The expression level of *CA11* mRNA and CARP XI protein showed a remarkable increase in the cells transfected with *CA11* compared with the GIST-T1 control cells. Interestingly, a very strong signal for CARP XI protein was observed in the cytoplasm of GIST-T1 cell bodies. There was a significant increase in cell proliferation and cell invasion in GIST-T1-*CA11* cells compared with GIST-T1 cells, suggesting that the CARP XI plays a role in the development and spread of GIST tumors. Additionally, the expression pattern of the human *CA11* gene at GeneSapiens bioportal indicates the upregulation of *CA11* mRNA in several cancers and in other pathological conditions (Kilpinen et al., 2008).

Recently, expression of CARP XI was studied in cultured neuronal cells expressing mutant ataxin 3 and in humans and mice with defects in ataxin 3 protein (Hsieh et al., 2013). It is well known that ataxin 3 contains CAG trinucleotide repeats and the mutations causing the expansion of CAG repeats cause a neurodegenerative disorder known as spinocerebellar ataxia 3 /Machado-Joseph disease (SCA3/MJD) in both humans and mice (Kawaguchi et al., 1994). Preliminary studies on the gene expression pattern of human neuroblastoma cells expressing mutant ataxin 3 showed upregulation of *CA11* mRNA (Hsieh et al., 2013). The results of the study led to further exploration of expression pattern of *CA11* gene in cultured neuronal cells transfected with mutant ataxin 3 gene and in a human patient with SCA 3 and in a transgenic mouse model with MJD. The results of the *in-vitro* study revealed an altered cellular localization of CARP XI in the cells expressing mutant ataxin 3 compared with the cells expressing WT ataxin 3 (Hsieh et al., 2013).

### 2.5.3 Catalytic activity and inhibition of mutant CARP XI

Mammalian CARP XI lacks all the three histidine residues required for the coordination of the $Zn^{2+}$ at the active site making it catalytically inactive (Fujikawa-Adachi et al., 1999; Lovejoy et al., 1998; Supuran, 2008). Recently, the catalytic activity of hCARP XI was restored by replacing the three missing histidines. (Nishimori et al., 2013). The mutated protein exhibited a very high catalytic activity. The catalytic activity of mutated protein was 82.6% of the hCAII and was effectively inhibited by acetazolamide, with the inhibition constant (KI) of 29 nM.

# 3 Aims and objectives of the study

The CARP VIII, X and XI sequences are highly conserved and, in human and mouse are, predominantly expressed in the brain, suggesting important physiological roles in higher organisms. In the present work, we planned to study the distribution of CARP sequences across the species and study the role of CARPs using zebrafish as a model organism as there are no knockout mouse models for CARP genes. In recent years, zebrafish has become an important model organism for studying the embryonic development which is rather similar to the humans. Besides, zebrafish embryos are transparent and develop externally and therefore can be manipulated easily.

**The specific aims of the study were to:**

Identify and evaluate the distribution of CARP genes in different taxonomic classes (across the species) and study the expression pattern of all the three CARPs in mouse, a mammalian model organism. (**I**)

Study the conserved residues of CARP VIII on a three dimensional protein structure and visualize the sites of pathogenic mutations in human CARP VIII. (**II**)

Elucidate the role of CARP VIII in zebrafish during embryonic development, another vertebrate animal model. (**III**)

Analyze the sequences and conserved residues of CARP X and CARP XI in vertebrate species and study their role in zebrafish embryonic development. (**IV**)

# 4 Materials and methods

## 4.1 Bioinformatic analysis of CARP VIII, X and XI sequences (**I**)

CARP sequences were retrieved from different databases (Ensembl, UniProt, and RefSeq) and at NCBI using Basic Local Alignment Search Tool (BLAST) search (Altschul et al., 1997; Pruitt et al., 2007). Further CARP sequences were generated using mammalian CARPs as query sequences for blast like search (BLAT) from the completed sequence of genomes (Kent, 2002). The obtained sequences were taken through the iterated cycles of multiple sequence alignment (MSA), evaluation and revision (Larkin et al., 2007). For revision of sequences, GeneWise was used for gene model generation with the genomic sequences from the University of California Santa Cruz (UCSC) Genome Browser for the sequences with imperfect matching and for the missing regions in the sequences (Birney et al., 2004; Kent et al., 2002). Gene models generated were confirmed using EST and mRNA sequence data, and to discover and assemble CARPs from less than genome-wide sequenced organisms. In total, we collected 84 full length CARP sequences for further analysis.

ClustalW was used for MSA of all the CARPs and the MSAs were visualized using GeneDoc software (Higgins et al., 1996; Nicholas, 1997). The molecular and evolutionary genetic analysis (MEGA) software (version 4.1), was used for the construction of a phylogenetic tree (Tamura et al., 2007). The evolutionary relationship of the CARPs was studied using Neighbor-Joining (NJ) method. A bootstrap test was performed using 1000 replicates and evolutionary distances were computed using the Poisson correction method with the complete deletion option.

## 4.2 Expression of CARP genes (**I, III,** and **IV**)

### 4.2.1 Extraction of mRNA from mouse and zebrafish

Tissue samples of adult mice were harvested and transferred to the tubes containing RNAlater (Ambion, Austin, TX, USA) (**I**). Similarly, tissue samples from different organs of adult zebrafish and embryos were collected in RNAlater (**III, IV**). RNA was isolated using RNeasy kit (Qiagen, Hilden, Germany).

**Table 2.** Primers for the study of *ca8*, *ca10a* and *ca10b* zebrafish genes (**III, IV**)

| Gene | Primer Name | Upstream (5'-3') Downstream (5'-3') primers | Size (bp) |
|---|---|---|---|
| ***ca8***[a] | *ca8*-G-DNA | GTATTGTGATACATCAGTTT<br>TTAAGCCAAACTGAGACAGG | 400 |
| | *ca8*-RT-PCR | TTCACTGGGGCAAAGAAAAC<br>ATGGCCTTCAGACCAAGATG | 100 |
| | *ca8*-RT-qPCR | CCCATGTTAAAGGAGCAGAGCTT<br>GGTTGGGTCGGTCTAAAGTTGT | - |
| | ITPR1-RT-qPCR | CGATAACCCCGGGTGAATG<br>CCTGGGAGCTTTCAATGTTTG | - |
| ***ca10a***[a] | *ca10a*-G-DNA | TCAGGGAAGCCACCCTTGAATGA<br>AGAGAAGGCCTGGCCATTGAGG | 400 |
| | *ca10a*-RT-PCR | ATGGATATAATCTGGGAAATATTTATTATTC<br>CTATTTCAGCAGCCATTCGTTC | Full Lengths |
| | *ca10a*-RT-PCR | TCTCTCGGGGCTAAACATTG<br>TTGACTTAGCAGTCGCATGG | 100 |
| | *ca10a*-RT-qPCR | GAAACCAGTCGCATGATTTTTG<br>TTGCGTTGCCCTGCATT | - |
| ***ca10b***[a] | *ca10b*-G-DNA | TAGTGTAAACGGGGCCTTACATTTTA<br>GATTGTCCTCACTGCCAAAGTG | 400 |
| | *ca10b*-RT-PCR | ATGCCGCACGTTTGGGAGTT<br>TTATTTCAGAAGCCATTCATTCACTC | Full Lengths |
| | *ca10b*-RT-PCR | TGGGGCTGAATATTGAGGAG<br>GGCTGGTTTTGACTGAGGAG | 100 |
| | *ca10b*-RT-qPCR | CCTGACACCACTGAGGCTCAA<br>CGGCCGGTGTTGTACATTG | - |
| ***CA10***[b] | *CA10*-PCR | CGCCTCGAGATGGAAATAGTCTGGGAGGTGCT<br>CCGGGATCCCTACTTGAGGAGCCATTCATT | Full Lengths |
| ***CA11***[b] | *CA11*-PCR | CGCTCTAGAATGGGGGCAGCTCGTCTG<br>CCGGAATTCTCAGCGACCATGGGGGACACC | Full Lengths |

[a]Zebrafish sequences, [b]human sequences for rescue of morphant zebrafish

### 4.2.2 Synthesis of single strand cDNA and RT-qPCR

cDNA was synthesized using first Strand cDNA Synthesis kit (High-Capacity cDNA RT Kits, Applied Biosystems, Foster City, CA). The primers were designed using Primer Express® Software (version 2.0) (Applied Biosystems) for the mouse CARPs genes deposited in the Gene Bank (Table 3). Similarly, primers for zebrafish *ca8* (ENSDART00000057097), *itpr1a* (ENSDART00000149019), *ca10a* (ENSDART00000074540), and *ca10b* (ENSDART00000055264) were designed using the cDNA sequences from ENSEMBL database (Table 2). RT-qPCR was performed using SYBR Green PCR Master Mix Kit according to the instructions (Applied Biosystems) using the initial denaturation step at 95ºC for 10 min followed by 40 cycles at 95ºC for 15 sec and elongation time of 1 min at 60ºC. Every PCR was performed in a total reaction volume of 15 µl containing 2 µl of the first strand cDNA (20 ng cDNA), 1x Power SYBR Green PCR Master Mix, and 0.5 µM of each

primer. The final results, expressed as the N-fold relative difference (ratio) in gene expression between the studied samples, internal control gene β-actin and the relative expressions were calculated according to Pfaffl's equation (Pfaffl, 2001). Each experiment was repeated thrice and average of the three values was taken.

**Table 3.** Mouse primer sequences used for RT-qPCR of mouse CARP genes (**I**)

| Gene | Primer | Sequence | RefSeq numbers |
|---|---|---|---|
| *Car8* | Forward<br>Reverse | 5'cgggattactgggtctatgaagg3'<br>5'ggctgggtaggtcggaaattgtc3' | NM_007592 |
| *Car10* | Forward<br>Reverse | 5'gagagcaagagcccagaactc3'<br>5'ctcaccagtggcagaaatggc3' | NM_028296 |
| *Car11* | Forward<br>Reverse | 5'gccggctctgaacaccagatc3'<br>5'gaggaggcgactgaggaatgg3' | NM_009800 |

### 4.2.3 Immunohistochemistry of CARPs in mouse and zebrafish (**I, III**)

The tissue specimens were fixed by immersion in 4% paraformaldehyde (PFA) in phosphate buffered saline (PBS). Samples were dehydrated in an alcohol series, treated with xylene, embedded in paraffin wax and 5 μm sections were cut and placed on Superfrost microscope slides. The paraffin was removed from the sections with xylene and the rehydrated sections were boiled in sodium citrate (0.01 M, pH 6.0) for 20 min and cooled down. The staining protocol was started by incubating the sections in methanol + 3% $H_2O_2$ for 5 min, rinsed with 1x Tris-buffered saline (TBS), pH 8.0, containing 0.05% Tween and blocked with Rodent Block M™ (Biocare Medical, Concord, CA) for 30 min. The samples were then incubated with primary rabbit anti-human CARP VIII, CARP X, and CARP XI antibodies ( Catalog # sc-67330, sc-67332 and sc-67333 respectively, Santa Cruz Biotechnology, Inc. Bergheimer Heidelberg, Germany) at a dilution of 1:350 in 1% bovine serum albumin (BSA) for 1 h at room temperature and rinsed with TBS containing 0.05% Tween (The specificity of the antibodies was verified by running a WB using lysate of mouse brain which gave a single band of expected size). The rabbit IgG was used as a control antibody and incubated with 2.5 ml of Rabbit (horseradish peroxidase) HRP-Polymer + 1-2 drops of XM Factor™ (Biocare Medical) for 30 min before rinsing with 1xTBS containing 0.05% Tween and the samples were treated with 3'-diaminobenzidine tetrahydrochloride (DAB) solution for 5 min prior to rinsing with $dH_2O$. Counterstaining was done with Mayer´s Hematoxylin for 1 to 3 sec and rinsed under tap water for 10 min. The slides were mounted with Entellan Neu™ (Merck; Darmstadt, Germany), examined and photographed using a microscope (Nikon Microphot-FXA, Japan).

The immunofluorescence staining was performed according to the following protocol: (i) incubation of the samples for 30 min in PBS containing 0.1% BSA, (ii) incubation with rabbit anti-human CARP VIII antibody (Santa Cruz Biotechnology,

Inc., Bergheimer Germany) diluted 1:20 for 1 h or normal rabbit serum diluted 1:20 in 0.1% BSA-PBS, (iii) rinsing of the samples three times for 5 min with 0.1% BSA-PBS, (iv) incubation for 1 h with 1:100 diluted Alexa Fluor 488 goat anti-rabbit IgG antibodies (Molecular Probes, Eugene, OR) in 0.1% BSA-PBS, and (v) rinsing of the samples twice 5 min each with 0.1% BSA-PBS and once with PBS. The stained sections were analyzed and photographed using a Zeiss LSM 700 Confocal laser scanning microscope.

### 4.2.4 Bioinformatic analysis of CARP VIII (**III**)

The CARP VIII sequences for the zebrafish (ID: ENSDARP00000057097), mouse (ID: ENSMUSP00000095891) and human (ENSP00000314407) were obtained from the database and ClustalW was used for MSA for calculating the percent identity of each aa. For *CA8* gene analysis, the transcripts were retrieved from Ensembl 2012 (zebrafish: ENSDART00000057098), (mouse: ENSMUST00000098290) and (human: ENST00000317995) and the exon structure analysis was done.

For co-evolution analysis the ITPR1 sequences used in the analysis were comprised of the region which binds to CARP VIII (Hirota et al., 2003), formed by four residues at the N-terminal and seven residues at the C-terminal region (corresponding to aa 1368–1649 in human ITPR1 isoform 1). Similarly, the CARP VIII sequences had the minimal ITPR1-binding fragment 45–291 (human numbering) and the sequences were chosen from the species which were identical for both proteins. The CARP VIII alignment had 31 sequences, while the alignment of ITPR1 included 37 due to an early duplication in the ray-finned fish lineage which has led to two co-orthologs of *ITPR1* (*itpr1 a and itpr1 b*) genes in fish genomes. A phylogenetic tree was reconstructed using the CARP VIII alignment with NJ method using fish sequence as the outgroup. Two alignments were built from the ITPR1 sequences so that the 25 tetrapod species were present in both, whereas the 12 sequences from 6 fish species were divided. The orthologs of zebrafish *itpr1a* were included in one alignment ('clade 1') and the orthologs of *itpr1b* in another alignment ('clade 2'). The two alignments of ITPR1 from the 31 species were analyzed separately for coevolution with the CARP VIII sequences. The CAPS program (Fares and McNally, 2006) (PMID: 17 005 535) was used with the MSAs and the phylogenetic tree to identify the likelihood of coevolution between sites of CARP VIII and ITPR1 proteins.

### 4.2.5 Bioinformatic analysis of CARP X and XI sequences (**IV**)

For sequence and phylogenetic analysis, 83 CARP X and 54 CARP XI sequences, and their corresponding coding regions of transcript sequences were obtained from

Ensembl. Due to the unique position of the jawless vertebrates in evolution, the two *L. japonicum* CARP X-like sequences which lacked an initiation codon (ATG) were also included in the analyses. The two sequences from *D. melanogaster* CARPs were RefSeq NM_132179 ("CARP-A") and NM_001258664 ("CARP-B") and a *cah-2* of *C. elegans* (RefSeq NM_063166.6) were used for comparison. The sequences were aligned using Clustal Omega (Sievers et al., 2011). To calculate amino acid identity percentages, the number of conserved amino acid residues in each aligned sequence pair was divided by the length of the shorter sequence. SignalP 4.1 (Petersen et al., 2011) and TargetP 1.1. (Emanuelsson et al., 2000) were used to predict signal peptides in the proteins. The default cutoff values were used in SignalP (chosen to optimize the performance), and predefined cutoffs for specificity >0.95 were used in TargetP. The C-terminal glycosylphoshpatidylinositol (GPI) anchor sites were predicted in the Pred-GPI server (Pierleoni et al., 2008) with the general model and taking "Highly probable" and "Probable" predictions (99.5% specificity cutoff) as positive. Potential N-glycosylation sites were identified by the sequence motif N – not P – S/T.

For the phylogenetic tree the 57 vertebrate CARP X/XI protein sequences were aligned with Clustal Omega and transformed into a codon-based cDNA alignment with the Pal2Nal web server (Suyama et al., 2006) with the remove gaps/internal stop codons option. MrBayes (Ronquist et al., 2012) was run to estimate a reliable set of model parameters. The tree was obtained using GTR+I (+G) model after 50,000 cycles. A 50% majority rule consensus tree was created, rooted by Archaeopteryx (Han and Zmasek, 2009) with the Drosophila sequence CARP-B (CG32698) as an outgroup. Final trees were drawn aided by the R package Ape (Paradis et al., 2004).

## 4.3 Molecular analysis of CARPs in zebrafish (**III, IV**)

### 4.3.1 Zebrafish husbandry for the knockdown experiments (**III, IV**)

The WT zebrafish of the AB strain were maintained at the zebrafish facility of the IBT. Embryos were collected from the breeder tanks and rinsed with embryonic medium (5 mM NaCl, 0.17 mM KCl, 0.33 mM $CaCl_2$, 0.33 mM $MgSO_4$ and 10–15% Methylene Blue) (Sarsted, Nümbrecht, Germany), transferred to Petri dishes and staged according to standard protocols (Kimmel et al., 1995). The embryos were kept in Petri dishes (50 embryos per dish) in embryonic medium at 28.5ºC. We used 0-5 dpf embryos for the knockdown of CARP genes using antisense MOs and hence, they did not require any ethical permission from the ethical committee. (http://www.laaninhallitus.fi/lh/etela/hankkeet/ellapro/home.nsf/pages/indexfin).

### 4.3.2 Sequencing of zebrafish CARP genes (**III, IV**)

Sequencing of *ca8, ca10a,* and *ca10b* genomic regions was performed to analyze polymorphism in the genomes. Similarly, sequencing of cDNAs of *ca8, ca10a,* and *ca10b* from zebrafish was also done using the primers presented in table 2. In a 10 µl reaction, we took 2 µl BigDye (BigDye® from Life Technologies), 2 µl sequencing buffer, 0.5 µl of 3.5 µM forward or reverse primer, 1 µl template DNA and 4.5 µl of $dH_2O$. The parameters used for PCR were: denaturation 96ºC for 10 sec, annealing at 50ºC for 5 sec and extension at 60ºC for 4 min with 25 cycles. PCR products were transferred to 1.5 ml tube containing 32 µl of $dH_2O$ and 8 µl of 95% ethanol and the DNA was precipitated by keeping the tubes at -20ºC for 30 min. The DNA was pelleted by centrifugation at 16,000 x g and washed with 70% ethanol and the DNA was sequenced.

### 4.3.3 Knockdown of CARP genes using morpholinos (**III, IV**)

Each zebrafish CARP gene was knocked down using two different antisense MOs. The antisense MOs and MOs for Tumor protein p53 **(***p53)* gene and Random Control (RC) MOs were obtained from GeneTools (Table 4) (GeneTools LLC, Philomath, OR). *ca8* gene was knocked down by MO1 which blocked the starting codon, ATG. The MO2 targeted the *ca8* gene at a splice site junction resulting in knocking down of one of the exons of *ca8* mRNA. For *ca10a* gene, we used a translational blocking MO (MO1) and a splice site blocking MO (MO2), but for *ca10b* gene both the MOs targeted two different exons. The RC-MOs were used as control MOs and *p53* MOs were used to suppress the *p53* mRNA.

The MOs were resuspended in dH2O at a 1 mM stock concentration. For the injections, the MOs were diluted to the intended concentration with 0.2 M, KCl, 1% phenol red (Sigma, Poole, UK) and 10% rhodamine B (Sigma-Aldrich) dyes were added to the diluted MOs to monitor the injection of morpholinos. We injected 1 nl of MOs into the yolk of one- to two-cell stage larvae. When p53 MO was included in the injections, the concentration of p53 MOs was one and a half times of the concentration of antisense MOs for *ca8*, *ca10a* or *ca10b*.

### 4.3.4 Analysis of CARP VIII protein and CARP mRNAs (**III, IV**)

For Western blotting (WB), morphant and WT zebrafish larvae were homogenized with a hand held pestle in a microcentrifuge tube with 50 µl of lysis buffer (50 mM Tris–HCl pH 7.4, 150 mM NaCl, 5 mM ethylene-diamine-tetra-acetic acid (EDTA), 1% NP40). The lysates were centrifuged at 10 000 x g for 5 min, 10 µl of the lysate was used per lane on a 10% sodium dodecyl sulfate (SDS) polyacrylamide gel along

with a protein marker (Bio-Rad, Hercules, CA) and ran the gel at 100 V for 10 min and then 200 V for 40 min. Separated proteins were transferred onto a polyvinylidene difluoride (PVDF) membrane (Immobilon, Millipore). CAPR VIII protein was detected by incubating the membrane with primary rabbit anti-human CARP VIII antibodies (1:50) (Santa Cruz Biotechnology) and horse radish peroxidase-conjugated goat anti-rabbit IgG (H + L) antibody. The signals were visualized using a chemiluminescence system (Western Lightning; Perkin Elmer Life Science). The total RNAs were isolated from 5 dpf WT and morphant fish, cDNA was prepared and PCR amplification was done as described above. The amplified products were separated on agarose gel and the bands were visualized and photographed.

**Table 4.** Morpholino sequences used to knock CARP genes down (**III, IV**)

| Gene | Name of morpholino | Sequence of morpholino |
|---|---|---|
| ***ca8*** | MO1-Translation blocking | 5′CGTGGAGAGAAGATTGAGTTGCCAT3′ |
| | MO2-Splice site blocking | 5′AGGATCATGCTGAAATCCAAATCTG3′ |
| ***ca10a*** | MO1-Translation blocking | 5'TGTCTTCATTCCAAGTCCATTGCGC3' |
| | MO2-Splice site blocking | 5'CATCTGTAAGGACAAGCAGAGGTTT3' |
| ***ca10b*** | MO1-Splice site blocking | 5'ACTGACCTGAAAAACACACCCAAAC3' |
| | MO2-Splice site blocking | 5'GACTGCATCTATGGAAATTCATTAT3' |
| **RC** | Control MO | 5'CCTCTTACCTCAGTTACAATTTATA3' |
| ***p53*** | *p53* MO | 5'GCGCCATTGCTTTGCAAGAATTG3' |

### 4.3.5 Live image analysis of zebrafish phenotypes (**III, IV**)

For phenotypic analysis the larvae were anesthetized using 5% Tricaine in embryo medium and embedded in 17% high molecular weight methyl cellulose on a transparent Petri dish. The behavioral studies of morphant larvae injected with antisense MOs were studied by analyzing the swim pattern of 5 dpf morphant larvae and comparing the swim pattern with the WT larvae. Morphant larvae were transferred (5 per well) into a 15×30 mm one-well Petri dish containing embryo medium and placed on a light stage with a transmitting light source. The movement of the larvae was observed for 10 min while simultaneously tracing the movements. Similarly, a 30s video of swim pattern was recorded for each group of larvae and images of 0-5 dpf larvae were taken using a Lumar (version1.12) fluorescence stereomicroscope (Carl Zeiss MicroImaging GmbH) and AxioVision software (versions 4.7 and 4.8). Each experiment was repeated a minimum of three times.

### 4.3.6 Histochemical analysis of morphant and control larvae (**III, IV**)

For histochemical analysis, 5 dpf morphant and WT zebrafish larvae were washed with PBS and fixed with 4% PFA in PBS for 3 h at room temperature. The larvae

were then transferred to 70% ethanol and stored at 4ºC. The larvae were placed on a paraffin block containing 1% low melting agarose and oriented dorsal side up before embedding in paraffin. Fixed sections of the larvae were deparaffinized in xylene, rehydrated in an alcohol series and histological staining was done with Mayer's hematoxylin and Eosin Y (Sigma-Aldrich). After dehydration, sections of the larvae were mounted with Entellan Neu™ (Merck, Darmstadt, Germany). Stained slides were examined and photographed using a Nikon Microphot microscope (Nikon Microphot-FXA, Japan).

### 4.3.7 Assay to detect apoptotic cell death in morphant fish (**III, IV**)

The morphant and WT zebrafish larvae were fixed in 4% PFA in PBS and stored in 70% ethanol. Fixed samples were then embedded in paraffin and sections of 5 μm were cut by a microtome. Terminal deoxynucleotidyl transferase dUTP nick end labeling (TUNEL) assay was performed using a QIA39 FragEL TMDNA Fragmentation Detection Kit, Fluorescent-TdT Enzyme (Merck Chemicals Ltd., Nottingham, UK). Proteinase K-treated and deparaffinized sections of larvae were incubated with TdT enzyme followed by incubation with anti-digoxigenin. Positive signals were detected by fluorescence microscopy and photographed using a Nikon Microphot microscope (Nikon Microphot-FXA, Japan). The assay was repeated twice for each zebrafish sample.

### 4.3.8 Electron microscope analysis (**III**)

Electron microscopy was used to study the ultrastructural changes in the cerebellum of *ca8* morphant fish. For electron microscopic study, the 5 dpf morphant zebrafish injected with 125 μM *ca8*-MO1 were fixed with 2% glutaraldehyde, 2% formaldehyde in 0.1 M sodium cacodylate buffer, pH 7.4 at 4ºC overnight. The rest of the procedure was carried out at the Electron Microscopy Unit, Institute of Biotechnology, University of Helsinki in collaboration with Dr. Eija Jokitalo. The samples were post-fixed with 1% reduced, buffered osmium tetroxide for 1 h at room temperature. The samples were dehydrated with a graded ethanol series and embedded into TAAB embedding resin (TAAB Ltd., UK). Semi-thin sections of the samples were cut and stained with Toluidine blue for light microscopy analysis. A suitable area was then selected for ultra-thin sectioning, and the sections were collected on pioloform-coated single-slot copper grids and post stained with uranyl acetate and lead citrate. The resulting sections were analyzed using a transmission electron microscope (Tecnai 12, FEI, Hilsboro, OR) operated at 80 kV, and images were acquired with a MultiScan 794 1K × 1K CCD camera (Gatan, Pleasanton, CA). In all comparisons, at least six larvae for each category were examined.

### 4.3.9 Cloning of human *CA10* and *CA11* genes in pcDNA3.1

Human *CA10* and *CA11* obtained from IMAGE (MGC Geneservice Ltd, Cambridge, UK) and were inserted into plasmid pcDNA3.1. The plasmid containing the inserts was cloned in One Shot® TOP10 *E. coli* cells (Invitrogen) by taking 1µl of the plasmid+25 µl competent cells and incubated on ice for 30 min. The cells were heat shocked at 42ºC for 30 sec and transferred to the ice for 2 min 125 µl of SOC medium was added to each tube and kept at 37ºC in a shaker at 225 rpm for 1 h. 20 µl of the cells were spread on (Luria-Bertani) LB agar plates and incubated at 37ºC for 16 h. The colonies were screened for the presence of inserts using the PCR conditions: denaturation at 98ºC for 2 min, 35 cycles of denaturation at 98ºC for 10 sec, annealing at 55ºC for 30 sec, extension at 72ºC for 1 min and extension at 72ºC for 10 min. Plasmid DNA was isolated from 3 ml of overnight culture using QIAprep Spin Miniprep Kit (Qiagen. Hilden, Germany)

For synthesis of capped mRNA, the plasmid was digested with KpnI and the linearized plasmid was treated with proteinase K (100-200 µg/ml) and 0.5% SDS for 30 min at 50ºC dry bath. To extract the DNA template, a mixture of phenol, chloroform and isoamyl alcohol (25:24:1) was added and vortexed for 20 sec and centrifuged at 16,000 x g for 5 min. The upper aqueous phase was carefully transferred to a fresh tube and the DNA was precipitated with 200 µl 95% ethanol at -80ºC for 1 h. The tubes were centrifuged at 4ºC for 30 min at 16,000 x g to pellet the DNA and was washed with 150 µl of 70% ethanol and centrifuged for 2 min at 4ºC at 16,000 x g. The DNA obtained as above was resuspended in 30 µl sterilized $dH_2O$. The DNA was quantitated using NanoDrop spectrophotometer.

### 4.3.10 Synthesis of mRNA and rescue of *ca10a* and *ca10b* morphants

The transcription of *CA10* and *CA11* genes was performed using mMESSAGE mMACHINE® T7 Kit from Ambion (Life technologies). A 20 µl reaction mixture (10 µl 2XNTP/CAP, 2 µl of 10X reaction buffer, 1 µg of the linear DNA template, 2 µl of enzyme mix and 5 µl of nuclease free water) was incubated at 37ºC for 1 h. After the incubation, 1 µl of TURBO DNase was added to the tube, mixed well and incubated at 37ºC for an additional 15 min. The capped RNA was recovered from the reaction mixture by adding 30 µl of Lithium Chloride (LiCl) to precipitate the RNA. The reaction mixture was chilled at -20ºC for 30 min and centrifuged at 4ºC for 15 min at 16,000 x g to pellet the RNA. The RNA pellet was washed with 1 ml of 70% ethanol and the RNA was resuspended in nuclease free $dH_2O$ and quantitated using NanoDrop spectrophotometer. For the rescue work, the embryos were divided into two groups. The first group of embryos was injected with 300 µM splice site blocking MOs and the second group co-injected with 80 pg of capped mRNA and 300 µM antisense MOs per embryo.

# 5 Results

## 5.1 Distribution and expression of CARP VIII, X and XI sequences

### 5.1.1 Distribution and evolutionary analysis of CARP sequences (**I**)

The number of CARPs has been increasing steadily with the completion of genome sequencing projects. Our bioinformatic analysis suggested that the annotation of CARPs is incomplete. The purpose of this study was to identify all the CARP sequences, evaluate their distribution across the species, and study their evolutionary relationship. We identified 84 CARP sequences from 38 organisms including 35 vertebrates and 3 invertebrates. The CARP VIII group was comprised of 33 sequences which included 3 sequences from deuterostome invertebrates. There were 31 sequences of CARP X and one of them belonged to a chordate (*B. floridae*). The 19 CARP XI sequences were found only in vertebrates (Table 1, **I)**. The sequence analysis of CARPs (Figs 1, 2, and 3, in **I**) displayed a minimum of 67% identity among the vertebrate CARP VIII sequences, while the sequence identities among the vertebrate CARP X and XI sequences were at least 70%. The invertebrate sequence identities of CARP VIII and CARP X were 40% to 45% compared with vertebrate orthologs.

The evolutionary relationship of CARPs was studied from the phylogenetic tree (Additional file 1, **I**) and the sequences in the tree showed two groups, group one included CARP VIII sequences, while the other group comprised of CARP X and XI sequences (Fig 4, **I**). Interestingly, the CARP X sequences formed three subgroups, group one comprised of the sequences from mammals, frog and lizard and the other two subgroups consisted of sequences from fish species. CARP XI sequences were derived from mammals, while CARP XI sequences from lizard and frog formed an out-group. The study suggested an independent duplication of *CA10* in the ray-finned fish lineage (actinopterygii), whereas *CA11* might have appeared from the second gene duplication after the separation of the actinopterygii and sarcopterygii lineages, or, alternatively, the duplication to *CA10* and *CA11* might have happened in early vertebrates, with a subsequent loss of *CA11* in the ray-finned fish lineage.

### 5.1.2 Expression analysis of CARPs in mouse tissues (**I**)

The studies on the tissue distribution of CARPs have been rare and produced slightly conflicting results. We studied the systematic distribution of CARPs at both mRNA and protein levels in mouse tissues. The results of RT-qPCR revealed that the *Car8* mRNA was predominantly expressed in the cerebellum and a high level of expression was also seen in the liver and lung. Low signal was also seen in the stomach, duodenum, ileum, jejunum, colon, spleen, kidney, heart, frontal cortex, parietal cortex, midbrain, and eye, and a faint signal was seen in the ovary, skeletal muscle, and the testis. *Car10* mRNA indicated strong signals in the cerebellum, frontal cortex, and parietal cortex, while midbrain and eye showed weaker expression. The expression of *Car11* mRNA was high in the frontal cortex, parietal cortex and cerebellum, and moderate expression was seen in the midbrain. A low signal for *Car11* was also seen in the colon, kidney, ovary, heart, and lung. A very faint signal for *Car11* was seen in liver, stomach, duodenum, ileum, jejunum, spleen, and eye. The expression of CARP mRNAs is summarized in table 5.

**Table 5.** Summary of the expression of CARP mRNAs in mouse tissues **(I)**

| Tissues | *Car8* | *Car10* | *Car11* |
|---|---|---|---|
| Cerebellum | +++ | +++ | ++ |
| Frontal cortex | + | ++ | +++ |
| Parietal cortex | + | ++ | +++ |
| Midbrain | + | + | + |
| Eye | + | +w | +w |
| Liver | ++ | - | - |
| Stomach | +w | - | - |
| Duodenum | + | - | - |
| Ileum | + | - | - |
| Jejunum | + | - | - |
| Colon | + | - | + |
| Pancreas | - | - | - |
| Spleen | +w | - | - |
| Kidney | + | - | + |
| Ovary | +w | - | + |
| Heart | + | - | + |
| Lung | ++ | - | +w |
| Skeletal Muscle | - | - | - |
| Testis | - | - | - |
| Uterus | - | - | - |

**Expression level:** +++ Strong, ++ Moderate, + Low, +w Very low, - No signal

The immunohistochemical analysis of CARP VIII displayed a broad expression pattern compared with the expression of CARP X and CARP XI (Figs 8, 9, 10 and 11, **I**). CARP VIII was predominantly expressed in the cerebellar PCs and cerebrum. Lower levels of expression were also seen in the liver, pancreatic Langerhans islets, submandibular gland, stomach, colon, kidney, and lung. An intense signal for CARP X was seen only in the respiratory epithelium of the lung and a faint signal for CARP

X was seen in the cerebellar capillaries and stomach. A very faint signal was detected in the heart muscle. CARP XI showed positive signals in cerebellum, cerebrum, liver, stomach, small intestine, colon, kidney, and testis. The cerebellar PCs also exhibited a prominent signal for CARP XI.

### 5.1.3 Comparative analysis of CARP VIII sequence (**II, III**)

The inactivity of CARPs has led scientists to suggest that CARPs might be involved in unknown functions by interacting with other proteins. Indeed, CARP VIII interacts with ITPR1 and is also associated with motor co-ordination function in mouse and human (Hirota et al., 2003; Jiao et al., 2005; Kaya et al., 2011; Turkmen et al., 2009). Based on the above information we performed further studies on CARP VIII to get better insights into its structure and function. The comparative analysis of hCARP VIII with hCA XIII and hCA II revealed that the CARP VIII sequence contains an additional Glu stretch at the N-terminal end up to 'WGYEE' encoded by the first exon (Fig 2, **II**). In CARP VIII, most active site residues are conserved except for His 94 and Gln 92, which are substituted by Arg117 and Glu115, respectively. Comparison of CARP VIII sequences from *S. purpuratus* showed the first exon is longer than the hCARP VIII sequence by an insertion of 18 residues, and it also suggested the absence of a Glu rich region. The Glu stretch was also found in fish and birds, but the number of Glu residues was fewer than in human sequences. The MSA of CARP VIII was done using sequences from vertebrate and invertebrate organisms, and the sequence identities were calculated from pairwise alignment (Fig 3 and Table 3, **II**). Results of the analysis indicated higher conservation of sequences among CARP VIII than among the active CAs.

Sequence conservation studies (11 CARP VIII sequences were used) of the CARP VIII structure, in comparison with hCA II, showed that a majority of the highly conserved residues in CA II are in the active site and in other structurally important sites of the protein core, while the protein surface exhibited high variability (Fig 6, **II**). Conversely, CARP VIII displayed a very high level of conservation on the surface. The structural basis of a misfolding of the CARP VIII protein with a mutation of S100P, in comparison with normal CARP VIII, showed the location of Ser 100 at the end of $\beta$ strand 6 (Fig 11, **II**). Replacement of Ser with Pro would cause a rigid bend in the peptide backbone that likely prevents β6 and/or the β6/β7 loop from assuming the conformations they have in the WT protein. The shorter and more conserved loop between strands β5 and β6 may amplify the problem in folding of the S100P mutant protein even further (**I**).

### 5.1.4 Bioinformatic analysis of zebrafish CARPs and their genes (**III, IV**)

Many human genes have orthologs in zebrafish with similar functions. We found orthologs of CARP genes in zebrafish (**I**). Therefore, we used zebrafish as a vertebrate model to get insights into the roles of CARP genes. To study the function of the CARP genes, we first used bioinformatic tools to analyze these genes and their corresponding protein products from zebrafish. For analysis of CARP VIII gene (**III**), we retrieved zebrafish, mouse and human *CA8* transcripts and their proteins from Ensembl. The *ca8* transcript was encoded by a 23.49 kb gene which is located on the forward strand of the chromosome 2 and had 9 exons, encoding 281 aa. The lengths of the mouse and human CARP VIII transcripts were above 90 kb and were located on reverse strands of chromosome 4 and 8, respectively. In zebrafish, a major portion of exon 1, part of exon 8 and entirety of exon 9 did not code for any aa, similar to the mouse and human genes (Fig 1A, **III**). The comparative analysis of zebrafish CARP VIII sequences with human and mouse CARP VIII showed a 79% overall aa identity, and the aa identity within ITPR1 binding region (aa 40-290 in human) was 85% (Fig 2A, **III**). The zebrafish CARP VIII sequence comprised 281 aa compared with mouse (291) and human (290) proteins due to absence of Glu residues at N-terminal end of zebrafish sequence. Sequencing of a zebrafish *ca8* gene revealed nucleotide changes at three places without any change in the protein (Fig S1, **III**).

CARP VIII binds to ITPR1 and takes part in the modulation of a $Ca^{2+}$ channel (Hirota et al., 2003). In the present work (**III**), we studied the functional association between ITPR1 and CARP VIII throughout the vertebrate evolution. The coevolution analysis of 31 ITPR1 sequences, (6 fish orthologs, version *itpr1a* and 25 tetrapod sequences) containing the ITPR1 region of 271 aa which interacts with CARP VIII, showed that the two proteins had several significant coevolving sites (P value of <0.001). Similar to the analysis of CARP VIII genes, we have done the analyses of CARP X and CARP XI genes. In zebrafish, the transcript for *ca10a* is encoded by a 252.67 kb gene located on the forward strand of chromosome 12 and the transcript for *ca10b* is encoded by short gene (61.86 kb) located on the forward strand of chromosome 3. The zebrafish *ca10a* and *ca10b* genes contain 9 exons similar to the human *CA10* gene and code for 328 and 326 aa, respectively.

### 5.1.5 Features of secretory proteins in CARPX-like sequences

Gene prediction analysis of CARP X and XI sequences improved 881 aa positions in incomplete sequences. Similarly, the analysis also restored 10 incomplete sequences to completeness (Table 3 and Supplementary file S1, **IV**). Sequencing of AB zebrafish strain *ca10a* and c*a10b* sequences did not indicate any change at the nucleotide level (data not presented). Zebrafish *ca10a* and *ca10b* are orthologs of *CA10 gene* (I), CARP Xa showing 90% similarity with hCARP X and CARP Xb

diverged slightly and has 75% identity with hCARP X (Table 4, **IV**). In addition to sequence percent identity, phylogenetic tree and MSA support that fish CARP Xa and Xb are closer to tetrapod CARP X than to CARP XI (Figs 1 and 2, **IV**). The transcript for *ca10a* is encoded by a 252.67 kb gene located on the forward strand of chromosome 12 and the transcript for *ca10b* is encoded by short gene (61.86 kb) located on the forward strand of chromosome 3. The zebrafish *ca10a* and *ca10b* genes contain 9 exons similar to the human *CA10* gene and code for 328 and 326 aa, respectively.

Analysis of CARP X-like sequences revealed the presence of signal peptide in 96% of sequences including the sequences from *D. melanogaster* and *C.elegans*. Interestingly, the signal peptide cleavage sites in hCARP X and XI, and zebrafish CARP Xa and Xb occur at the end of the sequences coded by the first exon in each gene (Fig 4, **IV**). All the protein sequences analyzed in the study showed conservation of three Cys residues at positions 60, 244, and 310 in hCARP X. An additional fourth Cys residue at position 296 hCARP X was conserved in all of the CARP X sequences in tetrapods, coelacanth, lamprey, and in all CARP Xa and CARP Xb, but not in CARP XI (Fig 4, **IV**). Similarly, two conserved N-glycosylation motifs were seen in CARP X-like proteins at N116 and N168 (hCARP X numbering). These positions corresponded to non-conserved surface residues, which are not part of glycosylation motif (n-not p-S/T) in any other human or zebrafish CAs, except for CARP X/XI/Xa/Xb. The third glycosylation site found in CARP XI was unique and another glycosylation site unique to CARP X/Xa/Xb (Fig 4, **IV**)

### 5.1.6 Expression analysis of CARP genes in zebrafish (**III, IV**)

We studied the expression pattern of zebrafish CARP genes in 0-5 dpf embryos and in a panel of adult zebrafish tissues to get insights into their distribution (Fig 3A, **III**). The expression analysis of *ca8* mRNA showed expression in all tissues analyzed (Table 6). The *ca8* gene was predominantly expressed in the brain and moderate levels of *ca8* mRNA were seen in the kidney, eye, gills, heart and tail. Low level of expression was seen in the testis, ovary, bowel, liver and gills. At the protein level immunohistochemistry exhibited the presence of CARP VIII in the cerebellar PCs (Fig 3C, **III**). The expression of *ca8* gene during development showed a significant signal at 0 hours post fertilization (hpf) suggesting a maternal origin. The high level of *ca8* mRNA throughout development further suggests its requirement during this phase (Supplementary Fig S3A, **III**). Similarly, we studied the expression of *itpr1a* mRNA to evaluate if the expression pattern of these genes (*ca8* and *itpr1a*) is the same. Indeed, the expression pattern suggested a significant presence of *itpr1a* mRNA at 0 hpf similar to *ca8* mRNA (Fig S3B, **III**).

Expression analysis of *ca10a* and *ca10b* in tissues revealed an intense signal for *ca10a* mRNA in brain, eye and heart. Low signal for *ca10a* was also seen in testis,

kidney, ovary, skin, spleen, swim bladder, fins, gills, intestine and muscle. No signal for *ca10a* was seen in the liver (Table 6). The *ca10b* gene was highly expressed in the ovary and high levels of *ca10b* were also seen in the brain. Positive signals for *ca10b* were also found in the swim bladder, spleen, testis and eye. Low level of *ca10b* was observed in the kidney, intestine, skin, heart, gills and fin (Table 6). The relative expression of *ca10a* and *ca10b* genes was studied during embryonic development (Fig 6A and B, **IV)**. High levels of *ca10a* were seen at 96 hpf followed by 120, 144, and 168. Low level expression for *ca10a* was seen at 72, 48, 24, 12, and 8 hpf and a very faint signal was also seen at 0 hpf and 4 hpf. These results indicate the requirement of *ca10a* expression throughout the development and especially after 72 hpf. The presence of *ca10b* at 0 hpf suggested that the *ca10b* is of maternal origin. An intense signal for *ca10b* was also seen at 72, 96, 120, 144 and 168 hpf and faint signal was observed at 12, 24 and 48 hpf (Fig 6B in **IV)**. The pattern of *ca10b* expression suggests its requirement in early embryonic development.

**Table 6.** Summary of the expression of CARP genes in zebrafish tissues (**III, IV**).

| Tissues | *ca8* | *ca10a* | *ca10b* |
|---|---|---|---|
| Brain | +++ | +++ | +++ |
| Eye | ++ | +++ | ++ |
| Heart | ++ | +++ | + |
| Muscle | +w | +w | - |
| Swim bladder | NA | + | +++ |
| Skin | + | + | + |
| Spleen | NA | + | ++ |
| Ovary | + | + | +++ |
| Intestine | + | +w | + |
| Gills | ++ | +w | +w |
| Liver | + | - | - |
| Kidney | ++ | + | + |
| Testis | NA | + | ++ |
| Fins | ++ | + | - |

Expression level: +++ Strong, ++ Moderate, + Low, +w Very low, - No signal, NA-Not analyzed

### 5.1.7 *ca8* knockdown leads to developmental defects in zebrafish (**III**)

We used two morpholinos, MO1 and MO2, to target translation of mRNA and splice site blocking (exon 4) of *ca8* gene, respectively. The RC-MOs were used as controls and *p53* MOs were used for correcting the potential off-target effects of antisense MOs. After the injection of MO1 and MO2, we studied the specificity of the MOs first by analyzing the CARP VIII protein (in case of MO1 injections) in the morphant and WT larvae by WB method. The results showed a complete absence of CARP VIII protein from 3 dpf larvae and appearance of a faint band in 5 dpf embryos which corresponded to CARP VIII protein when compared with the WB of lysates from WT embryos (Fig 4, B and C, **III**). Second, the analysis of *ca8* mRNA

from morphant embryos injected with MO2 showed a truncated mRNA in addition to a normal length mRNA (Fig D, **III**), suggesting a partial knockdown of *ca8* gene. The *CA8* morphants injected with 125 μM of MO1 exhibited abnormal changes in the head as early as 9 hpf (data not presented). The 5 dpf morphant embryos displayed a variety of defects, which included an abnormal head shape, fragile body and curved body axis, small eye size, absence of the swim bladder and otolith sacs, and pericardial edema (Fig 5A, **III**). The *ca8* morphants injected with MO2 demonstrated less severe phenotype (Fig 4 B, **III)**. The *ca8* morphant embryos injected with different concentrations of MO1 (ranging from 2 μM to 500 μM) showed a wide range of phenotypic changes from no obvious changes to severe phenotypic defects with increased mortality (Supplementary material, Fig S2 A-G and Table 2, **III**). The development of RC injected embryos and WT embryos was normal without any phenotypic defects. Similarly, co-injection of *p53* MO did not display any improvement in phenotype in 125 μM MO injected morphants.

### 5.1.8 Suppression of *ca10a* and *ca10b* genes leads to phenotypic defects (**IV**)

There are only a few reports available on *ca10a* and *ca10b* expression, these suggest that the genes are primarily expressed in CNS of mouse and human (Nishimori et al., 2003; Taniuchi et al., 2002a; Taniuchi et al., 2002b). In our study (**I**), the bioinformatics analyses of CARPs showed that the *CA10* and *CA11* genes are conserved across species and orthologs for these genes are found in zebrafish. Knockdown studies on *ca8* (**III**) encouraged us further to silence the *ca10a* and *ca10b* genes in order to get insights into their role in zebrafish. We used two antisense MOs for each *ca10a* and *ca10b* gene (Fig 7 A, B and C, **IV)**. The MO1 for *ca10a* targeted the translation of *ca10a* mRNA and the MO2 targeted the splice site junction (exon 8), resulting in the expression of a shorter length mRNA (Fig 7 D of **IV)**. The antisense MOs for *ca10b* gene (MO1 and MO2) targeted splice site junctions, resulting in the truncated *ca10b* mRNAs (Fig 7 E, **IV**). The presence of truncated mRNAs for *ca10a* and *ca10b* genes suggested that the MOs used were functional for targeting the *ca10a* and *ca10b* genes.

*ca10a* morphants injected with 200 μM of MO1 presented less severe phenotypic defects compared with the *ca10b* morphants injected with a similar concentration of MO1(Fig 8B, **IV**). The *ca10a* morphants exhibited defects in the head with abnormal body, small eye size and delayed hatching from the chorion after 1 dpf (Fig 8B, **IV**). As the development progressed, the larvae showed a long, tapering and curved tail, curved body, pericardial edema, and absence of swim bladder and otolith vesicles. Interestingly, the *ca10a* morphants injected with MO2 exhibited less severe abnormalities compared with the abnormalities produced by MO1.

The *ca10b* morphants injected with 200 μM concentration of MO1 exhibited an abnormal phenotype at 12 hpf (data not shown). After 1 dpf, the *ca10b* morphants showed a reduction in the length of the body and larvae were fragile with a high rate

of mortality (Fig 8C and Fig 9 and Table 3, **IV**). The *ca10b* morphants obtained with the injection of MO2 showed a milder phenotype compared with the phenotype obtained by MO1 injection and displayed abnormal body structure, sizes of the head and eye were smaller, mild pericardial edema, absence of otolith sacs, unutilized yolk sac and curved tail (Fig 8E, **IV**). The larvae injected with *p53* MOs did not show any difference either in phenotype or in the mortality rate (Fig 9 and Table 3, **IV**). The *ca10a* and *ca10b* morphants injected with 300 μM *ca10a* and *ca10b* MOs could be partially rescued by *hCA10* and *hCA11* mRNAs (Fig 11, **IV**).

### 5.1.9 Morphological changes and apoptosis in morphant fish (**III, IV**).

Histochemical staining revealed gross morphological changes in the cerebellum of *ca8* morphants (Fig 6 G and H, **III**) and the TUNEL assay suggested apoptotic cells in the brain (Fig 6 A, B, C and D, in **III**). Studies on ultrastructural changes using transmission electron microscopy showed increased neuronal cell death. The apoptotic changes included a condensed nucleus, fragmented mitochondrial profiles and debris of dead cells (Fig 6 E and F of **III)**. The histochemical studies on *ca10a* and *ca10b* morphants displayed gross morphological changes in the head and eye region (data not shown) compared with WT zebrafish larvae. The TUNEL assay on *ca10a* morphants indicated cells undergoing apoptosis in the head and eye regions (Fig 10 A and B, **IV**). Massive apoptosis was observed in the head and tail region of zebrafish larvae injected with *ca10b*-MOs (Fig 10 C and D, **IV**).

### 5.1.10 Abnormal swim pattern in *ca8*, *ca10a* and *ca10b* morphants (**III, IV**)

Earlier reports suggested that a mutation in the *CA8* gene is associated with gait disorder in waddle mice and ataxia in humans (Jiao et al., 2005; Kaya et al., 2011; Turkmen et al., 2009). Therefore, we studied whether the knockdown of CARP genes lead to any change in the swim pattern in the morphant embryos. For the swim pattern study, we injected the lowest concentration of antisense MOs at which no apparent phenotypic changes were seen in the morphants. In the *ca8* knockdown study (**III**), we used 5 dpf morphant embryos injected with 2 μM and 6 μM concentrations of *ca8*-MO1 which did not indicate any apparent physical deformity. Interestingly, the *ca8* morphants displayed difficulties in balancing the body with an increased turning angle compared with WT larvae (Fig 7B and movies S1-S4, supplementary material, **III)**. The swim pattern study was also carried out on *ca10a* and *ca10b* morphants injected with 50 μM MOs, which did not suggest any apparent physical deformities. The 5 dpf morphant larvae injected with *ca10a* and *ca10b* MOs exhibited clear change in the swim pattern compared with RC control larvae and WT larvae (Supplementary data, Movies 1-3, in Fig 12 and Fig 13 A-D of **IV)**.

# 6 Discussion

## 6.1 Bioinformatic and molecular analysis of CARP sequences

### 6.1.1 The CARPs are widely distributed across species (**I, IV**)

Previous studies on the occurrence of CARP sequences were limited to few species (Bellingham et al., 1998; Fujikawa-Adachi et al., 1999; Kato, 1990b; Okamoto et al., 2001). Therefore, one aim of this study was to analyze the distribution of CARP sequences in multiple species, and indeed, we identified 84 full length sequences including 22 novel sequences. Among the novel sequences, 8 sequences were previously unannotated and 14 sequences came from the partial correction of already available sequences. The CARP VIII and X sequences were found in all the available vertebrate genomes. However, CARP XI sequences were limited to mammals, frogs, lizards, and lobe-finned fish. Our bioinformatic analysis suggested that the *CA11* gene emerged through gene duplication from *CA10* either after the divergence of the fish and tetrapod lineages, or from the whole-genome duplication in early vertebrates. The *CA11* gene was not found in the two bird genomes available for study I, and not in the four bird genomes at the time of writing of this thesis, so I assume it was lost in the bird lineage. Interestingly, the fish CARP X-like sequences formed two sub-groups of their own, suggesting that they appeared by *CA10* gene duplication in the ray-finned fish lineage. The unexpected discovery of the study was the identification of CARP VIII-like sequences from deuterostomes. The finding of CARP VIII like sequences in deuterostomes suggested that these sequences might have originated after the separation of Protostomia and Deuterostomia lineages.

After the publication of the first study of this thesis (I), a CARP VIII-like protein has been reported in the pearl oyster, *Pinctada fucata* (Miyamoto, 2012), and a mollusc, i.e. a protostome. More recently, three additional CARP VIII-like protostomal sequences have been added to online databases, namely two from other molluscs (*Lottia gigantea*, giant owl limpet, UniProt V4C962_LOTGI, January 2014); and *Aplysia californica*, California sea hare, RefSeq XP_005107445.1, July 2013) and one from an annelid worm (*Capitella teleta*, a bristle worm, GenBank ELT96119.1, January 2013). Their high sequence similarity, 50% to 58% identity with human CARP VIII (compared to 30% to 34% identity with human CARP X) proves a close relationship, and all of these sequences miss one or two of the zinc-binding histidines. Therefore, I need to reject our previous hypothesis on the origin of CARP VIII in

deuterostomes, as it appears in molluscs and annelids as well. Its origin must date back to protostomes, but it remains unexplained why it is not found in arthropods or nematodes. Miyamoto suggests (Miyamoto, 2012) that the mollusc CARPs would have originated independently from deuterostome CARP VIII, but other plausible explanations might include lineage-specific gene losses or horizontal gene transfer between an early deuterostome and an ancestor of molluscs and annelids.

I have prepared a further phylogenetic tree for this thesis to illustrate the phylogenetic position of the invertebrate CARPs relative to vertebrate CARPs. As seen in figure 6 below, the genes coding for Drosophila and *C. elegans* CARPs are most similar to the CARP X/XI group of vertebrates, and need to be considered as many-to-many orthologs (co-orthologs) of *CA10* and *CA11* in human, whereas we have not discovered multiple *CA8*–like sequences in any genome yet.

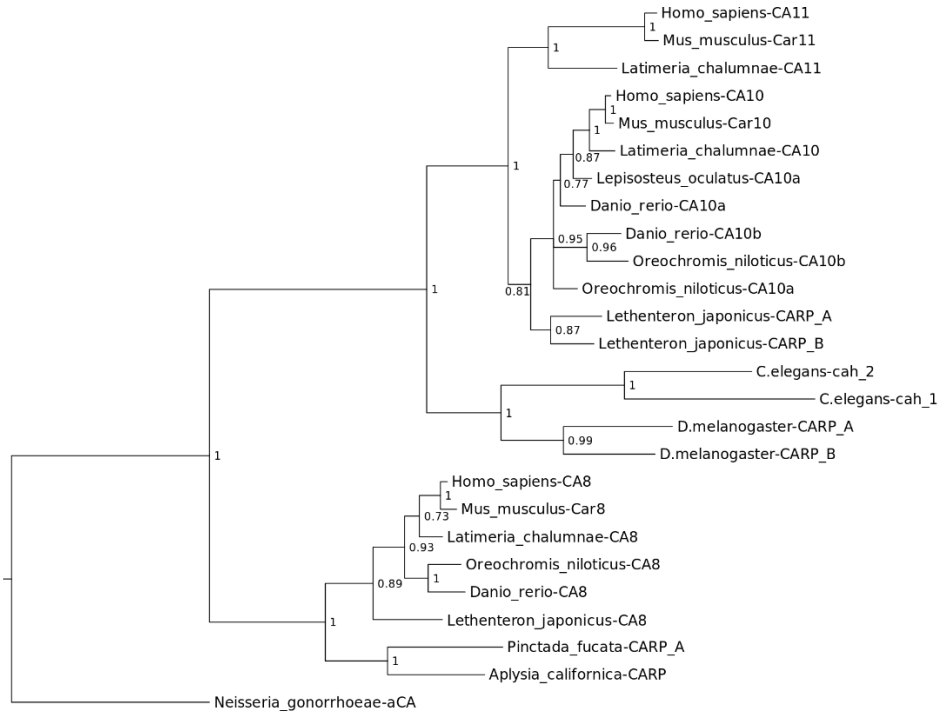


**Figure 6**. A phylogenetic tree made of the coding sequences of 26 CARP genes. Neisseria gonorrhoeae alpha CA served as an outgroup. In preparation, a protein alignment was created using Clustal Omega (Sievers et al., 2011). The amino acid positions were used as a guide from which a codon alignment was made using the Pal2Nal program (Suyama et al., 2006). Finally a phylogenetic tree based on the generalized time-Reversible (GTR) model was computed in the Mr. Bayes program (Ronquist et al., 2012). After 10 million generations the average standard deviation of split frequencies was 0.008. The numbers at the nodes represent the posterior probabilities of each node.

The ancestor of *CA8* remains an open question that awaits further study, even though *CA10*-like genes would be the obvious candidate. Despite their presence in all major groups of bilaterian animals, CARP X-like sequences are seemingly missing from some species. For example, our studies have not found them in the genomes of *Ciona intestinalis* or *Ciona savignyi*. The question whether this proves gene loss in the evolution of *Ciona* or whether these genes have escaped sequencing can only be answered when genomes with higher coverage become available.

### 6.1.2 CARPs are mainly expressed in the CNS (I)

In the past, RT-PCR and WB showed the presence of CARPs in the brain and few other tissues, often with conflicting results (Akisawa et al., 2003; Hirasawa et al., 2007; Hirota et al., 2003; Jiao et al., 2005; Taniuchi et al., 2002a). Hence, the purpose of the study (I) was to comprehensively analyze the expression pattern of the CARP genes in mouse, which is an important mammalian model organism.

Previous studies on the expression of *CA8* gene were done in several human tissues and showed that the *CA8* is mainly expressed in the brain, while additionally expressed in the lung, liver, heart, skeletal muscle and low level of expression in the kidney (Okamoto et al., 2001). In the present study, the expression of *Car8* mRNA was predominantly high in the cerebellum followed by liver and lung. Low to faint signals for *Car8* mRNA were also seen in almost all the tissues we studied. Our findings on *Car8* expression pattern agreed quite well with Okamoto´s results (Okamoto et al., 2001). In this study, immunohistochemistry showed strong signal for the presence of the CARP VIII protein in cerebellum and cerebrum which agree with the results of other previous studies (Hirota et al., 2003; Jiao et al., 2005; Lakkis et al., 1997b; Taniuchi et al., 2002a; Taniuchi et al., 2002b). Surprisingly, strong localized signals were also observed in the stomach, Fig 9 D (I) compared to the levels of mRNA in the stomach. We believe that the difference between the expression of CARP VIII protein and mRNA in the stomach might be due to the region of the stomach used for the analysis of *Car8* mRNA as the expression of CARP VIII protein is localized in the stomach. The predominant expression of CARP VIII in the brain and high level of expression in several other tissues suggesting that CARP VIII might play a physiological role in these tissues.

Earlier studies showed moderate to low levels of *CA10* mRNA in the human brain, testis, salivary glands, kidney, pancreas, liver and testis (Okamoto et al., 2001). At protein level, human cerebellar PCs displayed a weak signal for CARP X (Nishimori et al., 2003; Taniuchi et al., 2002a). In our study, the strong signal for *Car10* mRNA was seen in the cerebellum, parietal cortex and frontal cortex and a faint signal was seen in the midbrain and eye. The immunohistochemical study showed a localized signal for CARP X in the respiratory epithelium of the lung and a weak signal in the stomach and cerebral capillaries.

In the present study, CARP XI expression analyses showed a widespread distribution of *Car11* mRNA with an exceptionally high level in the frontal cortex, parietal cortex, cerebellum and midbrain. Previously, high levels of *CA11* mRNA was seen in all parts of the human brain and low levels in several other tissues, which included the kidney, liver, salivary glands, lung, skeletal muscle, pancreas and liver (Fujikawa-Adachi et al., 1999). The results of our RT-qPCR showed *Car11* mRNA in the colon, kidney, ovary, heart and lung, which is in agreement with the results of the above study. The presence of high levels of CARP XI in the human and mouse CNS suggests a role for CARP XI in mammals. In the present study, the signal for CARP XI in the mouse brain was less intense in comparison with CARP VIII staining, which agrees with the results of a previous study on the human brain (Taniuchi et al., 2002a).

### 6.1.3 Sequence and structural analysis of CARP VIII (**II**)

There are several pieces of evidence showing that CARP VIII is an important protein in various species: First, our results showed that CARP VIII is highly conserved across the species, which can be considered one sign for an evolutionally important role (**I**). Second, interaction of CARP VIII with ITPR1, a $Ca^{2+}$ channel protein is well known (Hirota et al., 2003). Third, defects in the CARP VIII gene lead to ataxia in mouse and human (Jiao et al., 2005; Kaya et al., 2011; Turkmen et al., 2009). The crystal structure of CARP VIII has been resolved and the basis of its inactivity has been reported (Picaud et al., 2009). Based on the above information, we have analyzed CARP VIII at structural level to get some novel insights into its possible functions (**II, III**).

Comparative analysis of human CARP VIII (hCARP VIII) sequence with hCAs (hCAII, and hCA XIII) showed the presence of Glu stretch at N-terminal region of CARP VIII. The analysis also revealed the conservation of aa residues at the active site except His94 and Gln92, which were replaced by Arg117 and Glu115 in CARP VIII respectively. The Glu residues which are encoded by GAG repeats are found in all the mammalian CARP VIII proteins. It is well known that the expansion mutation in trinucleotide repeats lead to neurodegenerative disorders in humans (Plassart and Fontaine, 1994). It is speculated that the expansion mutation of GAG repeats in *CA8* gene might lead to neurological disorders in humans. Similarly, it has been reported that the transcriptional activators GAL4, GCN4, and Herpesvirus VP16 contain a glutamic acid-rich region (Melcher, 2000; Tavernarakis and Thireos, 1995; Triezenberg et al., 1988). Therefore, the presence of a glutamic acid stretch in CARP VIII may be involved in the regulation of transcription (Miyaji et al., 2003) (**II**). Analysis of conserved residues in hCARP VIII compared with hCAII from a number of species showed a very high conservation of residues on the surface CARP VIII. The conservation of residues on the surface of protein suggests that these residues might be involved in the interaction with other proteins.

A homozygous missense mutation in the *CA8* gene, resulting in substitution of Ser 100 by a Pro residue, was found in members of Iraqi family (Turkmen et al., 2009). The affected members of the family exhibited a quadrupedal gait with mild mental retardation. The *in-vitro* studies showed that the S100P aa change caused proteasomal mediated degradation of CARP VIII protein due to misfolding which lead to decreased levels of CARP VIII protein. This is a common mechanism for loss of function mutations associated with human disease (Wang and Moult, 2001). We studied the structural basis of misfolding in the S100P mutant protein showing the location of Ser 100 at the end of β strand β6. The substitution of Ser with Pro causes a rigid bend in the peptide backbone and thus preventing the β6 and or the β6/ β7 loop from assuming the confirmation similar to WT protein. The misfolding of CARP VIII would then lead to the proteasomal mediated degradation of the protein in the members of Iraqi family with a mutation in *CA8* gene.

### 6.1.4 Zebrafish CARP VIII and ITPR1 sequences are coevolved (**III**)

CARP VIII and ITPR1 are co-expressed in the cerebellar PCs and are known to interact with each other (Hirota et al., 2003). The coevolution (a change in the gene product of one gene reflects a change in the gene product of another gene to retain the functional interaction) analysis of 31 vertebrate CARP VIII and ITPR1 sequences, which included 6 ITPR1a/ ITPR1b sequences from fish, showed a strong correlation with ITPR1a suggesting that ITPR1a and CARP VIII evolved together. The measurement of *itpr1a* and *ca8* mRNAs indicated a similar expression pattern during the embryonic development, supporting the co-evolution of both genes and their functional association. In our study, the abnormal development of zebrafish larvae might be due to knockdown of *ca8* gene leading to an improper modulation of ITPR1 function in $Ca^{2+}$ signaling. Similarly, gait disorder and ataxia in mouse and human with a mutation in *Car8* or *CA8* gene may be due to improper interaction of CARP VIII with ITPR1. The mutations in ITPR1 gene also lead to ataxia in mice and SCA 15 in humans (van de Leemput et al., 2007).

### 6.1.5 The *ca8* morphants displayed abnormal swim pattern (**III**)

CARP VIII is abundantly expressed in the human and mouse brain (Hirota et al., 2003; Jiao et al., 2005; Taniuchi et al., 2002a; Taniuchi et al., 2002b). Studies in the past showed that a spontaneously occurring mutation in *CA8* gene leads to ataxia and mental retardation in humans (Kaya et al., 2011; Turkmen et al., 2009). However, no studies on the role of CARP VIII during embryonic development are available.

The genes involved in the neurodegenerative disorders play a crucial role in the development of the brain early in embryogenesis and the molecular basis of brain development is similar in all the vertebrates. Lately, zebrafish has emerged as an

attractive model to study development in vertebrates, due to easy tractability and common biological relevance (Carradice and Lieschke, 2008; Lohi et al., 2013).

In this study, we knocked down the *ca8* gene to understand its consequences on the zebrafish brain at the ultrastructural level and behavioral consequences in morphant zebrafish. Zebrafish CARP VIII sequence analysis showed 84% similarity with hCARP VIII sequence in the core domain. Developmental expression analysis of *ca8* gene indicated the presence of a high level of *ca8* mRNA at 0 hpf, suggesting that the mRNA is of maternal origin and is required very early in development. Few reports are available on the developmental expression of the CARP VIII gene in mouse and human (Lakkis et al., 1997a; Taniuchi et al., 2002a; Taniuchi et al., 2002b). In one study, the expression of *Car8* mRNA was studied by *in-situ* hybridization in mouse, which showed a positive signal at 9.5 days of gestation, while the expression data before 9.5 days of gestation was not available (Lakkis et al., 1997a). In the second study, the developmental expression of *Car8* was investigated starting at 7 days of gestation until 17 days after fertilization (Taniuchi et al., 2002b). The RT-PCR and NB analyses suggested slightly conflicting results with positive signals at 11 and 15 days of gestation respectively. Similarly, the developmental expression studies in human showed *CA8* expression at 84 days of gestation with some discrepant findings between the results of NB and immunohistochemistry (Taniuchi et al., 2002a). The reinvestigation of CARP VIII gene expression is needed in another mammalian model to get a better picture of CARP VIII gene expression during development.

The expression pattern of zebrafish *ca8* gene was studied using RT-qPCR in a panel of adult zebrafish tissues. Predominantly, expression of the *ca8* gene was seen in the brain, with moderate to low levels of expression in several other tissues (**III**). At the protein level, expression of CARP VIII was seen in cerebellar PCs (**III**). The expression pattern of the *ca8* gene in this study is fairly similar to the expression pattern in mouse (**I**) and human (Taniuchi et al., 2002a). The expression pattern of CARP VIII gene in the zebrafish brain – similar to mouse and human - further indicated a possible role for *CA8* in vertebrates.

The presence of similarities between the zebrafish, mouse, and human CARP VIII gene at both sequence and expression levels prompted us to silence the *ca8* gene in zebrafish larvae to study if we could observe a phenotype similar to mouse and human patients with a defect in the CARP VIII gene. The morphant zebrafish injected with *CA8*-MOs (125 μM) exhibited several phenotypic defects (**I**). The injections of two different sets of MOs resulted in the similar phenotypic defects in the morphant embryos and injection of control MOs showed phenotypes similar to WT embryos. The injection of *p53* MOs could not improve the defective phenotype of the morphant embryos, suggesting the phenotype obtained was due to the knockdown effect of MOs. The efficacy of the translation blocking MOs was further confirmed by a WB of lysates from 3 dpf embryos and analyzing the length of *ca8* mRNA in MO2 morphant zebrafish.

Previous studies of the cerebellum of *wdl* mice showed defects in the morphology of the synapse, suggesting a critical role for CARP VIII in formation and/or maintenance of synapse and its excitatory function in the cerebellum (Hirasawa et al., 2007). Another study showed a loss in the cerebellar volume proportional to the age in members of Saudi family (Kaya et al., 2011). In the present study, *ca8* morphant fish exhibited abnormal development of the head at 1 dpf stage, the time point at which differentiation of neurons occurs. Histological studies on 5 dpf morphant fish revealed gross morphological changes in the cerebellar region. In addition, TUNEL assay indicated apoptosis of neurons in the cerebellum and electron microscopy also showed increased neuronal cell death. The changes observed in the cerebellum of 5 dpf morphant zebrafish may be similar to the changes found in the cerebellum of human patients (Kaya et al., 2011). In the present study, we found that an increase in the concentration of c*a8*-MOs lead to more severe phenotype in the morphant fish. More importantly, the morphant fish injected with lower concentration of *ca8*-MOs, with a phenotypic appearance similar to the WT fish, displayed abnormal swim pattern. Taken together, the *ca8* morphant fish mimicked the phenotype observed in *wdl* mouse and human patients who had a mutation in *CA8* gene (Jiao et al., 2005; Kaya et al., 2011; Turkmen et al., 2009).

Taken together, our studies suggest that down regulation of CARP VIII expression might disturb the $Ca^{2+}$ ion channel in the endoplasmic reticulum by increasing the sensitivity of $IP_3$ to ITPR1 in the absence of CARP VIII protein. Thus releasing large amount of $Ca^{2+}$ from intracellular reserves activating and deactivating many genes including the genes involved in apoptotic pathway leading to neuronal cell death and ataxia in the present study and human patients and mouse with a mutation in CARP VIII gene. Indeed, analysis of expression profile of genes from the mouse with a spontaneous mutation in CARP VIII gene showed dysregulation of many genes which play important roles in the brain

### 6.1.6 Zebrafish *ca10a* and *ca10b* genes are widely expressed (**IV**)

Similar to CARP VIII, the sequences of CARP X and XI are highly conserved across species. Unlike CARP VIII, very few reports are available on CARP X and CARP XI, which makes these two proteins even more attractive research targets. First, we performed bioinformatic analysis on CARP Xa and CARP Xb sequences to understand their evolutionary relationship and conservation.

In the past, some studies suggested the presence of signal peptides in CARP X and CARP XI (Bellingham et al., 1998; Fujikawa-Adachi et al., 1999; Okamoto et al., 2001), and later on another study suggested cytoplasmic localization for CARP X and CARP XI based on the results of phylogeny and histochemical staining (Taniuchi et al., 2002b). To resolve the earlier contradictory findings we used bioinformatic tools to look at the features, such as disulfides and N-glycosylation motifs that have functional significance in secreted proteins. Our sequence analysis

revealed the presence of a signal peptide in all the CARP X and XI sequences we analyzed (Fig 4, **IV**). Similarly, the sequence analyses revealed a pair of cysteines in the same location where all the active extracellular CA isoforms have a disulfide bridge. In addition, we found two conserved N-glycosylation motifs in all the sequences analyzed in the study (Fig 4, **IV**). The above finding of our study strongly suggests that the CARP Xa and Xb sequences and their vertebrate and invertebrate orthologs are secretory proteins.

Expression analysis suggested that the *ca10a* and *ca10b* mRNAs are present throughout the development of zebrafish. The highest level of *ca10a* mRNA was found after 96 hpf. The presence of high levels *ca10b* mRNA at 0 hpf suggested that it is of maternal origin. Similarly, the presence of a high level of *ca10b* mRNA between 48 hpf and 168 hpf suggests a possible role in the development of zebrafish. In the past, developmental expression studies of CARP X and CARP XI genes were done in mouse whole embryos and in the human fetal brain (Taniuchi et al., 2002a; Taniuchi et al., 2002b). In mouse embryos, the expression of *Car10* and *Car11* genes was studied only at four different stages of development (E7, E11, E15 and E17). The presence of the *Car10* gene was observed in the middle of gestation (E15) and *Car11* appeared early in the development (Taniuchi et al., 2002b). In the human fetal brain, expression of CARP X and CARP XI was studied using immunohistochemistry at five different stages of development (Taniuchi et al., 2002a). In this study too, the signal for CARP X appeared late during the development (121$^{st}$ day of gestation) compared with the signal for CARP XI, which appeared at 84$^{th}$ and 95$^{th}$ day of gestation. The results of these studies are in agreement with the results of the present study in the zebrafish model.

Previous studies showed that the CARP X and CARP XI genes are predominantly expressed in the human and mouse CNS (Bellingham et al., 1998; Okamoto et al., 2001; Taniuchi et al., 2002a; Taniuchi et al., 2002b). In the present study, the expression pattern of *ca10a* and *ca10b* genes in adult zebrafish tissues showed that the *ca10a* gene is predominantly expressed in the brain and also exhibited high level of *ca10b* gene in the brain. Thus these results agree well with the results of above studies. Surprisingly, the highest level of *ca10b* signal was detected in the zebrafish ovary, which is in contrast with the expression pattern in human and mouse. Interestingly, *D. melanogaster* contains two CARP sequences. CARP A, which is similar to CARP X, is expressed in the brain and CARP B, which is similar to CARP XI, is predominantly expressed in the reproductive tissues followed by CNS (Ortutay et al., 2010, Tolvanen et al unpublished results). Similarly, *C. elegans* contains two copies of CARP X like genes known as *cah-1* and *cah-2* which are expressed in several types of neurons (Spencer et al., 2011). Taken together, the results of the expression patterns of *ca10a* and *ca10b* genes suggest that these genes may play an important but yet unknown roles for these genes in the brain.

### 6.1.7 Ataxia and apoptosis in *ca10a* and *ca10b* morphants (**IV**)

Recent study showed an upregulation of CARP XI and altered localization in cultured neuronal cells expressing the mutant ataxin 3 (Hsieh et al., 2013). Further analysis of expression of CARP XI in SCA 3 and in MJD mouse revealed results similar to neuronal cells expressing mutant ataxin 3. It was suggested that CARP XI might interact with ITPR1 and control the release of $Ca^{2+}$ similar to CARP VIII (Chen et al., 2008; Hsieh et al., 2013). Taken together, the results of the present study suggest that the *ca10a* and *ca10b* genes are required for the normal development of the brain during embryogenesis and the suppression of these genes lead to ataxic phenotype in the zebrafish. However, more studies are needed to understand the precise function of the CARP X and CARP XI proteins.

# 7 Summary and future directions

In the present work, I have studied the distribution and phylogenesis of CARP VIII, CARP X, and CARP XI sequences from all the available databases and studied the expression of all the three CARPs both at the gene and protein levels in mouse. I also studied the functional role of CARP VIII, CARP X and CARP XI proteins in zebrafish using antisense morpholinos to silence the *ca8*, *ca10a* and *ca10b* genes.

Bioinformatic analysis showed a very high conservation of CARP VIII, X and XI sequences across the species studied. The study revealed unusually high similarity within CARP VIII and X groups, even between invertebrate and vertebrate sequences. The high conservation of CARPs suggests conserved functions across the vertebrate species. Results of the phylogenetic analysis further revealed that duplication of *CA10* gene followed different paths in the fish and tetrapod lineages. The expression analyses of *CARP* genes suggested that the *Car8* gene is expressed in a wide variety of tissues in the mouse with a predominantly high level of expression in the cerebellum. The strongest expression of *Car10* and *Car11* genes was seen in the CNS. The expression patterns of CARP genes suggest that these proteins may be involved in the development of the nervous system and nerve system functions, such as motor coordination. In addition, they may have still unknown physiological roles in other tissues.

In zebrafish, CARP VIII was expressed in the brain and in several other tissues, which is similar to the expression pattern in mouse and human tissues. The presence of *CA8* gene product in 0 hpf embryos suggested that the gene is of maternal origin. Knockdown of the *CA8* gene led to abnormal swim pattern in morphant fish with a reduction in cerebellar volume. The morphant zebrafish displayed ataxic movement similar to *wdl* mice and human patients. The study provides evidence that CARP VIII is required in early development in zebrafish, especially for the normal development of the brain.

Studies carried out on CARP X and CARP XI proteins showed that they are highly expressed in the CNS of the zebrafish. Data on the developmental expression pattern of *ca10a* and *ca10b* genes in zebrafish are novel and suggest important but unknown roles for these genes in embryonic development. This is the first study to demonstrate that silencing of *ca10a* or *ca10b* gene leads to abnormal embryonic development. Knockdown of *ca10a* and *ca10b* genes results in an abnormal swim pattern in the morphant zebrafish and suggests that these genes might regulate motor coordination. Further experiments are needed to precisely define the role of CARP X and CARP XI proteins in mammals.

It is well established that the CARP VIII is predominantly expressed in cerebellar Purkinje cells in human, mouse and zebrafish and it also interacts with ITPR1 receptor in these cells. Association of CARP VIII with motor coordination function and in neurodevelopmental disorder has been demonstrated in human and mouse. The association of CARP VIII has been also studied in human cancers and cancer cell lines. However, the precise role of CARP VIII still remains elusive. The progress made so far on CARP VIII research will be helpful to design future course of research to define the precise role of CARP VIII both in motor coordination function and human cancers. In fact, in our laboratory work is in progress in cultured cells and in human cancers to study the mechanism by which CARP VIII exerts its functions in both cancers and in neurodevelopmental disorder.

Studies done in the past showed that similar to CARP VIII expression CARP X and CARP XI are also predominantly expressed in the CNS. In the present study the experiments in zebrafish showed that the CARP X and CARP XI play a crucial role during embryonic development and play a role in motor coordination function. However, unlike CARP VIII very little is known about their mode of action and their precise roles. The research so far showed that the CARPs function by interacting with other proteins. It will be interesting to find binding partners for CARP X and CARP XI using different molecular techniques. More information and better insights into the role of CARP X and CARP XI can be obtained by knocking down *Car10* and *Car11* genes individually (single knockout) and together (double knockout) in a mouse model. The *CA10* gene is known to contain CCG repeats and any expansion mutation in these repeats might lead to a neurodegenerative disease in humans. It will be interesting to do the large scale screening of the patients with unknown neurological disorders for the expansion mutations in *CA10* gene. To get better insights into the biological role of CAPR X and CARP XI in human cancers we plan to use cell culture techniques and analyze human cancer tissues.

# Acknowledgements

This research was carried out at the Institute of Biomedical Technology (IBT), now BioMediTech and Department of Anatomy, School of Medicine, University of Tampere, Finland in the years 2010-14.

I am deeply indebted to my supervisors, Prof. Mauno Vihinen, PhD., and Prof Seppo Parkkila, MD., PhD. To Prof. Mauno, for accepting me for master's study in his department and giving me an opportunity to study bioinformatics. Perhaps most importantly, I am thankful for him sharing his enthusiasm for research, further encouraging me, accepting me as a PhD candidate, for his positive feedback, and for giving me help throughout the program, without which this thesis would not have been possible.

I will always be grateful to Prof. Seppo Parkkila first, for providing me a position in his group and then giving all the freedom I could ever ask for, and showing faith in me. I consider myself privileged to work in his group and it was a real turning point in my research carrier. Biological research has always been close to my heart and working with Seppo made me enjoy biological research more than ever. I thank him for investing in me, and making sure no opportunity for a challenge, competition, scholarship, presentation/poster, or conference passed by. Beyond science, you have mentored my growth as a person throughout these years, and have encouraged me to never fall short of my dreams. That is a tremendous gift, and I owe you infinite gratitude. I am grateful for his guidance and encouragement during these years, as well as his patience and flexibility as I struggled to combine work and family life successfully.

I express my sincere thanks to Assoc. Prof. Martti Tolvanen PhD, Bioinformatics Unit, University of Tampere and presently at University of Turku. Martti is my teacher, colleague and friend and introduced me to research these fascinating proteins, CARPs. Without Martti's contribution to the CARP project, my thesis would be incomplete. His endless discussions, be it one to one or in the group meetings, and his practical guidance on the thesis project, were of immense value. His collaboration in the research projects, including CARPs, have produced several high impact factor publications apart from my PhD thesis. His patience and generosity be it in research or outside of research, has taught me many things that will go a long way in life. If I had a problem, however big or small, if I turned to Martti for help, he would help me every single time. Apart from research, I enjoyed my time with him on numerous occasions. Be it in Tampere, or in conferences such as Florence, Italy and Antalya, Turkey, just sipping beer, watching movies in theater, having food (we both enjoy all kinds of foods in the world), and it was a

pleasure cooking and sharing Indian food with Martti. Thank you very much Martti for your kindness and help, which made all these years enjoyable and the memories will always remain with me.

Sometimes you become friends with someone and feel that you have always known that person. It was so nice to meet Harlan Barker (M.Sc. Bioinformatics) through peer-tutoring when he came from the US in 2011 for a bioinformatics program at the University of Tampere. Later, it was a great pleasure to have him sitting in the same office next to me as a colleague. Indeed, I owe many thanks to Harlan for his help in many things in and outside of research. It was great fun to discuss many topics ranging from research to as wide as politics, movies and life. We had great time together in the lab chatting, meeting over food and beer, watching movies in the theater thanks for that. His contribution to my PhD thesis as a co-author and his invaluable help with the English language corrections in the PhD thesis manuscripts are greatly appreciated.

I wish to thank my thesis committee members, Docent Dr. Csaba Ortutay, PhD, Bioinformatics group, University of Tampere and Prof. Heikki Kainulainen MD, PhD, Department of Biology of Physical Activity University of Jyväskylä for their timely assessment and annual reports for TGPBB. I would also like to thank Dr. Ortutay for his collaboration with the PhD thesis project and for the bioinformatic analysis work that lead to many good publications together.

I would like to acknowledge the director of the Institute of Biomedical Technology and the Director of BioMediTech, Dr. Hannu Hanhijärvi, DDS, Ph.D., for providing me the research facilities for this study. My thanks are also due to the administrative staff of the institute and Medical School, especially, Riitta Aallos, Marjatta Viilo, Jaana Anttila-Salmensivu, Merja Koivula, Östring Anne-Marja, Mira Pihlström, I express my gratitude to Sari Luokkala, the computer administrator B-building, for all the help with my computers during the course of my research which was so invaluable. I am grateful to Jukka Lehtiniemi for the help with movement pattern videos for research articles, and for my information at IBT web page. My special thanks are also due to Dr. Henna Mattila, PhD, and the Tampere Graduate Program in Biomedicine and Biotechnology (TGPBB), for supporting me and for the courses that were of immense help to me to grow as a researcher in particular, and as a person in general, and for the financial support for attending the international conferences. I would also like to thank Docent Vesa Hytönen, PhD for his help with experiments and for the discussions related to my research and my PhD project and his guidance. Dr. Hytönen's enthusiastic attitude towards science and his endless thirst for knowledge have been very inspiring and encouraging. I greatly appreciate and thank Prof. Abdul Waheed, PhD, Saint Louis University School of Medicine, USA, for the discussion and guidance on my thesis project and for sharing his wisdom and enthusiasm in several conference meetings and during his visits to School of Medicine, Tampere. I am thankful to Dr. Jarko Valjakka and Janette Hinkka from FinMedi1 for their kindness and all the help every time I went to their office if I needed anything. I want to express my deepest

gratitude to all my colleagues at IMT and to thank the former and current attendants for always being so helpful and keeping things running.

The official reviewers of my thesis, Prof. Todd Alexander, MD, PhD, FRCP, Associate Professor, University of Alberta, Canada and Prof. Matti Airaksinen, MD, PhD, Professor of Neuroscience, University of Helsinki, Finland are warmly thanked for their constructive criticism and feedback that lead to an improvement in the quality of my thesis. It is an honor to have Prof. Erik Pettersen, University of Oslo, Norway as the opponent of my thesis and I am grateful to him for accepting the invitation.

I would like to thank my collaborators and co-authors, without their contribution, this thesis would not have been completed. Most of my thesis work is based on functional studies of CARPs using morpholino (MO) knockdown technology in a zebrafish model. I am grateful to Prof. Mika Rämet MD, PhD, Experimental Immunology group, BioMediTech, Unversity of Tampere, for the collaboration with knockdown experiments in zebrafish that produced some wonderful results and manuscripts. I thank Prof. Rämet for extending me all the help and freedom I needed throughout the work. I appreciate the critical review of the manuscripts, input, and the discussions that were of immense help for the thesis and for me personally. I am grateful to Dr. Mataleena Parikka, DDE, PhD, for teaching and helping me with basics of zebrafish experiments, MO injections, handling and manipulation of zebrafish embryos, and for being there for me every time I needed her help and for her critical comments and review of the manuscripts. I appreciate and thank Sanna-Kaisa E. Harjula, M.Sc., for her immense help especially during the MO injections and also with using the microscope and taking the swim pattern videos. I greatly appreciate the help of Leena Makinen for doing morpholino injections for knockdown of CARP genes and arranging the embryos and adult fish for my experiments within one day of request. I would thank Hannaleena Piipo for all the arrangements and help with zebrafish embryos and with MO knockdown experiments during the research. I thank Matilda Martikainen and Kaisa Oksanen for technical assistance during the MO knockdown experiments. I would also like to thank Docent Hannu Turpeinen, PhD for the help and discussion regarding the rescue of morphant fish. Thanks are also due to Annemari Uusimäki for her technical help and for the cDNAs from zebrafish adult tissues. I appreciate Dr. Kaisa Teittinen, PhD for the help with pDNA3.1 for the synthesis of CARP mRNA for the experiments. I would like to thank Dr. Eija Jokitalo PhD, Electron Microscopy Unit, Institute of Biotechnology, University of Helsinki for her collaboration with ca8 morphants electron microscope studies, which produced wonderful results and lead to a good publication.

I consider myself lucky to have wonderful colleagues and friends in the laboratory and at the IBT. It was pleasure working with Dr. Peiwen Pan PhD, Marianne Kuuslahti, Aulikki Lehmus, Dr. Leo Syrjänen MD, Dr. Heini Kallio, PhD, Maarit Patrikainen M.Sc, and Reza Zolfaghari Emameh M.Sc, Saku Peltari, Prajwol Manandhar, Lydia Isokangas and Rawnak Jahan Hoque. I would especially like to

thank Leo and Heini for their friendship and help in the lab with the experimental work that were of immense help during my initial days in the CA group. In the later part of my graduate program, it was great pleasure to work with Maarit on CA related projects. Together we have produced a lot of important scientific data that is in the process of publication in high impact factor journals. My special thanks go to Peiwen for her friendship and the wonderful time we had in the lab, be it doing experiments or discussion about research. Apart from research, I appreciate her help and guidance in my personal life and several get togethers we had with Dr. Yuemei Fan, PhD for Chinese and Indian food and long discussions about life and other things in general, but also for the many interesting discussions we've had in appreciation of our different cultures and languages thank you Yuemei and Peiwen. Marianne has my appreciation and deserves a huge thanks for all the technical help and assistance with the experiments and discussions, without which my thesis would be incomplete. My special thanks are also due to Aulikki Lehmus for all the help in the lab and her expert technical assistance and guidance in the laboratory and for your kindness. I would like to thank Dr. Pasi Pennanen, PhD for his help from time to time in the department and invaluable help with qPCR calculations every single time I needed. It was indeed a pleasure to work alongside with Dr. Heimo Syvälä, PhD, Sami Purmonen, M.Sc, Prof. Teemu Ylikomi, MD, PhD, Ninni Ikkonen, Arja Ahola, and Ilka Mäkinen. I would like to thank Arja specially for giving me day-to-day help in the department whenever I needed it and it was always a pleasure talking to her, who is ever smiling and enthusiastic and who would always lift my mood. My thanks also go to the past CA group members Alejandra, Mikä, and Fatemeh.

I am thankful to my friends, especially FCA. Naveen Raj from India for being with me in all the situations, Dr. Peter Carvalho PhD (Org Chem) from Germany for being a great buddy and helping me with many things and spending endless hours talking about research and life in the GCH Hostel, Mumbai, India that helped me learn many things and my thanks to Dr. Hormudz Mulla PhD (Org Chem), Arizona University, Head R&D at Sudarshan Chemicals Limited's Pigments Pune, India for the friendship. I do not have words to express my gratitude to Prof. Iqbal Hamza PhD, Dept. of Animal & Avian Sciences, University of Maryland, USA, your friendship and association had a great influence on me ever since we became friends at The Institute of Science, Mumbai and it will always have the same effect. Thanks for teaching me the things that nobody would teach and one cannot learn at schools, I am indebted to you for the same.

I would like to thank my friends and colleagues in Tampere, especially the late Ayodeji Olatubosun, Gabriel Teku, Mesue Kolle, Sreevani Kotha and Rishi Mohanta for being with me when I needed them and helping me academically as well as personally and making my stay in Tampere pleasant. My special thanks go to Chandrasekhar Challagonda and Vijender Reddy for their generous help in the initial period of my stay in Tampere and for their friendship. My sincere thanks go to our family friends Imre and Daniela Balog for their friendship and for their generosity and for being there for us for any help we need.

This study was financially supported by the Fimlabs Research Fund, the Pirkanmaa District Hospital, Medical Research Fund of Tampere University Hospital, The Sigrid Juselius Foundation, Academy of Finland, Tampere University Foundation, the Scientific Foundation of the City of Tampere, and Jane and Aatos Erkko Foundation.

I thank my late parents for the love and support and for inculcating good values in me without which I would never have reached where I am today. I am grateful to Amma, Bapu and Akkalu, Geetha and Srilatha and their families for giving me unconditional love and support, which means a lot to me. I thank my girlfriend Sanji, for being there for me and for her love and support, which will always mean a lot to me and I thank my son Atharva, whom I love very much, for being my source of strength and inspiration and my son Shiv who is a source of joy and motivation and to both my sons for providing a reason to live my life. Indeed, I am grateful to the God for giving me strength to carry through the difficult times and for being kind to me.

Tampere, October 2014

Ashok Aspatwar

# References


Akisawa, Y., Nishimori, I., Taniuchi, K., Okamoto, N., Takeuchi, T., Sonobe, H., Ohtsuki, Y., and Onishi, S. (2003). Expression of carbonic anhydrase-related protein CA-RP VIII in non-small cell lung cancer. Virchows Arch *442*, 66-70.

Altschul, S.F., Madden, T.L., Schaffer, A.A., Zhang, J., Zhang, Z., Miller, W., and Lipman, D.J. (1997). Gapped BLAST and PSI-BLAST: a new generation of protein database search programs. Nucleic Acids Res *25*, 3389-3402.

Andersen, J.N., Jansen, P.G., Echwald, S.M., Mortensen, O.H., Fukada, T., Del Vecchio, R., Tonks, N.K., and Moller, N.P. (2004). A genomic perspective on protein tyrosine phosphatases: gene structure, pseudogenes, and genetic disease linkage. FASEB J *18*, 8-30.

Barnea, G., Silvennoinen, O., Shaanan, B., Honegger, A.M., Canoll, P.D., D'Eustachio, P., Morse, B., Levy, J.B., Laforgia, S., Huebner, K.*, et al.* (1993). Identification of a carbonic anhydrase-like domain in the extracellular region of RPTP gamma defines a new subfamily of receptor tyrosine phosphatases. Mol Cell Biol *13*, 1497-1506.

Bataller, L., Sabater, L., Saiz, A., Serra, C., Claramonte, B., and Graus, F. (2004). Carbonic anhydrase-related protein VIII: autoantigen in paraneoplastic cerebellar degeneration. Ann Neurol *56*, 575-579.

Behravan, G., Jonsson, B.H., and Lindskog, S. (1991). Fine tuning of the catalytic properties of human carbonic anhydrase II. Effects of varying active-site residue 200. Eur J Biochem *195*, 393-396.

Bellingham, J., Gregory-Evans, K., and Gregory-Evans, C.Y. (1998). Sequence and tissue expression of a novel human carbonic anhydrase-related protein, CARP-2, mapping to chromosome 19q13.3. Biochem Biophys Res Commun *253*, 364-367.

Birney, E., Clamp, M., and Durbin, R. (2004). GeneWise and Genomewise. Genome Res *14*, 988-995.

Bosanac, I., Alattia, J.R., Mal, T.K., Chan, J., Talarico, S., Tong, F.K., Tong, K.I., Yoshikawa, F., Furuichi, T., Iwai, M.*, et al.* (2002). Structure of the inositol 1,4,5-trisphosphate receptor binding core in complex with its ligand. Nature *420*, 696-700.

Carradice, D., and Lieschke, G.J. (2008). Zebrafish in hematology: sushi or science? Blood *111*, 3331-3342.

Chen, X., Tang, T.S., Tu, H., Nelson, O., Pook, M., Hammer, R., Nukina, N., and Bezprozvanny, I. (2008). Deranged calcium signaling and neurodegeneration in spinocerebellar ataxia type 3. J Neurosci *28*, 12713-12724.

Elleby, B., Sjoblom, B., and Lindskog, S. (1999). Changing the efficiency and specificity of the esterase activity of human carbonic anhydrase II by site-specific mutagenesis. Eur J Biochem *262*, 516-521.

Elleby, B., Sjoblom, B., Tu, C., Silverman, D.N., and Lindskog, S. (2000). Enhancement of catalytic efficiency by the combination of site-specific mutations in a carbonic anhydrase-related protein. Eur J Biochem *267*, 5908-5915.

Emanuelsson, O., Nielsen, H., Brunak, S., and von Heijne, G. (2000). Predicting subcellular localization of proteins based on their N-terminal amino acid sequence. J Mol Biol *300*, 1005-1016.
Fares, M.A., and McNally, D. (2006). CAPS: coevolution analysis using protein sequences. Bioinformatics *22*, 2821-2822.
Fujikawa-Adachi, K., Nishimori, I., Taguchi, T., Yuri, K., and Onishi, S. (1999). cDNA sequence, mRNA expression, and chromosomal localization of human carbonic anhydrase-related protein, CA-RP XI. Biochimica et biophysica acta *1431*, 518-524.
Gavrieli, Y., Sherman, Y., and Ben-Sasson, S.A. (1992). Identification of programmed cell death in situ via specific labeling of nuclear DNA fragmentation. J Cell Biol *119*, 493-501.
Han, M.V., and Zmasek, C.M. (2009). PhyloXML: XML for evolutionary biology and comparative genomics. BMC Bioinformatics *10*, 356.
Hewett-Emmett, D., 2000. Evolution and distribution of the carbonic anhydrase gene families. In: Chegwidden, W.R., Carter, N.D., Edwards, Y.H. (Eds.), Evolution and distribution of the carbonic anhydrase gene families. The Carbonic Anhydrases: New Horizons. Birkhauser Verlag, Boston, pp. 29–76.
Hewett-Emmett, D., and Tashian, R.E. (1996). Functional diversity, conservation, and convergence in the evolution of the a-, b-, and g-carbonic anhydrase gene families. Mol Phylogenet Evol *5*, 50-77.
Higgins, D.G., Thompson, J.D., and Gibson, T.J. (1996). Using CLUSTAL for multiple sequence alignments. Methods Enzymol *266*, 383-402.
Hirasawa, M., Xu, X., Trask, R.B., Maddatu, T.P., Johnson, B.A., Naggert, J.K., Nishina, P.M., and Ikeda, A. (2007). Carbonic anhydrase related protein 8 mutation results in aberrant synaptic morphology and excitatory synaptic function in the cerebellum. Mol Cell Neurosci *35*, 161-170.
Hirota, J., Ando, H., Hamada, K., and Mikoshiba, K. (2003). Carbonic anhydrase-related protein is a novel binding protein for inositol 1,4,5-trisphosphate receptor type 1. Biochem J *372*, 435-441.
Hsieh, M., Chang, W.H., Hsu, C.F., Nishimori, I., Kuo, C.L., and Minakuchi, T. (2013). Altered expression of carbonic anhydrase-related protein XI in neuronal cells expressing mutant ataxin-3. Cerebellum *12*:338–349
Ishihara, T., Takeuchi, T., Nishimori, I., Adachi, Y., Minakuchi, T., Fujita, J., Sonobe, H., Ohtsuki, Y., and Onishi, S. (2006). Carbonic anhydrase-related protein VIII increases invasiveness of non-small cell lung adenocarcinoma. Virchows Arch *448*, 830-837.
Jiao, Y., Yan, J., Zhao, Y., Donahue, L.R., Beamer, W.G., Li, X., Roe, B.A., Ledoux, M.S., and Gu, W. (2005). Carbonic anhydrase-related protein VIII deficiency is associated with a distinctive lifelong gait disorder in waddles mice. Genetics *171*, 1239-1246.
Kastury, K., Ohta, M., Lasota, J., Moir, D., Dorman, T., LaForgia, S., Druck, T., and Huebner, K. (1996). Structure of the human receptor tyrosine phosphatase gamma gene (PTPRG) and relation to the familial RCC t(3;8) chromosome translocation. Genomics *32*, 225-235.
Kato, K. (1990a). A Collection of cDNA Clones with Specific Expression Patterns in Mouse Brain. Eur J Neurosci *2*, 704-711.
Kato, K. (1990b). Sequence of a novel carbonic anhydrase-related polypeptide and its exclusive presence in Purkinje cells. FEBS Lett *271*, 137-140.
Kawaguchi, Y., Okamoto, T., Taniwaki, M., Aizawa, M., Inoue, M., Katayama, S., Kawakami, H., Nakamura, S., Nishimura, M., Akiguchi, I.*, et al.* (1994). CAG expansions in a novel gene for Machado-Joseph disease at chromosome 14q32.1. Nat Genet *8*, 221-228.

Kaya, N., Aldhalaan, H., Al-Younes, B., Colak, D., Shuaib, T., Al-Mohaileb, F., Al-Sugair, A., Nester, M., Al-Yamani, S., Al-Bakheet, A., *et al.* (2011). Phenotypical spectrum of cerebellar ataxia associated with a novel mutation in the CA8 gene, encoding carbonic anhydrase (CA) VIII. Am J Med Genet B Neuropsychiatr Genet *156*, 826-834.
Kent, W.J. (2002). BLAT--the BLAST-like alignment tool. Genome Res *12*, 656-664.
Kent, W.J., Sugnet, C.W., Furey, T.S., Roskin, K.M., Pringle, T.H., Zahler, A.M., and Haussler, D. (2002). The human genome browser at UCSC. Genome Res *12*, 996-1006.
Kiefer, L.L., Paterno, S.A. and Fierke, C.A. (1995). Hydrogen bond network in the metal binding site of carbonic anhydrase enhances zinc affinity and catalytic efficiency. J. Am. Chem.Soc *117*, 6831-45837.
Kilpinen, S., Autio, R., Ojala, K., Iljin, K., Bucher, E., Sara, H., Pisto, T., Saarela, M., Skotheim, R.I., Bjorkman, M., *et al.* (2008). Systematic bioinformatic analysis of expression levels of 17,330 human genes across 9,783 samples from 175 types of healthy and pathological tissues. Genome Biol *9*, R139.
Kim, D.S., Ross, S.E., Trimarchi, J.M., Aach, J., Greenberg, M.E., and Cepko, C.L. (2008). Identification of molecular markers of bipolar cells in the murine retina. The Journal of comparative neurology *507*, 1795-1810.
Kimmel, C.B., Ballard, W.W., Kimmel, S.R., Ullmann, B., and Schilling, T.F. (1995). Stages of embryonic development of the zebrafish. Developmental dynamics : an official publication of the American Association of Anatomists *203*, 253-310.
Kleiderlein, J.J., Nisson, P.E., Jessee, J., Li, W.B., Becker, K.G., Derby, M.L., Ross, C.A., and Margolis, R.L. (1998). CCG repeats in cDNAs from human brain. Hum Genet *103*, 666-673.
LaForgia, S., Morse, B., Levy, J., Barnea, G., *et al.* (1991). Receptor protein-tyrosine phosphatase gamma is a candidate tumor suppressor gene at human chromosome region 3p21. Proc Natl Acad Sci U S A *88*, 5036-5040.
Lakkis, M.M., Bergenhem, N.C., O'Shea, K.S., and Tashian, R.E. (1997a). Expression of the acatalytic carbonic anhydrase VIII gene, Car8, during mouse embryonic development. Histochem J *29*, 135-141.
Lakkis, M.M., O'Shea, K.S., and Tashian, R.E. (1997b). Differential expression of the carbonic anhydrase genes for CA VII (Car7) and CA-RP VIII (Car8) in mouse brain. J Histochem Cytochem *45*, 657-662.
Lamprianou, S., Vacaresse, N., Suzuki, Y., Meziane, H., Buxbaum, J.D., Schlessinger, J., and Harroch, S. (2006). Receptor protein tyrosine phosphatase gamma is a marker for pyramidal cells and sensory neurons in the nervous system and is not necessary for normal development. Mol Cell Biol *26*, 5106-5119.
Larkin, M.A., Blackshields, G., Brown, N.P., Chenna, R., McGettigan, P.A., McWilliam, H., Valentin, F., Wallace, I.M., Wilm, A., Lopez, R., *et al.* (2007). Clustal W and Clustal X version 2.0. Bioinformatics *23*, 2947-2948.
Levy, J.B., Canoll, P.D., Silvennoinen, O., Barnea, G., Morse, B., Honegger, A.M., Huang, J.T., Cannizzaro, L.A., Park, S.H., Druck, T., *et al.* (1993). The cloning of a receptor-type protein tyrosine phosphatase expressed in the central nervous system. J Biol Chem *268*, 10573-10581.
Lohi, O., Parikka, M., and Ramet, M. (2013). The zebrafish as a model for paediatric diseases. Acta paediatrica *102*, 104-110.
Lovejoy, D.A., Hewett-Emmett, D., Porter, C.A., Cepoi, D., Sheffield, A., Vale, W.W., and Tashian, R.E. (1998). Evolutionarily conserved, "acatalytic" carbonic anhydrase-related protein XI contains a sequence motif present in the neuropeptide sauvagine: the human CA-

RP XI gene (CA11) is embedded between the secretor gene cluster and the DBP gene at 19q13.3. Genomics *54*, 484-493.
Lu, S.H., Takeuchi, T., Fujita, J., Ishida, T., Akisawa, Y., Nishimori, I., Kohsaki, T., Onishi, S., Sonobe, H., and Ohtsuki, Y. (2004). Effect of carbonic anhydrase-related protein VIII expression on lung adenocarcinoma cell growth. Lung Cancer *44*, 273-280.
Lukacs, G.L., and Verkman, A.S. (2012). CFTR: folding, misfolding and correcting the DeltaF508 conformational defect. Trends Mol Med *18*, 81-91.
Maa, J.S., Rodriguez, J.F., and Esteban, M. (1990). Structural and functional characterization of a cell surface binding protein of vaccinia virus. J Biol Chem *265*, 1569-1577.
Melcher, K. (2000). The strength of acidic activation domains correlates with their affinity for both transcriptional and non-transcriptional proteins. J Mol Biol *301*, 1097-1112.
Mikoshiba, K. (2007). IP3 receptor/Ca2+ channel: from discovery to new signaling concepts. J Neurochem *102*, 1426-1446.
Mikoshiba, K., Okano, H., Miyawaki, A., Furuichi, T., and Ikenaka, K. (1995). Molecular genetic analyses of myelin deficiency and cerebellar ataxia. Prog Brain Res *105*, 23-41.
Miyaji E, Nishimori I, Taniuchi K, Takeuchi T, Ohtsuki Y, and Onishi, S. (2003). Overexpression of carbonic anhydrase-related protein VIII in human colorectal cancer. J Pathol. *201*, 37-45.
Miyaji, E., Nishimori, I., Taniuchi, K., Takeuchi, T., Ohtsuki, Y., and Onishi, S. (2003). Overexpression of carbonic anhydrase-related protein VIII in human colorectal cancer. J Pathol *201*, 37-45.
Miyamoto, H. (2012). Sequence of the pearl oyster carbonic anhydrase-related protein and its evolutionary implications. Biochem Genet *50*, 269-276.
Mori, S., Kou, I., Sato, H., Emi, M., Ito, H., Hosoi, T., and Ikegawa, S. (2009). Nucleotide variations in genes encoding carbonic anhydrase 8 and 10 associated with femoral bone mineral density in Japanese female with osteoporosis. J Bone Miner Metab *27*, 213-216.
Morimoto, K., Nishimori, I., Takeuchi, T., Kohsaki, T., Okamoto, N., Taguchi, T., Yunoki, S., Watanabe, R., Ohtsuki, Y., and Onishi, S. (2005). Overexpression of carbonic anhydrase-related protein XI promotes proliferation and invasion of gastrointestinal stromal tumors. Virchows Arch *447*, 66-73.
Nicholas, K.B., Nicholas H.B. Jr., and Deerfield, D.W. II (1997). GeneDoc: Analysis and Visualization of Genetic Variation,. EMBNEW.NEWS *4:14*.
Nishikata, M., Nishimori, I., Taniuchi, K., Takeuchi, T., Minakuchi, T., Kohsaki, T., Adachi, Y., Ohtsuki, Y., and Onishi, S. (2007). Carbonic anhydrase-related protein VIII promotes colon cancer cell growth. Mol Carcinog *46*, 208-214.
Nishimori, I., Takeuchi, T., Morimoto, K., Taniuchi, K., Okamoto, N., and Onishi, S. (2003). Expression of carbonic anhydrase-related protein VIII, X and XI in the enteric autonomic nervous system. Biomed Res *14*, 70–74.
Nishimori, I., Vullo, D., Minakuchi, T., Scozzafava, A., Capasso, C., and Supuran, C.T. (2013). Restoring catalytic activity to the human carbonic anhydrase (CA) related proteins VIII, X and XI affords isoforms with high catalytic efficiency and susceptibility to anion inhibition. Bioorg Med Chem Lett *23*, 256-260.
Nogradi, A., Jonsson, N., Walker, R., Caddy, K., Carter, N., and Kelly, C. (1997). Carbonic anhydrase II and carbonic anhydrase-related protein in the cerebellar cortex of normal and lurcher mice. Brain Res Dev Brain Res *98*, 91-101.
Ohradanova, A., Vullo, D., Kopacek, J., Temperini, C., Betakova, T., Pastorekova, S., Pastorek, J., and Supuran, C.T. (2007). Reconstitution of carbonic anhydrase activity of the cell-surface-binding protein of vaccinia virus. Biochem J *407*, 61-67.

Okamoto, N., Fujikawa-Adachi, K., Nishimori, I., Taniuchi, K., and Onishi, S. (2001). cDNA sequence of human carbonic anhydrase-related protein, CA-RP X: mRNA expressions of CA-RP X and XI in human brain. Biochimica et biophysica acta *1518*, 311-316.
Ortutay C, Olatubosun A, Parkkila S, Vihinen M, Tolvanen M. (2010). An Evolutionary Analysis of Insect Carbonic Anhydrases. In Advances in Medicine and Biology Volume 7. Volume 7. Edited by Berhardt LV. New York: Nova Science Pub Inc;. 145-168.
Paradis, E., Claude, J., and Strimmer, K. (2004). APE: Analyses of Phylogenetics and Evolution in R language. Bioinformatics *20*, 289-290.
Peles, E., Nativ, M., Campbell, P.L., Sakurai, T., Martinez, R., Lev, S., Clary, D.O., Schilling, J., Barnea, G., Plowman, G.D.*, et al.* (1995). The carbonic anhydrase domain of receptor tyrosine phosphatase beta is a functional ligand for the axonal cell recognition molecule contactin. Cell *82*, 251-260.
Petersen, T.N., Brunak, S., von Heijne, G., and Nielsen, H. (2011). SignalP 4.0: discriminating signal peptides from transmembrane regions. Nat Methods *8*, 785-786.
Pfaffl, M.W. (2001). A new mathematical model for relative quantification in real-time RT-PCR. Nucleic Acids Res *29*, e45.
Picaud, S.S., Muniz, J.R., Kramm, A., Pilka, E.S., Kochan, G., Oppermann, U., and Yue, W.W. (2009). Crystal structure of human carbonic anhydrase-related protein VIII reveals the basis for catalytic silencing. Proteins *76*, 507-511.
Pierleoni, A., Martelli, P.L., and Casadio, R. (2008). PredGPI: a GPI-anchor predictor. BMC Bioinformatics *9*, 392.
Plassart, E., and Fontaine, B. (1994). Genes with triplet repeats: a new class of mutations causing neurological diseases. Biomed Pharmacother *48*, 191-197.
Pruitt, K.D., Tatusova, T., and Maglott, D.R. (2007). NCBI reference sequences (RefSeq): a curated non-redundant sequence database of genomes, transcripts and proteins. Nucleic Acids Res *35*, D61-65.
Puthussery, T., Gayet-Primo, J., and Taylor, W.R. (2011). Carbonic anhydrase-related protein VIII is expressed in rod bipolar cells and alters signaling at the rod bipolar to AII-amacrine cell synapse in the mammalian retina. Eur J Neurosci *34*, 1419-1431.
Ronquist, F., Teslenko, M., van der Mark, P., Ayres, D.L., Darling, A., Hohna, S., Larget, B., Liu, L., Suchard, M.A., and Huelsenbeck, J.P. (2012). MrBayes 3.2: efficient Bayesian phylogenetic inference and model choice across a large model space. Syst Biol *61*, 539-542.
Sievers, F., Wilm, A., Dineen, D., Gibson, T.J., Karplus, K., Li, W., Lopez, R., McWilliam, H., Remmert, M., Soding, J.*, et al.* (2011). Fast, scalable generation of high-quality protein multiple sequence alignments using Clustal Omega. Mol Syst Biol *7*, 539.
Sjoblom, B., Elleby, B., Wallgren, K., Jonsson, B.H., and Lindskog, S. (1996). Two point mutations convert a catalytically inactive carbonic anhydrase-related protein (CARP) to an active enzyme. FEBS Lett *398*, 322-325.
Skaggs, L.A., Bergenhem, N.C., Venta, P.J., and Tashian, R.E. (1993). The deduced amino acid sequence of human carbonic anhydrase-related protein (CARP) is 98% identical to the mouse homologue. Gene *126*, 291-292.
Sly, W.S., and Hu, P.Y. (1995). Human carbonic anhydrases and carbonic anhydrase deficiencies. Annu Rev Biochem *64*, 375-401.
Spencer, W.C., Zeller, G., Watson, J.D., Henz, S.R., Watkins, K.L., McWhirter, R.D., Petersen, S., Sreedharan, V.T., Widmer, C., Jo, J.*, et al.* (2011). A spatial and temporal map of C. elegans gene expression. Genome Res *21*, 325-341.
Supuran, C., Scozzafava A, and Conway, J, ed. (2004). Carbonic Anhydrase: Its Inhibitors and Activators (Washington, D.C.: CRC PR E S S).

Supuran, C.T. (2008). Carbonic anhydrases: novel therapeutic applications for inhibitors and activators. Nat Rev Drug Discov *7*, 168-181.
Suyama, M., Torrents, D., and Bork, P. (2006). PAL2NAL: robust conversion of protein sequence alignments into the corresponding codon alignments. Nucleic Acids Res *34*, W609-612.
Tamura, K., Dudley, J., Nei, M., and Kumar, S. (2007). MEGA4: Molecular Evolutionary Genetics Analysis (MEGA) software version 4.0. Mol Biol Evol *24*, 1596-1599.
Taniuchi, K., Nishimori, I., Takeuchi, T., Fujikawa-Adachi, K., Ohtsuki, Y., and Onishi, S. (2002a). Developmental expression of carbonic anhydrase-related proteins VIII, X, and XI in the human brain. Neuroscience *112*, 93-99.
Taniuchi, K., Nishimori, I., Takeuchi, T., Ohtsuki, Y., and Onishi, S. (2002b). cDNA cloning and developmental expression of murine carbonic anhydrase-related proteins VIII, X, and XI. Brain Res Mol Brain Res *109*, 207-215.
Tashian, R.E. (1989). The carbonic anhydrases: widening perspectives on their evolution, expression and function. Bioessays *10*, 186-192.
Tashian, R.E.; Hewett-Emmett, D.; Carter, N.D. and Bergenhem, N.C.H. (2000). Carbonic anhydrase (CA)-related proteins (CA-RPs) and transmembrane proteins with CA or CA-RP domains. In: Chegwidden, W.R.; Carter, N.D. & Edwards, Y.H. (Eds.), Carbonic anhydrase (CA)-related proteins (CA-RPs) and transmembrane proteins with CA or CA-RP domains. The Carbonic Anhydases: New Horizons. Birkhauser, Basel, pp. 105–120.
Tavernarakis, N., and Thireos, G. (1995). Transcriptional interference caused by GCN4 overexpression reveals multiple interactions mediating transcriptional activation. Mol Gen Genet *247*, 571-578.
Tolvanen, M.E., Ortutay, C., Barker, H.R., Aspatwar, A., Patrikainen, M., and Parkkila, S. (2013). Analysis of evolution of carbonic anhydrases IV and XV reveals a rich history of gene duplications and a new group of isozymes. Bioorg Med Chem *21*, 1503-1510.
Triezenberg, S.J., Kingsbury, R.C., and McKnight, S.L. (1988). Functional dissection of VP16, the trans-activator of herpes simplex virus immediate early gene expression. Genes Dev *2*, 718-729.
Turkmen, S., Guo, G., Garshasbi, M., Hoffmann, K., Alshalah, A.J., Mischung, C., Kuss, A., Humphrey, N., Mundlos, S., and Robinson, P.N. (2009). CA8 mutations cause a novel syndrome characterized by ataxia and mild mental retardation with predisposition to quadrupedal gait. PLoS Genet *5*, e1000487.
van de Leemput, J., Chandran, J., Knight, M.A., Holtzclaw, L.A., Scholz, S., Cookson, M.R., Houlden, H., Gwinn-Hardy, K., Fung, H.C., Lin, X.*, et al.* (2007). Deletion at ITPR1 underlies ataxia in mice and spinocerebellar ataxia 15 in humans. PLoS Genet *3*, e108.
Wang, Z., & Moult, J. (2001). SNPs, protein structure, and disease. Hum Mutat *17*, 263-270.
Wen, F.C., Li, Y.H., Tsai, H.F., Lin, C.H., Li, C., Liu, C.S., Lii, C.K., Nukina, N., and Hsieh, M. (2003). Down-regulation of heat shock protein 27 in neuronal cells and non-neuronal cells expressing mutant ataxin-3. FEBS Lett *546*, 307-314.
Wu, C., Orozco, C., Boyer, J., Leglise, M., Goodale, J., Batalov, S., Hodge, C.L., Haase, J., Janes, J., Huss, J.W., 3rd*, et al.* (2009). BioGPS: an extensible and customizable portal for querying and organizing gene annotation resources. Genome Biol *10*, R130.
Yan, J., Jiao, Y., Jiao, F., Stuart, J., *et al.* (2007). Effects of carbonic anhydrase VIII deficiency on cerebellar gene expression profiles in the wdl mouse. Neurosci Lett *413*, 196-201.
Yoon , C.H. (1959). Waddler, a new mutation, and its interaction with quivering. J Hered *50*, 238-244.

# Original communications

BMC Molecular Biology

RESEARCH ARTICLE Open Access

# Phylogeny and expression of carbonic anhydrase-related proteins

Ashok Aspatwar*[1,2,3], Martti EE Tolvanen[1] and Seppo Parkkila[2,3]

## Abstract

**Background:** Carbonic anhydrases (CAs) are found in many organisms, in which they contribute to several important biological processes. The vertebrate α-CA family consists of 16 subfamilies, three of which (VIII, X and XI) consist of acatalytic proteins. These are named carbonic anhydrase related proteins (CARPs), and their inactivity is due to absence of one or more Zn-binding histidine residues. In this study, we analyzed and evaluated the distribution of genes encoding CARPs in different organisms using bioinformatic methods, and studied their expression in mouse tissues using immunohistochemistry and real-time quantitative PCR.

**Results:** We collected 84 sequences, of which 22 came from novel or improved gene models which we created from genome data. The distribution of CARP VIII covers vertebrates and deuterostomes, and CARP X appears to be universal in the animal kingdom. *CA10*-like genes have had a separate history of duplications in the tetrapod and fish lineages. Our phylogenetic analysis showed that duplication of *CA10* into *CA11* has occurred only in tetrapods (found in mammals, frogs, and lizards), whereas an independent duplication of *CA10* was found in fishes. We suggest the name *CA10b* for the second fish isoform. Immunohistochemical analysis showed a high expression level of CARP VIII in the mouse cerebellum, cerebrum, and also moderate expression in the lung, liver, salivary gland, and stomach. These results also demonstrated low expression in the colon, kidney, and Langerhans islets. CARP X was moderately expressed in the cerebral capillaries and the lung and very weakly in the stomach and heart. Positive signals for CARP XI were observed in the cerebellum, cerebrum, liver, stomach, small intestine, colon, kidney, and testis. In addition, the results of real-time quantitative PCR confirmed a wide distribution for the *Car8* and *Car11* mRNAs, whereas the expression of the *Car10* mRNA was restricted to the frontal cortex, parietal cortex, cerebellum, midbrain, and eye.

**Conclusions:** CARP sequences have been strongly conserved between different species, and all three CARPs show high expression in the mouse brain and CARP VIII is also expressed in several other tissues. These findings suggest an important functional role for these proteins in mammals.

## Background

Carbonic anhydrases (CAs), EC 4.2.1.1, are metal-containing enzymes that occur abundantly in nature and are found in almost all organisms that have been studied [1]. CAs are fundamental to many biological processes, such as photosynthesis, respiration, renal tubular acidification, and bone resorption [2-5]. These enzymes are encoded by five distinct and evolutionarily unrelated gene families known as α, β, γ, δ, and ζ CAs [6]. Interestingly, there is no sequence similarity between these different families. Thus, the CA families are excellent examples of the convergent evolution of catalytic function. The animal kingdom CAs belong to a single gene family known as α-CAs that contain zinc as a metal ion in the active site. The main chemical reaction catalyzed by CAs involves the reversible hydration of $CO_2$ ($CO_2$+$H_2O$ ($HCO_3^-$+$H^+$).

In mammals, α-CAs are characterized by 16 different isoforms, 13 of which (CA I, II, III, IV, VA, VB, VI, VII, IX, XII, XIII, XIV, and XV) are enzymatically active, whereas the other 3, namely, the CA-related proteins (CARPs) VIII, X, and XI, appear to lack CA activity because of substitutions to 1 or more of the 3 functionally important histidine residues [3,7,8]. In addition, the receptor-type protein tyrosine phosphatases β and γ (RPTP β, RPTP γ) also contain 'CA-like' domains [3,9]. The 13 active CA isozymes differ in their subcellular

* Correspondence: ashok.aspatwar@uta.fi
[1] Bioinformatics Group, Institute of Medical Technology, 33014 University of Tampere, Tampere, Finland
Full list of author information is available at the end of the article

localizations such that CAs I, II, III, VII, and XIII are all cytosolic enzymes, CAs IV, IX, XII, XIV, and XV are all membrane-associated enzymes, CAs VA and VB are mitochondrial, and CA VI is a secreted protein.

Previous studies on the distribution of CARPs using either western blot analysis or RT-PCR methods have shown a wide expression profile in all parts of the brain in both humans and mice [10-13]. Notably, immunohistochemical studies on CARPs have been mainly focused on brain tissues. The results have shown predominant expression of CARP VIII in the mouse and human cerebellum, especially in the Purkinje cells. Studies on CARP X and XI have revealed a lower level of expression in the cerebellum [14-16]. Previous investigations using reverse transcription polymerase chain reaction (RT-PCR), northern blot analysis, western blot assays or dot blots have reported restricted expression of all CARPs in some mouse and human tissues including the brain [13,17]. The presence of CARPs in the human and mouse brain has suggested important roles for these proteins in the brain development and/or neural functions [12,16]. Interestingly, CARP VIII and XI may also be involved in cancer development in the gastrointestinal tract and lungs [13,18-21].

The pivotal physiological function of CARP VIII became clearly evident in recently published reports on CARP VIII mutations in both human and mouse. A study of waddle mice characterized by a spontaneous mutation in the *Car8* gene showed ataxia and a distinctive lifelong gait disorder [22]. Another recent study described mild mental retardation, quadrupedal gait and ataxia in members of an Iraqi family who each possessed a defect in the *CA8* gene [23]. These studies clearly indicated that CARP VIII plays an important role in motor coordination.

The three-dimensional structure of CARP VIII has been recently solved [24], as the only protein in the CARP subfamily. The structural basis of catalytic inactivity is confirmed in this study, but currently there is no interpretation to correlate the structure to any function.

The CARP sequences are well conserved throughout all vertebrates, suggesting that CARPs may play biologically important roles in higher organisms. The number of members in the CARP families has increased with the completion of vertebrate genome sequencing projects, but many sequences have been annotated in incomplete or even partly incorrect forms. To date there are no systematic studies on the distribution and phylogenetic analysis of CARP genes across species nor does there exist any parallel study on the distribution of all three CARP proteins and their mRNA levels in mouse tissues. Therefore, we first used bioinformatic methods to identify and evaluate the distribution of CARP genes across different species. We subsequently performed sequence and phylogenetic analysis of CARPs VIII, X, and XI, focusing on vertebrates, and studied the distribution of the three CARP mRNAs using real-time quantitative PCR (qPCR) and the corresponding proteins using immunohistochemistry in different mouse tissues.

## Results

### Bioinformatic survey and comparison of CARP sequences

Detailed information and database sources from which sequences were obtained are shown in Table 1. In total, 84 full-length sequences were obtained from 38 organisms (3 invertebrates and 35 vertebrates). Thirty-three gene sequences encoding for CARP VIII were identified, of which 3 sequences were from deuterostome invertebrates, namely, *Branchiostoma floridae*, *Trichoplax adhaerens*, and *Strongylocentrotus purpuratus*, and 30 were from vertebrates. We identified 31 sequences of CARP X and 19 sequences of CARP XI in these vertebrates, which included a single CARP X gene from a chordate (*Branchiostoma floridae*). CARP X-like sequences in invertebrates were discovered in both protostomes and deuterostomes. A detailed analysis of invertebrate CARP X homologs will be reported elsewhere. Multiple sequence alignments (MSAs) of the CARP VIII, X, and XI protein sequences are presented in Figures 1, 2, and 3, respectively.

Among vertebrate sequences, the protein sequence identities ranged from 67% to 100% for CARP VIII, from 70% to 100% for CARP X and from 70% to 100% for CARP XI. The 100% values were observed between primate sequences. However, even between humans and mice, identities of CARP orthologs were 98%, 100%, and 96% for CARP VIII, X, and XI, respectively. When the invertebrate CARP VIII and CARP X sequences used in this study were compared to their vertebrate orthologs, the sequence identities were only 40% to 45%. For comparison, in case of enzymatically active CAs, protein sequence identity between human and mouse are 94%, 93%, 92%, and 91% for CAs VII, Vb, III, and XIII, respectively, and 50% to 83% for other pairs of isozymes. Thus, sequence conservation was found to be higher in all CARPs than in any of the active CAs.

### Phylogenetic analysis

The phylogenetic tree of the CARP protein sequences is shown in Figure 4. The full MSA from which the tree was calculated is provided as Additional file 1. The tree shows two distinct sequence pools, including one pool for CARP VIII and the other pool for CARPs X and XI. The CARP VIII pool subscribes to the expected animal taxonomy, except for mammals, which are not resolved due to sequence identities near 100%. The second sequence pool is comprised of the CARP X and CARP XI sequences. CARP X forms three subgroups, including the large subgroup consisting of sequences from mammals, frogs, and

**Table 1: Details of the carbonic anhydrase-related protein (CARP) sequences used in this study**

| Group | Organism | Scientific Name | CARPs | Acc. No./ID | Length (aa) | Description1 |
|---|---|---|---|---|---|---|
| | Cow | *Bos taurus* | VIII | NP_001077159 | 290 | NCBI_RefSeq |
| | | | X | A0JN41 | 328 | Uniprot |
| | | | XI | NP_783648.1 | 328 | NCBI_RefSeq |
| | Marmoset | *Callithrix jacchus* | VIII | - | 290 | UCSC_BLAT |
| | | | X | - | 328 | UCSC_BLAT |
| | | | XI | A6MLD1 | 321 | Uniprot _UCSC_BLAT |
| | Dog | *Canis familiaris* | VIII | XP_544094.2 | 290 | NCBI_RefSeq |
| | | | X | XP_866307.1 | 328 | Ensembl_UCSC_BLAT |
| | | | XI | XP_852031.1 | 328 | NCBI_RefSeq |
| | Guinea Pig | *Cavia porcellus* | VIII | ENSCPOP00000017966 | 256 | Ensembl |
| | | | X | ENSCPOP00000013970 | 328 | Ensembl |
| | | | XI | ENSCPOP00000011461 | 332 | Ensembl |
| | Armadillo | *Dasypus novemcinctus* | X | ENSDNOP00000008341 | 327 | Ensembl |
| | Horse | *Equus caballus* | VIII | XP_001496523.1 | 290 | NCBI_RefSeq |
| | | | X | XP_001503286.2 | 328 | NCBI_RefSeq |
| | | | XI | ENSECAP00000015876 | 278 | Ensembl |
| | Cat | Felis catus | X | ENSFCAP00000002102 | 326 | Ensembl_UCSC_BLAT |
| | | | XI | ENSFCAP00000006798 | 265 | Ensembl |
| | Human | *Homo sapiens* | VIII | P35219 | 290 | Uniprot |
| | | | X | Q9NS85 | 328 | Uniprot |
| | | | XI | O75493 | 328 | Uniprot |
| | Mouse | *Mus musculus* | VIII | P28651 | 291 | Uniprot |
| | | | X | P61215 | 328 | Uniprot |
| | | | XI | O70354 | 328 | Uniprot |
| | Macaque | *Macaca mulatta* | VIII | XP_001088977.1 | 290 | NCBI_RefSeq |
| | | | X | XP_001101492.1 | 334 | NCBI_RefSeq |
| | | | XI | XP_001113730.1 | 328 | RefSeq_UCSC_BLAT |
| | Rhesus Monkey | *Macaca fascicularis* | X | Q9N085 | 328 | Uniprot |
| | Mouse Lemur | *Microcebus murinus* | VIII | ENSMICP00000001089 | 286 | Ensembl |
| **Mammals** | Opossum | *Monodelphis domestica* | VIII | ENSMODP00000010658 | 289 | Ensembl_UCSC_BLAT |
| | | | X | ENSMODP00000015705 | 328 | Ensembl_UCSC_BLAT |
| | | | XI | ENSMODP00000017625 | 332 | Ensembl |
| | Microbat | *Myotis lucifugus* | VIII | ENSMLUP00000008230 | 275 | Ensembl |
| | Pika | *Ochotonidae princeps* | VIII | ENSOPRP00000014387 | 290 | Ensembl |
| | Platypus | *Ornithorhynchus anatinus* | VIII | ENSOANP00000008002 | 267 | Ensembl |
| | | | X | ENSOANP00000003611 | 308 | Ensembl_UCSC_BLAT |
| | Rabbit | *Oryctolagus cuniculus* | X | ENSOCUP00000002025 | 333 | Ensembl |
| | Bushbaby | *Otolemur garnettii* | X | ENSOGAP00000004458 | 327 | Ensembl |
| | Chimpanzee | *Pan troglodytes* | VIII | XP_519778.2 | 290 | NCBI_RefSeq |
| | | | X | XP_001171455.1 | 328 | NCBI_RefSeq |
| | | | XI | XP_001171520.1 | 328 | RefSeq_UCSC_BLAT |
| | Sumatran Orangutan | *Pongo abelii* | VIII | - | 290 | UCSC_BLAT |
| | | | X | Q5R4U0 | 328 | Uniprot |
| | | | XI | NP_001128968.1 | 328 | NCBI_RefSeq |

**Table 1: Details of the carbonic anhydrase-related protein (CARP) sequences used in this study (Continued)**

| | | | | | | |
|---|---|---|---|---|---|---|
| | Orangutan | *Pongo pygmaeus* | VIII | ENSPPYP00000020875 | 290 | Ensembl |
| | | | X | ENSPPYP00000009287 | 328 | Ensembl |
| | | | XI | ENSPPYP00000011415 | 328 | Ensembl |
| | Rat | *Rattus norvegicus* | VIII | Q5PPN4 | 290 | Uniprot |
| | | | X | EDM05681 | 319 | NCBI_RefSeq |
| | | | XI | NP_783639 | 328 | NCBI_RefSeq |
| | Pig | *Sus scrofa* | VIII | XP_001926916 | 291 | NCBI_RefSeq_EST |
| | | | XI | Q866X6 | 331 | Uniprot |
| | Tarsier | *Tarsius syrichta* | VIII | ENSTSYP00000009029 | 256 | Ensembl |
| | Dolphin | *Tursiops truncatus* | VIII | ENSTTRP00000015250 | 256 | Ensembl |
| | | | X | ENSTTRP00000001587 | 308 | Ensembl |
| | | | XI | ENSTTRP00000007758 | 320 | Ensembl |
| | Sheep | *Ovis aries* | XI | Q95203 | 328 | Uniprot |
| | Anole Lizard | *Anolis carolinensis* | VIII | - | 257 | UCSC_BLAT |
| | | | X | - | 321 | UCSC_BLAT |
| | | | XI | ENSACAP00000015571 | 289 | Ensembl |
| | Chicken | *Gallus gallus* | VIII | ENSGALP00000024873 | 283 | Ensembl |
| | | | X | XP_415644.1 | 328 | NCBI_RefSeq |
| | Zebra Finch | *Taeniopygia guttata* | VIII | ENSTGUP00000011522 | 258 | Ensembl |
| | | | X | ENSTGUP00000009733 | 328 | Ensembl |
| | Frog | Xenopus tropicalis | VIII | Q5M8Z5 | 282 | Uniprot |
| | | | X | ENSXETP00000002773 | 321 | Ensembl_UCSC_BLAT |
| | | | XI | - | 303 | UCSC_BLAT |
| | Zebrafish | Danio rerio | VIII | NP_001017571.1 | 281 | NCBI_RefSeq |
| Other | | | Xa | NP_001032198.1 | 328 | NCBI_RefSeq |
| vertebrates | | | Xb | XP_696967.2 | 308 | NCBI_RefSeq |
| | Stickleback | Gasterosteus aculeatus | VIII | ENSGACP00000019684 | 281 | Ensembl |
| | | | Xa | ENSGACP00000020102 | 323 | Ensembl_UCSC_BLAT |
| | | | Xb | ENSGACP00000000619 | 328 | Ensembl |
| | Rainbow trout | Oncorhynchus mykiss | VIII | Q5I2J1 | 281 | Uniprot |
| | Medaka | Oryzias latipes | VIII | ENSORLP00000016815 | 281 | Ensembl |
| | Fugu | Takifugu rubripes | VIII | ENSTRUP00000009702 | 282 | Ensembl |
| | | | Xa | ENSTRUP00000007839 | 297 | Ensembl_UCSC_BLAT |
| | | | Xb | ENSTRUP00000032938 | 328 | Ensembl_UCSC_BLAT |
| | Pufferfish | Tetraodon nigroviridis | VIII | ENSTNIP00000005959 | 272 | Ensembl |
| | | | Xa | ENSTNIP00000017020 | 328 | Ensembl_UCSC_BLAT |
| | Lancelet | Branchiostoma lancelet | VIII | C3XTT7 | 256 | Uniprot_UCSC_BLAT |
| | | | X | - | 319 | UCSC_BLAT |
| Invertebrates | Trichoplax | Trichoplax adhaerens | VIII | XP_002111595.1 | 348 | NCBI_RefSeq |
| | Sea urchin | Strongylocentrotus purpuratus | VIII | XP_795365.2 | 312 | NCBI_RefSeq |

[1] The sources of the best protein sequences. NCBI, RefSeq, UniProt and Ensembl refer to the respective databases, and UCSC_BLAT refers to discovery of novel genes/exons using the UCSC genome browser and subsequent gene model building, as detailed in Materials and Methods. EST means that a further EST sequence was used to extend an incomplete genome sequence.

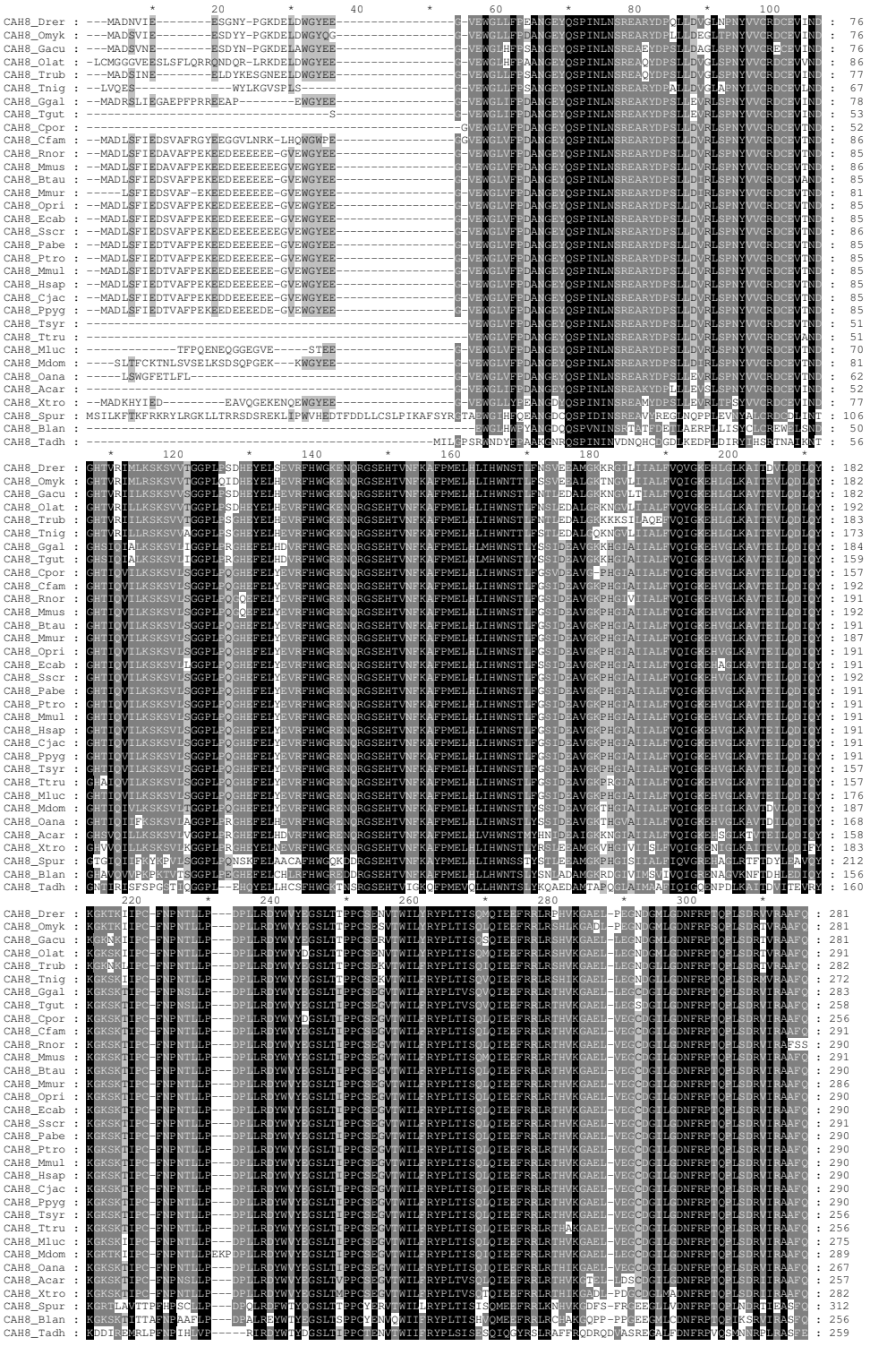

**Figure 1 Multiple sequence alignment of CARP VIII sequences**. Comparison of 33 CARP VIII sequences by multiple sequence alignment. Short names (first letter of the genus and first three letters of the species) are provided on the left side and residue numbers are provided on the right side of the figure. Details of the sequences and full species names are provided in Table 1. The sequences of CAH8_Rnor and CAH8_Spur are trimmed in the end by 21 and 89 residues, respectively.

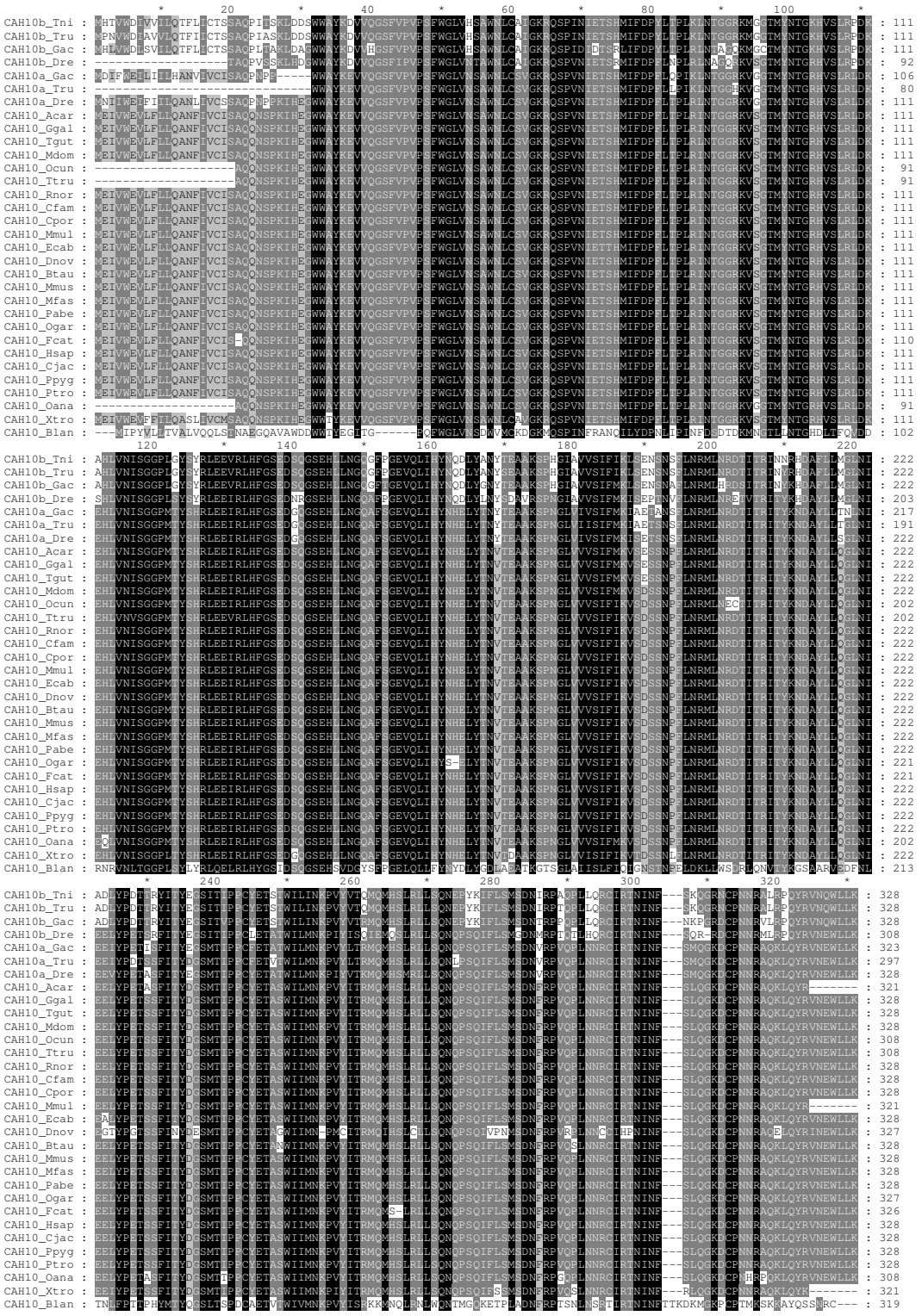

**Figure 2 Multiple sequence alignment of CARP X sequences**. Comparison of 32 CARP X sequences by multiple sequence alignment. Short names (first letter of the genus and first three letters of the species) are provided on the left side and residue numbers are provided on the right. Details of the sequences and full species names are provided in Table 1.

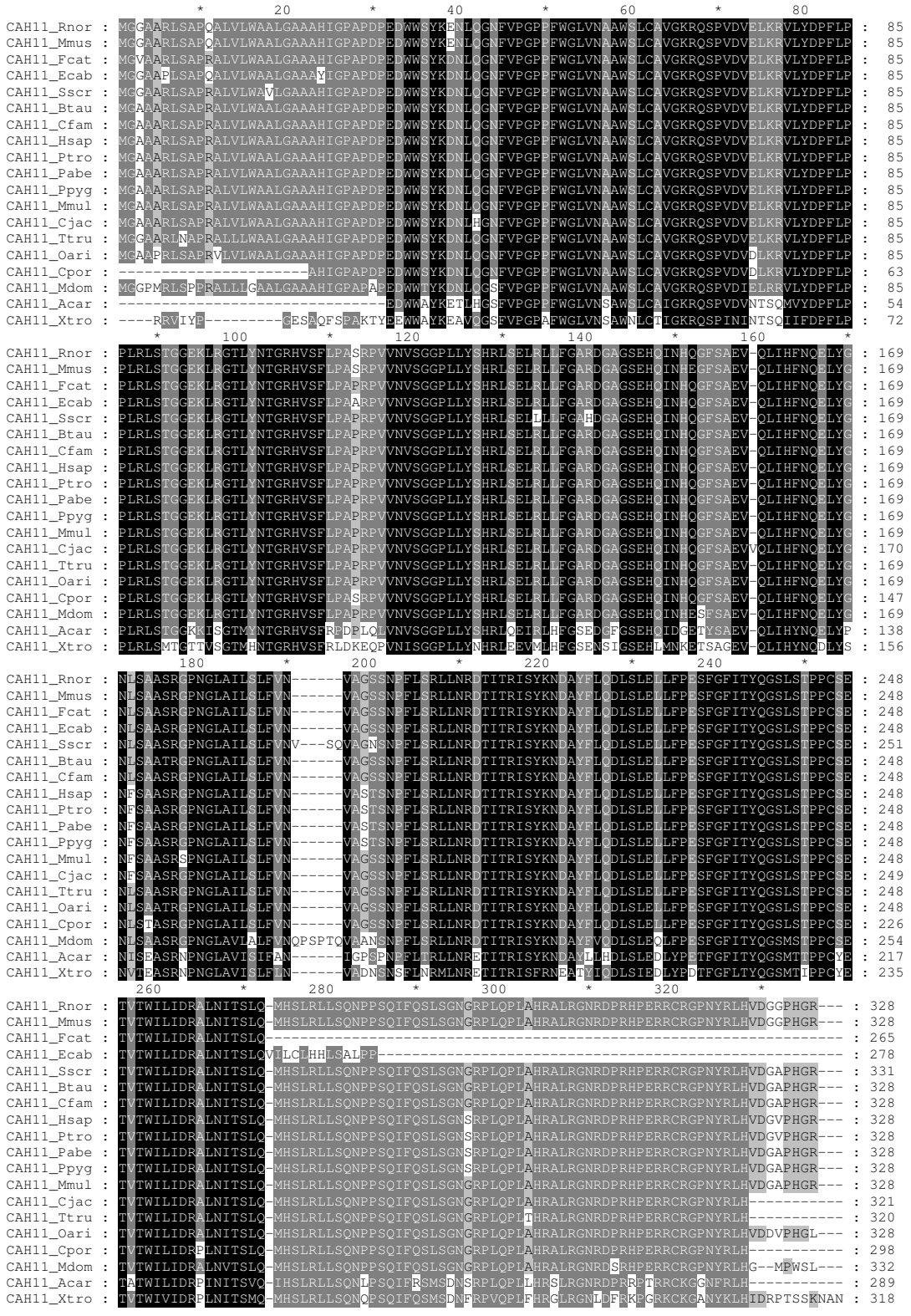

**Figure 3 Multiple sequence alignment of CARP XI sequences**. Comparison of 19 CARP XI sequences by multiple sequence alignment. Short names (first letter of the genus and first three letters of the species) are provided on the left side and residue numbers are provided on the right. Details of the sequences and full species names are provided in Table 1.

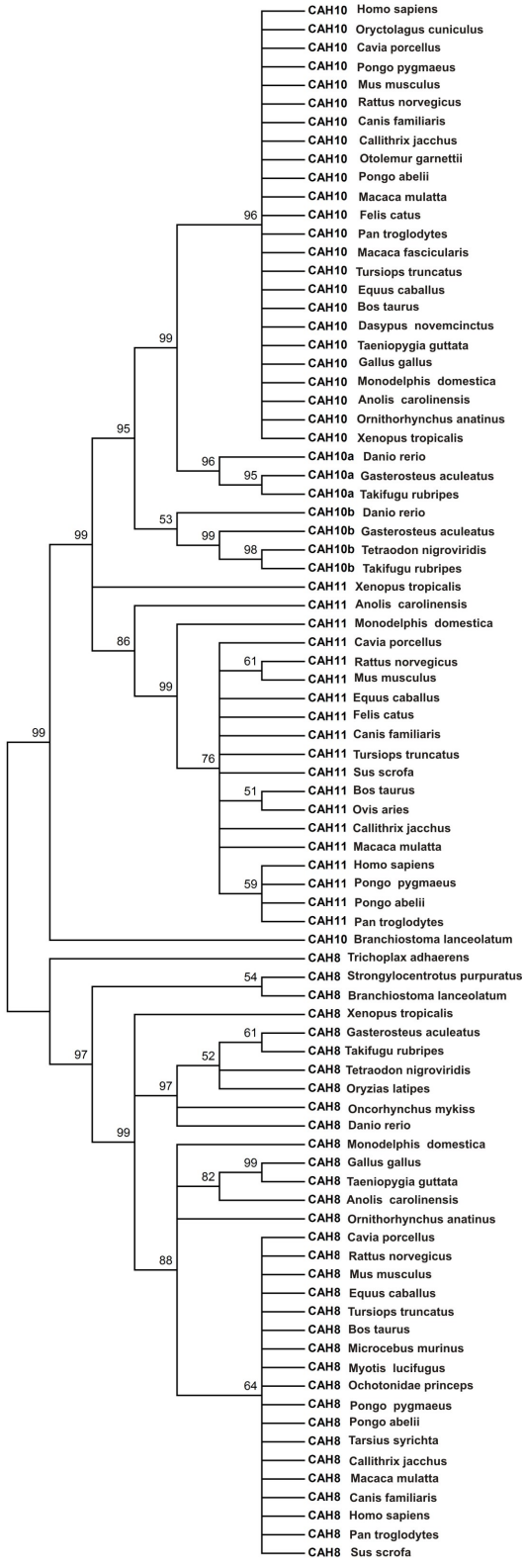


**Figure 4 Evolutionary relationships of CARP sequences**. The phylogenetic tree of 84 CARP sequences used in the study was inferred using the Neighbor-Joining method. The percentage of replicate trees in which the associated sequences clustered together in the bootstrap test is shown above the branches.

lizards, and two smaller groups containing sequences from fishes (Figure 4). The CARP XI group contains a major branch, consisting of mammalian sequences, while the sequences from lizard and frog form an outgroup. The tree indicates that there has been an independent duplication of the ancestral vertebrate *CA10* gene in the fish lineage, whereas we conclude that the *CA11* gene has emerged from another gene duplication after the separation of the fish and tetrapod lineages.

### Quantitative analysis of Car 8, Car10, Car11 mRNA expression in mouse tissues

We studied the expression of all three CARP mRNAs in 20 different mouse tissues. The expression patterns of each mRNA are shown in Figures 5 through 7. As predicted based on previous studies [15], *Car8* mRNA expression was found to be highest in the cerebellum, and high levels were also detected in the liver and the lung (Figure 5). Low expression was observed in the stomach, duodenum, ileum, jejunum, colon, spleen, kidney, heart, frontal cortex, parietal cortex, midbrain, and eye, while extremely low expression was observed in the ovary, skeletal muscle, and testis.

The expression profile for *Car10* mRNA is presented in Figure 6. The *Car10* mRNA levels were high in the cerebellum, frontal cortex, and parietal cortex, low in the midbrain, and extremely low in the eye. The distribution of *Car11* mRNA expression was broad, and the highest signals were observed in the cerebellum and cerebral cortex (Figure 7) while the midbrain showed moderate levels of expression. In addition to the brain, low expression was detected in the colon, kidney, ovary, heart, and lung. Moreover, barely detectable expression was observed in the liver, stomach, duodenum, ileum, jejunum, spleen, and eye.

### Distribution of CARP VIII, X, and XI proteins in mouse tissues

We studied the expression of CARP VIII, X, and XI proteins in mouse tissues using immunohistochemistry as shown in Figures 8 through 11 and in Table 2. CARP VIII was expressed in most of the tissues analyzed, indicating a wider distribution profile compared to CARP X and CARP XI expression. Strong expression for CARP VIII was observed in the cerebellum and cerebrum while weaker expression was observed in several other tissues including the liver, pancreatic Langerhans islets, submandibular gland, stomach, colon, kidney, and lung (Figures 8 and 9). In the cerebellum, the highest staining intensity was present in the Purkinje cells and a slightly lower staining intensity was associated with the molecular layer. The cerebrum showed an intense and punctate staining pattern, indicating the strongest expression in the axons and dendrites. In the kidney, very weak positive staining

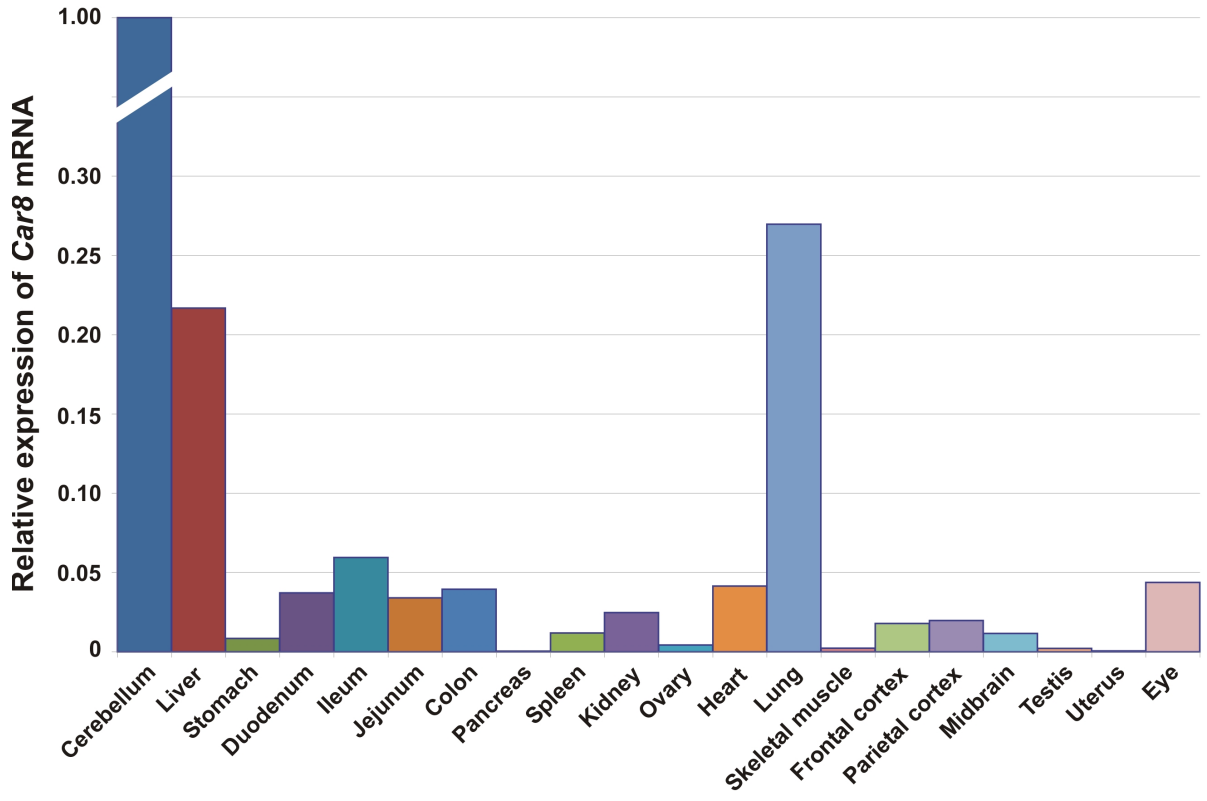


**Figure 5 Expression pattern of *Car8* mRNA in different murine tissues**.

was observed in a few epithelial cells of the renal tubules. The liver showed moderate immunostaining in the hepatocytes. In the lung, staining was observed in both the respiratory epithelium and the rounded alveolar cells, most likely representing the type II pneumocytes. The submandibular gland showed strong immunoreactions in both the acinar and ductal epithelial cells. The gastric and colonic glands were also positively stained for CARP VIII.

A significant amount of CARP X expression was observed only in the lung where the staining was localized to the respiratory epithelium. In addition, positive signals were occasionally detected in the cerebral capillaries and the stomach (Figures 8 and 10 and Table 2). Barely detectable staining was occasionally observed in the heart muscle cells.

CARP XI showed a broader expression profile than CARP X. Its overall distribution was fairly similar to that for CARP VIII, although the staining intensity was clearly less intense. Positive signal for CARP XI was observed in the cerebellum, cerebrum, liver, stomach, small intestine, colon, kidney, and testis (Figures 8 and 11 and Table 2). In the cerebellum, the most prominent signal was located in the Purkinje cells.

## Discussion

Previous bioinformatic investigations have described individual CARP sequences only for human, mouse, and other mammals [10,11,25,26]. Using a variety of bioinformatic tools we identified 84 full-length sequences from genome and sequence databases, including 22 coming from novel or improved gene models and combining mRNA data to genome data. Of these 22 sequences, 8 are novel and previously unannotated, and 14 comprise extended and/or partially corrected sequences. Sequences encoding CARP VIII and CARP X were identified in all available vertebrate genomes, even if many sequences were present only as gene fragments. In contrast, CARP XI was found only in mammals, frogs (*X. tropicalis*), and lizards (*A. carolinensis*). Our results indicate that the *CA11* gene emerged through a process of gene duplication from *CA10* after the divergence of the fish and tetrapod lineages. In addition, we failed to identify any CARP XI sequences from birds, but since there are only two genomes available, the *CA11* gene may have been either missed as a consequence of the incomplete genome coverage or alternatively the gene may have been lost in the bird lineage.

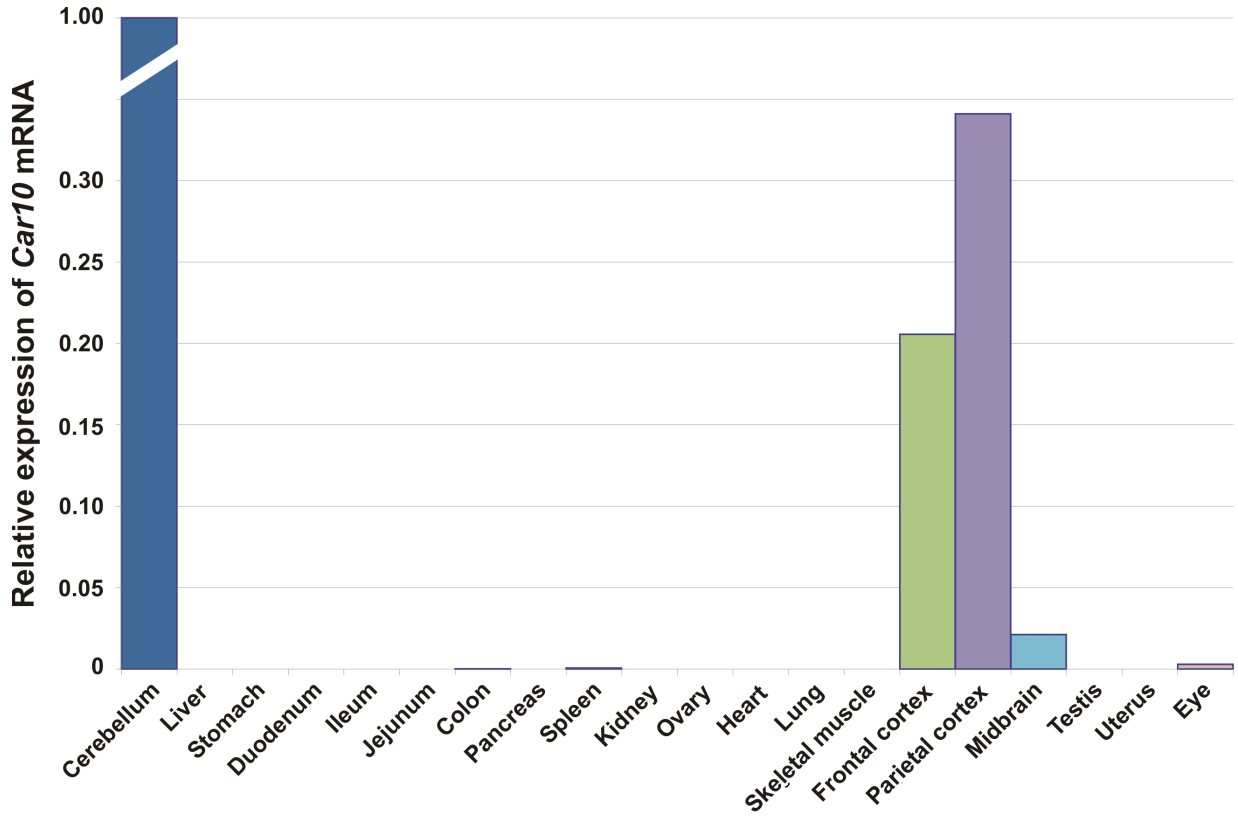


**Figure 6 Expression profile of *Car10* mRNA in murine tissues**.

The fish CARP X-like sequences form two distinct subgroups, both of which are more closely related to CARP X than CARP XI. This indicates that these sequences have arisen by gene duplication from the *CA10* gene in the fish lineage. We suggest names *CA10a* and *CA10b* for these genes and CARP Xa and CARP Xb for the proteins to distinguish them from *CA11*/CARP XI, which is specific to tetrapods.

Sequences found in three deuterostomes (*B. floridae*, *T. adhaerens*, and *S. purpuratus*) that were similar to CARP VIII, with sequence similarities between 40% and 45% when compared to vertebrate CARP VIII sequences, were novel and unexpected discoveries. No CARP VIII orthologs were likewise discovered in protostomes. According to these findings, the origin of CARP VIII would have occurred sometime after the separation of the Protostomia and Deuterostomia lineages. In contrast, CARP X-like sequences are widely found in invertebrates, including all available insect and nematode genomes. Further analysis of the invertebrate CARP X homologs will be presented elsewhere.

Earlier studies reported the expression of human or mouse CARP mRNAs and their corresponding proteins using immunohistochemistry, western blot analysis, northern blot assays, dot blots, and RT-PCR mostly in the brain and in a few cases in other tissues, often with slightly conflicting results [12,13,16,22,27-30]. However, a comprehensive distribution of all CARPs and their corresponding mRNAs has yet to be completely elucidated. In fact, the present study revealed for the first time the distribution of all CARP proteins and their mRNAs in a wide variety of adult mouse tissues using immunohistochemistry and real-time qPCR.

The expression of *Car8* mRNA has been previously studied in some other tissues besides from the brain using RT-PCR and dot blot analysis. Multiple transcripts were reported to be expressed in the brain, lung, and liver, and a single transcript was found in the heart, skeletal muscle, and kidney, though to a lesser extent [11]. In the present study, we observed high expression of *Car8* mRNA in the cerebellum, liver, and lung. Low expression of *Car8* mRNA was observed in all other tissues except for the pancreas and uterus. In brief, the expression pat-

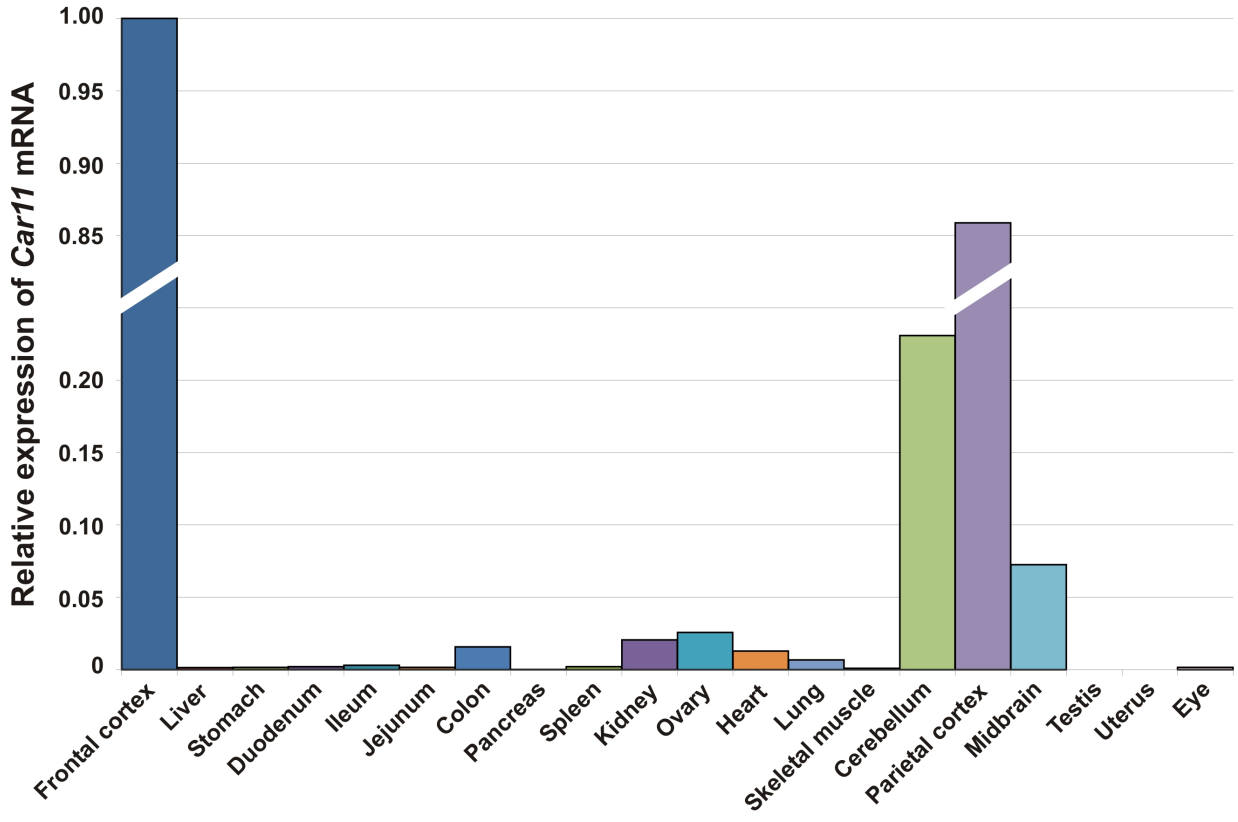


**Figure 7 Distribution of *Car11* mRNA in murine tissues**.

tern we observed by RT-qPCR was similar to the earlier results [11]. The immunohistochemical findings show high levels of CARP VIII expression in the cerebellum and cerebrum. In previous studies, immunohistochemical staining, northern blot studies, and RT-PCR analyses have shown abundant expression of CARP VIII in the human and mouse brain, and immunohistochemical studies have further defined its expression especially in the cerebellar Purkinje cells [12,13,16,22,27-30], all of which are in agreement with the results of our study. Lower CARP VIII expression has been reported in other murine tissues including the lung, liver, and stomach using western blot analysis [30]. Our study confirmed the expression using immunohistochemical staining in these organs. High level expression of *Car8* mRNA and CARP VIII protein in the brain and in a wide variety of other tissues suggests important roles for this protein in normal physiology. Indeed the role of CARP VIII is evident from the recently published reports showing ataxia and gait disorders in both mice and humans due to mutations in the *CA8* gene [22,23].

RT-PCR analyses have previously shown the expression of *Car10* mRNA in the human brain, testis, salivary glands, and kidney, while lower expression levels were reported in the pancreas, liver, and testis [11]. Using northern blot analysis, the expression was observed in the kidney and the brain [11]. Incidentally, there have been only a few previous reports in the literature regarding the expression of the CARP X protein in the human and mouse brain. The expression was shown to be weak in the cerebellar Purkinje cells [14,16]. Herein we report strong positive signal intensities only in the cerebellum followed by the parietal cortex and the frontal cortex, low expression in the midbrain, and extremely low expression in the eye. Using immunohistochemical studies, we observed clearly localized signal only in the respiratory epithelium of the lung, and weak signals in the stomach and cerebral capillaries. Our real-time qPCR results do not agree with previous results on human tissues (except for the brain) nor do they agree with the present immunohistochemical findings. The discrepancies between immununohistochemistry and RT-qPCR may be due to (i) a low amount of mRNA that is translated into protein; (ii) rapid

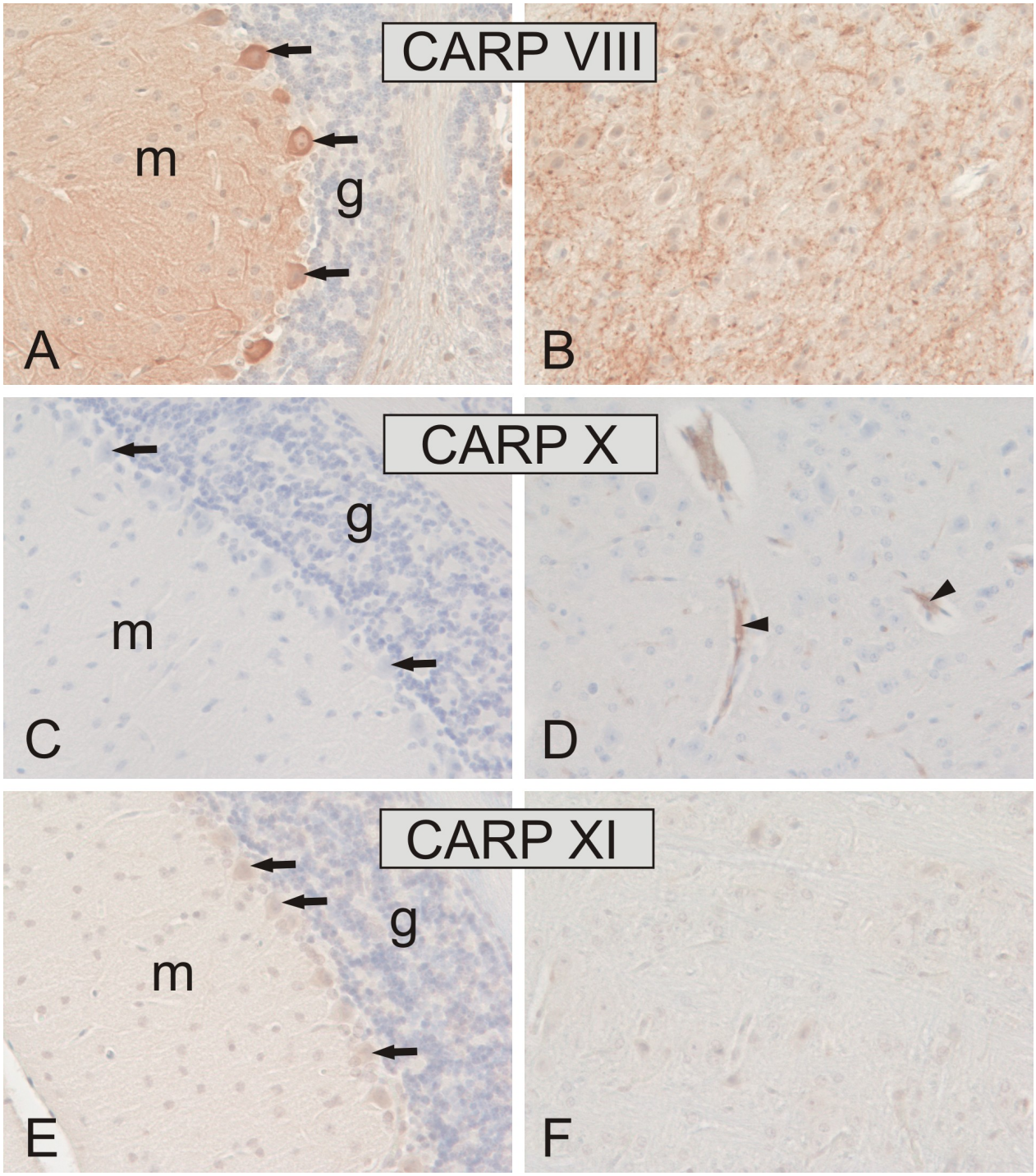


**Figure 8 Immunohistochemical staining of CARP VIII, CARP X, and CARP XI proteins in mouse cerebellum (A, C, E) and cerebrum (B, D, F)**. Arrows indicate the location of the Purkinje cells, which are strongly positive for CARP VIII and moderately positive for CARP XI. The molecular layer (m) of the cerebellum is also intensely labeled with CARP VIII, whereas the granular cell layer is negative (g). Panel B shows strong punctuate immunostaining for CARP VIII in the cerebrum. The arrowheads in panel D indicate CARP X-positive microcapillaries in the cerebrum. Immunostaining reactions for CARP XI remained very weak in the cerebrum (F). Original magnifications are at × 20.

degradation of the protein; (iii) the low signal from immunochemical staining, which could be due to the loss of antigenicity in some tissues during the processing and storage of slides; (iv) differences in the species or strains used. Further immunohistochemical studies using new antibodies along with analysis of mRNA transcripts will

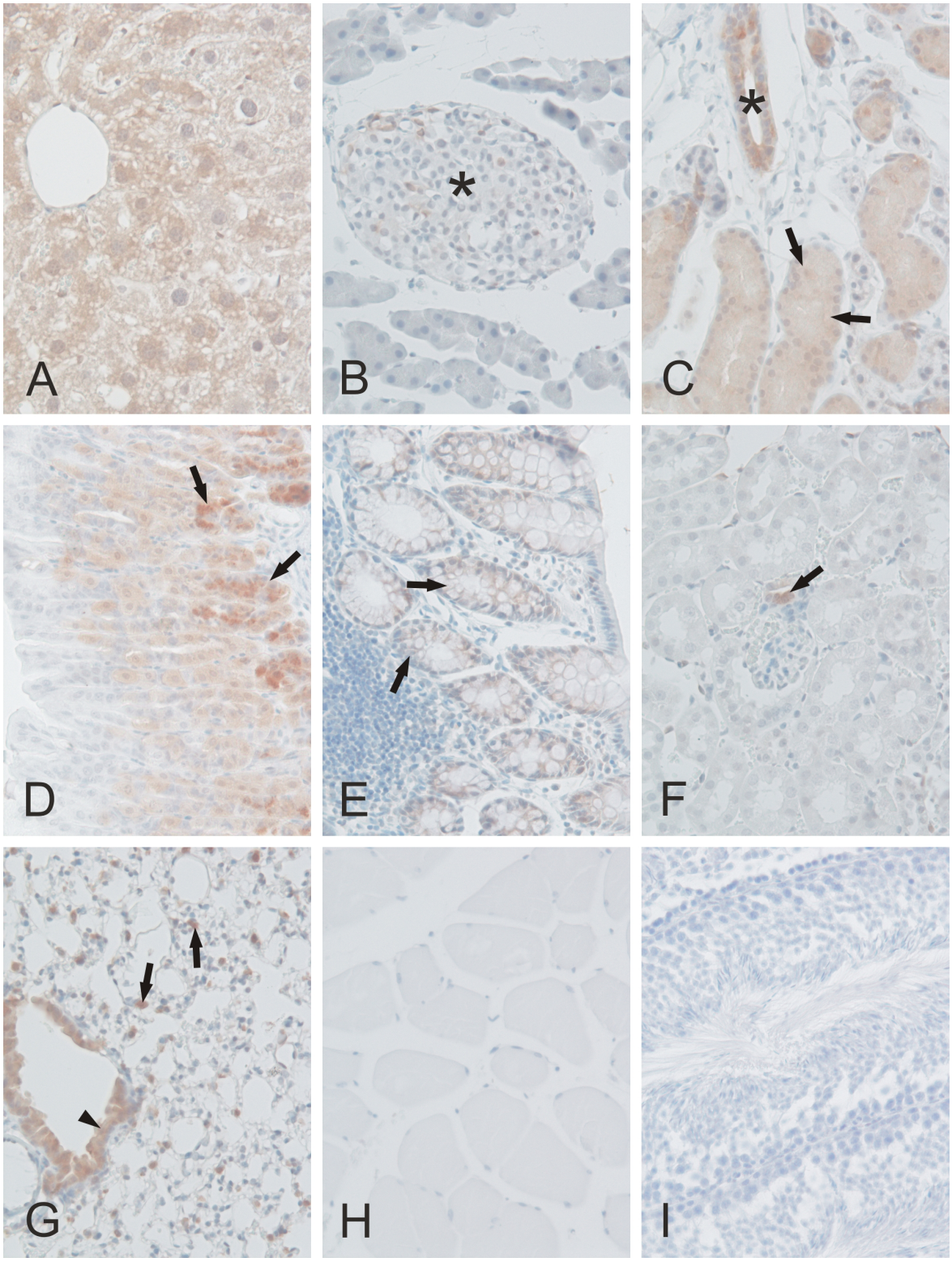


**Figure 9 Immunohistochemical staining of CARP VIII proteins in mouse tissues**. CARP VIII was observed moderately in the liver hepatocytes (A), ducts (*) and acini (arrows) of the submandibular gland (C), gastric glands (arrows in D), respiratory epithelium (arrowhead), and rounded alveolar cells (arrows) of the lung (G). Extremely low expression was observed in the pancreatic Langerhans islets (*in B), colonic glands (arrows in E), and occasionally in the tubule cells of the kidney (arrow in F indicates positive macula densa cells). No staining was present in the skeletal muscle (H) and testis (I). Original magnifications are at × 20.

**Table 2: Expression profile of CARP VIII, X, and XI in mouse tissues using immunohistochemistry**

| Tissue | CARP VIII | CARP X | CARP XI |
|---|---|---|---|
| Cerebellum | +++ | --- | ++- |
| Cerebrum | +++ | ++- | +-- |
| Liver | ++- | --- | +-- |
| Pancreas | +-- | --- | --- |
| Submandibular gland | ++- | --- | --- |
| Stomach | ++- | +-- | +-- |
| Colon | +-- | --- | +-- |
| Kidney | +-- | ++- | +-- |
| Lung | ++- | --- | --- |
| Skeletal muscle | --- | --- | -- |
| Testis | --- | NA | +- |
| Ovary | NA | -- | NA |
| Heart | NA | +-- | NA |
| Epididymis | NA | --- | --- |
| Small intestine | --- | --- | +-- |

+++ Strong, ++Moderate, +-Weak, ---No signal, and NA-Not analyzed

be important for understanding the discrepancies observed.

In a previous paper, Okamoto et al. [11] reported that the *Car10* sequence contains seven CCG repeats in the 5'-untranslated region followed by two CCG repeats located 16 bp downstream from the aforementioned repeats. These repeats have been associated with various neurological disorders [31]. The presence of the CCG repeats in the *Car10* gene makes it a potential candidate gene that might contribute to the development of neurodegenerative disorders. Therefore, it will be of interest to explore the expansion mutations of *Car10* gene in patients with neurological symptoms [8].

Our study revealed widespread expression of CARP XI in most of the tissues studied by using both immunohistochemistry and real-time qPCR. Compared to CARP VIII, the intensity of CARP XI immunostaining was clearly weaker. In a previous study, immunochemical staining of the human brain indicated that the signal for CARP XI was lower compared to CARP VIII but higher than CARP X [16]. Thus, our findings were in agreement with these aforementioned results. The present real-time qPCR analysis, surprisingly, showed very high expression of the *Car11* mRNA in all of the brain segments analyzed, especially in the frontal cortex followed by the parietal cortex, cerebellum, and midbrain. These results were in agreement with an earlier report showing *Car11* mRNA expression in all parts of the human brain [10]. The same study demonstrated *Car11* mRNA expression in the kidney, liver, and salivary glands, and low expression levels in the lung, skeletal muscle, kidney, pancreas, and liver [10]. In our study, low levels of *Car11* mRNA were observed in the colon, kidney, ovary, heart, and lung. The presence of CARP XI in several regions of the brain suggests an important, yet undefined role for CARP XI in the central nervous system.

## Conclusions

The present investigation describes a comprehensive bioinformatic study of CARP gene sequences and also elucidates the distribution of three CARPs in mouse tissues using real-time qPCR and immunohistochemistry. We have observed a very high conservation of all the three CARP sequences across the species. In the cases of CARP VIII and CARP X, we found unusually high similarity between vertebrate and invertebrate sequences. Based on our results, the duplication history of the *CA10* gene has followed different paths in the fish and tetrapod lineages. Our results contribute to a deeper understanding of CARP evolution across species.

The expression of CARP VIII was found to be widespread in the tissues analyzed, and the highest mRNA signals were detected in the cerebellum, lung, and liver. Both CARP X and XI showed the strongest mRNA expression in the nervous tissues. The distribution patterns suggest that CARPs may contribute to the development of the nervous system, motor coordination functions, and yet unknown physiological roles in other tissues. It will be of interest to determine the specific function of all CARPs by producing and analyzing suitable single, double, and

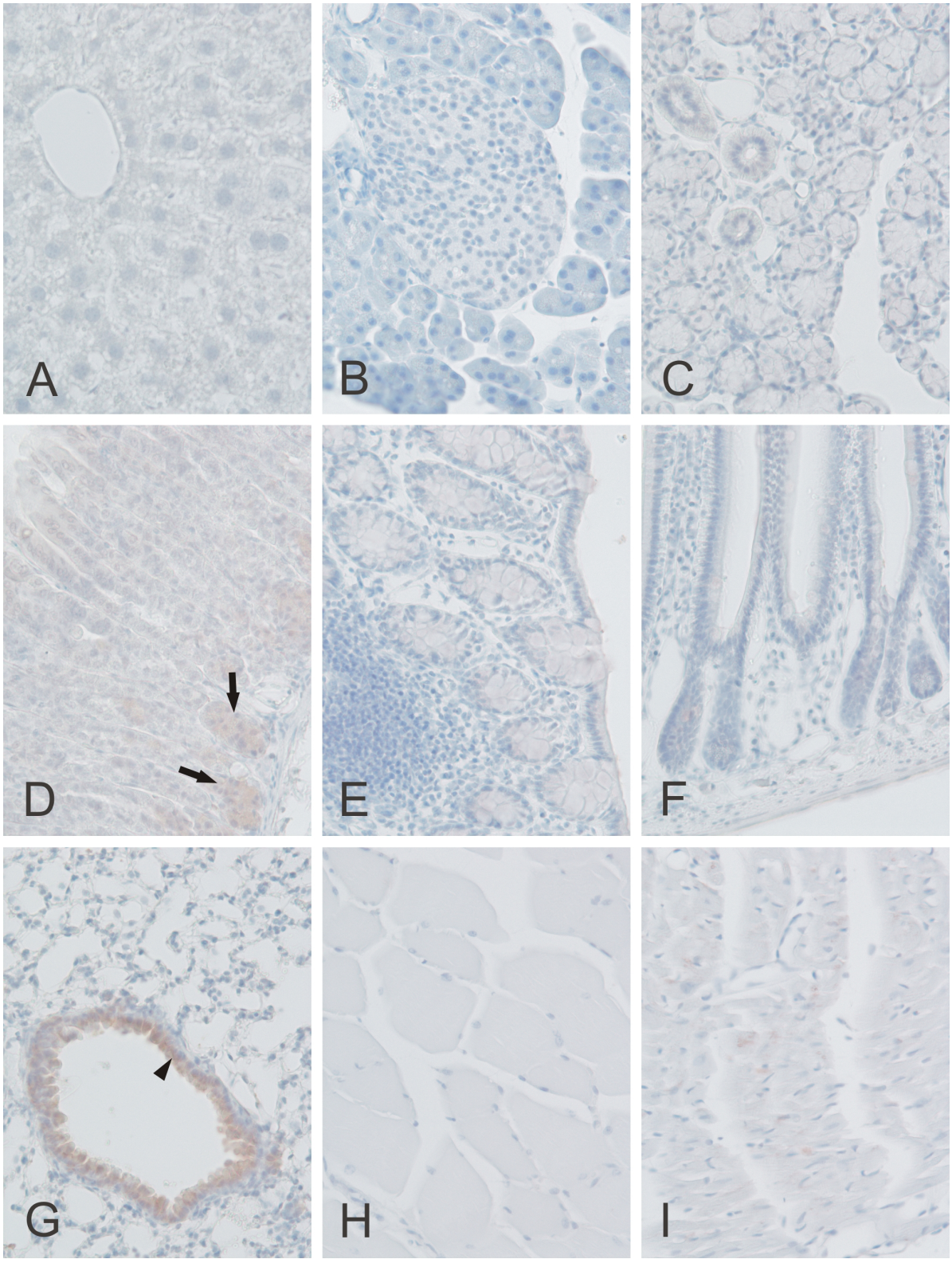


**Figure 10 Immunohistochemical staining of CARP X protein in mouse tissues**. Moderate CARP X expression was observed in the respiratory epithelium (arrowhead) of the lung (G). Moderate expression was also present in the gastric glands (arrows in panel D). The heart muscle cells occasionally showed extremely weak signals (I). The other tissues including the liver (A), pancreas (B), submandibular gland (C), colon (E), small intestine (F), skeletal muscle (H) remained negative. Original magnifications are at × 20.

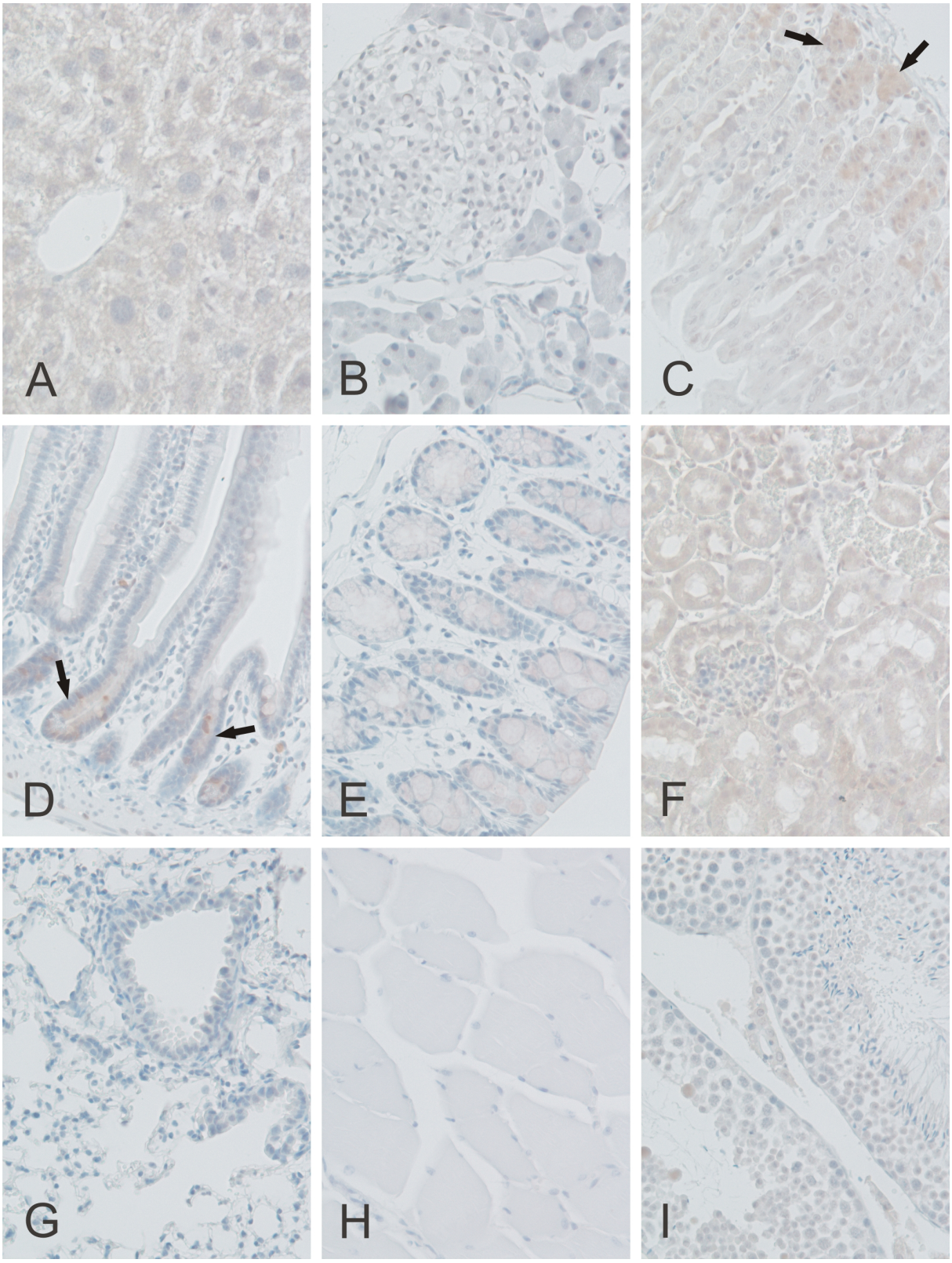


**Figure 11 Immunohistochemical staining of CARP XI protein in mouse tissues**. Weak immunoreactions for CARP XI were observed in the crypts of Lieberkuhn (arrows in D), gastric glands (arrows in C), and renal tubule cells (F). Extremely weak signals can also be observed in the liver (A), colon (E), and testis (I). The pancreas (B), lung (G), and skeletal muscle (H) were all negative. Original magnifications are at × 20.

triple knockout animal models and also by screening neurological patients for trinucleotide repeats or other mutations in CARP genes.

## Methods

### Sequence retrieval

The available CARP protein sequences were obtained from Ensembl [32], UniProt [33], and RefSeq [34] and further sequences were searched using BLAST from NCBI protein databases [35] and via BLAT searches from complete genomes [36] using human and mouse CARPs as initial query sequences, and zebrafish, lancelet and sea urchin CARPs later as they were discovered and confirmed. Duplicate sequences were rejected, after which the remaining sequences were taken through iterated cycles of multiple sequence alignment [37], evaluation, and revision. For revision, sequences with poorly matching or missing regions were subjected to gene model generation with GeneWise [38] taking the genomic sequences from the UCSC Genome Browser [36]. EST and mRNA sequence data were used to confirm gene models, to bridge gaps or fill ends in the genomic sequences, and to discover and assemble CARPs from less than genome-wide sequenced organisms. Finally, incomplete sequences were rejected, with the exception of marginally shortened ends, which were allowed.

### Multiple sequence alignment

Individual multiple sequence alignments (MSAs) were calculated for CARP VIII, CARP X, and CARP XI using ClustalW [39] and visualized using GeneDoc software [40]. Furthermore, all of the 84 CARP protein sequences were aligned together for the phylogenetic tree.

### Phylogenetic analysis

The phylogenetic tree of all CARP protein sequences was constructed from the MSA of 84 sequences using the MEGA software, version 4.1 [41]. Evolutionary relationships were inferred using the Neighbor-Joining method. A bootstrap test was performed using 1000 replicates and evolutionary distances were computed using the Poisson correction method with the complete deletion option.

### Immunohistochemistry

The tissue specimens from the normal mice were fixed in 4% neutral-buffered formaldehyde at +4°C for 8 to 27 days. The samples were then dehydrated in an alcohol series, treated with xylene, embedded in paraffin wax, and 4 μm sections were cut and placed on Superfrost microscope slides. After removal of the paraffin with xylene, the rehydrated sections were boiled in sodium citrate (0.01 M, pH 6.0) for 20 min and cooled down. The sections were immunohistochemically stained according to the following procedure: (i) incubating the sample in methanol + 3% $H_2O_2$ for 5 min; (ii) rinsing with 1 × Tris-buffered saline (TBS), pH 8.0, containing 0.05% Tween; (iii) blocking with Rodent Block M™(Biocare Medical, Concord, CA) for 30 min; (iv) incubating with primary rabbit anti-human CARP VIII, CARP X, and CARP XI antibodies (Santa Cruz Biotechnology, Inc. Bergheimer Heidelberg, Germany) raised against amino acids 1 to 100 (CARP VIII), 1 to 50 (CARP X) and 279 to 328 (CARP XI) diluted 1:350 in 1% bovine serum albumin (BSA) in phosphate-buffered saline (PBS) for 1 hour at room temperature and rinsing with TBS containing 0.05% Tween. Notably, rabbit IgG was used as a control instead of the primary antibodies; (v) incubation with Rabbit HRP-Polymer + XM Factor™(Biocare Medical, Concord, CA) (2.5 ml HRP-Polymer + 1 to 2 drops XM Factor) for 30 min prior to rinsing with 1 × TBS containing 0.05% Tween; (vi) treatment with 1 × 3,3'-diaminobenzidine tetrahydrochloride (DAB) solution for 5 min prior to rinsing with distilled water; (vii) counterstaining of the slides with Mayer's Hematoxylin for 1 to 3 sec and rinsing under tap water for 10 min. After dehydration, the slides were mounted with Entellan Neu™ (Merck; Darmstadt, Germany), examined and photographed using Nikon Microphot microscope (Nikon Microphot-FXA, Japan). All of the procedures were carried out at room temperature.

### RNA Extraction

Specimens from 20 tissue samples were collected from six normal NMRI mice. The tissue samples used for mRNA isolation were stabilized in RNAlater (Ambion, Austin, TX, USA) immediately after collection, and the total RNA was isolated from 30 mg of tissue samples using the RNeasy Mini kit (Qiagen, Hilden, Germany) by following the manufacturer's instructions. The concentration and purity of RNA was determined using a spectrophotometric method at 260 and 280 nm.

### Quantitative real-time PCR

Reverse transcriptase PCR was performed using 50 μg of total RNA to synthesize the first strand of cDNA using First Strand cDNA Synthesis kits (High-Capacity cDNA Reverse Transcription Kits, Applied Biosystems, Foster City, CA) with random primers and MultiScribe™ Reverse Transcriptase according to the protocol recommended by the manufacturer.

Real-time qPCR primers were designed based on the complete cDNA sequences deposited in the GenBank (RefSeq accession numbers: *Car8* [NCBI: NM_007592], *Car10* [NCBI: NM_028296], and *Car11* [NCBI: NM_009800]). Primer sequences for *Car8* included the Forward primer (5'-3') cgggattactgggtctatgaagg and the Reverse primer (5'-3') ggctgggtaggtcggaaattgtc, while the primer sequences for *Car10* included the Forward primer

(5'-3') gagagcaagagcccagaactc and the Reverse primer (5'-3') ctcaccagtggcagaaatggc. In addition, the *Car11* primer sequences were (5'-3') gccggctctgaacaccagatc (for the Forward primer) and (5'-3') gaggaggcgactgaggaatgg (for the Reverse primer).

Real-time qPCR was performed using the SYBR Green PCR Master Mix Kit in an ABI PRISM 7000 Detection System™ according to the manufacturer's instructions (Applied Biosystems). The PCR conditions consisted of an initial denaturation step at 95°C for 10 min followed by 40 cycles at 95°C for 15 sec (denaturation) and 60°C for 1 min (elongation). The data were analyzed using the ABI PRISM 7000 SDS™ software (Applied Biosystems). Every PCR was performed in a total reaction volume of 15 μl containing 2 μl of first strand cDNA (20 ng cDNA), 1 × Power SYBR green PCR Master Mix™ (Applied Biosystems, Foster City, CA 94404, USA), and 0.5 μM of each primer. The final results, expressed as the *N*-fold relative difference (ratio) in gene expression between the studied samples, were calculated according to the Pfaffl's equation with appropriate modification [42].

## Additional material

**Additional file 1 Multiple sequence alignment of CARP VIII, X, and XI sequences**. Multiple sequence alignment of the 84 CARP protein sequences analyzed in the study which was used for the construction of the phylogenetic tree.

### Authors' contributions

All authors participated in the design of the study. AA is the corresponding author who performed the experimental work and drafted the first version of the manuscript. AA and MT jointly performed the bioinformatic analyses, under supervision of MT. In addition, AA and SP performed essential microscopic analyses. All authors contributed to the writing of the document and approved the final version of the manuscript.

### Acknowledgements

We thank Marianne Kuuslahti and Aulikki Lehmus for their skilful technical assistance with the experiments and Csaba Ortutay for helpful discussions. This work was supported by the Competitive Research Funding of the Tampere University Hospital (Grant 9L071) and a grant from Academy of Finland.

### Author Details

[1]Bioinformatics Group, Institute of Medical Technology, 33014 University of Tampere, Tampere, Finland, [2]Institute of Medical Technology and School of Medicine, University of Tampere, 33520 Tampere, Finland and [3]Centre for Laboratory Medicine, Tampere University Hospital, 33520 Tampere, Finland

Received: 24 November 2009 Accepted: 31 March 2010
Published: 31 March 2010

### References

1. Henry RP: **Multiple roles of carbonic anhydrase in cellular transport and metabolism.** *Annu Rev Physiol* 1996, **58:**523-538.
2. Supuran CT: **Carbonic anhydrases: novel therapeutic applications for inhibitors and activators.** *Nat Rev Drug Discov* 2008, **7(2):**168-181.
3. Sly WS, Hu PY: **Human carbonic anhydrases and carbonic anhydrase deficiencies.** *Annu Rev Biochem* 1995, **64:**375-401.
4. Tashian RE: **The carbonic anhydrases: widening perspectives on their evolution, expression and function.** *Bioessays* 1989, **10(6):**186-192.
5. Tashian RE: **Genetics of the mammalian carbonic anhydrases.** *Adv Genet* 1992, **30:**321-356.
6. Bertucci A, Innocenti A, Zoccola D, Scozzafava A, Tambutte S, Supuran CT: **Carbonic anhydrase inhibitors. Inhibition studies of a coral secretory isoform by sulfonamides.** *Bioorg Med Chem* 2009, **17(14):**5054-5058.
7. Tashian REH-ED, Carter ND, Bergenhem NCH, (ed): **Carbonic anhydrase (CA)-related proteins (CA-RPs), and trans-membrane proteins with CA or CA RP membrane proteins with CA or CA RP domains.** Basel: New Horizons, Birkhauser; 2000.
8. Nishimori I: **Acatalytic CAs: Carbonic anhydrase-related proteins.** In *Carbonic anhydrases: Its inhibitors and activators. CRC enzyme inhibitor series* Edited by: Supuran CT, Scozzfava A, Conway J. CRC press; 2004:25-43.
9. Barnea G, Silvennoinen O, Shaanan B, Honegger AM, Canoll PD, D'Eustachio P, Morse B, Levy JB, Laforgia S, Huebner K, *et al.*: **Identification of a carbonic anhydrase-like domain in the extracellular region of RPTP gamma defines a new subfamily of receptor tyrosine phosphatases.** *Mol Cell Biol* 1993, **13(3):**1497-1506.
10. Fujikawa-Adachi K, Nishimori I, Taguchi T, Yuri K, Onishi S: **cDNA sequence, mRNA expression, and chromosomal localization of human carbonic anhydrase-related protein, CA-RP XI.** *Biochim Biophys Acta* 1999, **1431(2):**518-524.
11. Okamoto N, Fujikawa-Adachi K, Nishimori I, Taniuchi K, Onishi S: **cDNA sequence of human carbonic anhydrase-related protein, CA-RP X: mRNA expressions of CA-RP X and XI in human brain.** *Biochim Biophys Acta* 2001, **1518(3):**311-316.
12. Taniuchi K, Nishimori I, Takeuchi T, Fujikawa-Adachi K, Ohtsuki Y, Onishi S: **Developmental expression of carbonic anhydrase-related proteins VIII, X, and XI in the human brain.** *Neuroscience* 2002, **112(1):**93-99.
13. Akisawa Y, Nishimori I, Taniuchi K, Okamoto N, Takeuchi T, Sonobe H, Ohtsuki Y, Onishi S: **Expression of carbonic anhydrase-related protein CA-RP VIII in non-small cell lung cancer.** *Virchows Arch* 2003, **442(1):**66-70.
14. Nishimori I, Takeuchi H, Morimoto K, Taniuchi K, Okamoto N, Onishi S, Ohtsuki Y: **Expression of carbonic anhydrase-related protein VIII, X and XI in the enteric autonomic nervous system.** *Biomed Res* 2003, **14(1):**69-73.
15. Taniuchi K, Nishimori I, Takeuchi T, Ohtsuki Y, Onishi S: **cDNA cloning and developmental expression of murine carbonic anhydrase-related proteins VIII, X, and XI.** *Brain Res Mol Brain Res* 2002, **109(1-2):**207-215.
16. K Taniuchi IN, Takeuchi T, Fujikawa-Adachi K, Ohtsuki Y, Onishi S: **Developmental expression of carbonic anhydrase-related proteins VIII, X, and XI in the human brain.** *Neuroscience* 2002, **112:**93-99.
17. Miyaji E, Nishimori I, Taniuchi K, Takeuchi T, Ohtsuki Y, Onishi S: **Overexpression of carbonic anhydrase-related protein VIII in human colorectal cancer.** *J Pathol* 2003, **201(1):**37-45.
18. Morimoto K, Nishimori I, Takeuchi T, Kohsaki T, Okamoto N, Taguchi T, Yunoki S, Watanabe R, Ohtsuki Y, Onishi S: **Overexpression of carbonic anhydrase-related protein XI promotes proliferation and invasion of gastrointestinal stromal tumors.** *Virchows Arch* 2005, **447(1):**66-73.
19. Lu SH, Takeuchi T, Fujita J, Ishida T, Akisawa Y, Nishimori I, Kohsaki T, Onishi S, Sonobe H, Ohtsuki Y: **Effect of carbonic anhydrase-related protein VIII expression on lung adenocarcinoma cell growth.** *Lung Cancer* 2004, **44(3):**273-280.
20. Ishihara T, Takeuchi T, Nishimori I, Adachi Y, Minakuchi T, Fujita J, Sonobe H, Ohtsuki Y, Onishi S: **Carbonic anhydrase-related protein VIII increases invasiveness of non-small cell lung adenocarcinoma.** *Virchows Arch* 2006, **448(6):**830-837.
21. Nishikata M, Nishimori I, Taniuchi K, Takeuchi T, Minakuchi T, Kohsaki T, Adachi Y, Ohtsuki Y, Onishi S: **Carbonic anhydrase-related protein VIII promotes colon cancer cell growth.** *Mol Carcinog* 2007, **46(3):**208-214.
22. Jiao Y, Yan J, Zhao Y, Donahue LR, Beamer WG, Li X, Roe BA, Ledoux MS, Gu W: **Carbonic anhydrase-related protein VIII deficiency is associated with a distinctive lifelong gait disorder in waddles mice.** *Genetics* 2005, **171(3):**1239-1246.
23. Turkmen S, Guo G, Garshasbi M, Hoffmann K, Alshalah AJ, Mischung C, Kuss A, Humphrey N, Mundlos S, Robinson PN: **CA8 mutations cause a novel syndrome characterized by ataxia and mild mental retardation with predisposition to quadrupedal gait.** *PLoS Genet* 2009, **5(5):**e1000487.
24. Picaud SS, Muniz JR, Kramm A, Pilka ES, Kochan G, Oppermann U, Yue WW: **Crystal structure of human carbonic anhydrase-related protein VIII reveals the basis for catalytic silencing.** *Proteins* 2009, **76(2):**507-511.

25. Kato K: **Sequence of a novel carbonic anhydrase-related polypeptide and its exclusive presence in Purkinje cells.** *FEBS Lett* 1990, **271(1-2):**137-140.
26. Bellingham J, Gregory-Evans K, Gregory-Evans CY: **Sequence and tissue expression of a novel human carbonic anhydrase-related protein, CARP-2, mapping to chromosome 19q13.3.** *Biochem Biophys Res Commun* 1998, **253(2):**364-367.
27. Hirasawa M, Xu X, Trask RB, Maddatu TP, Johnson BA, Naggert JK, Nishina PM, Ikeda A: **Carbonic anhydrase related protein 8 mutation results in aberrant synaptic morphology and excitatory synaptic function in the cerebellum.** *Mol Cell Neurosci* 2007, **35(1):**161-170.
28. Antal Nógrádi NJ, Richard Walker, Keith Caddy, Nick Carter, Christiane Kelly: **Carbonic anhydrase II and carbonic anhydrase-related protein in the cerebellar cortex of normal and lurcher mice.** *Developmental Brain Research* 1997, **98:**91-101.
29. Lakkis MM, O'Shea KS, Tashian RE: **Differential expression of the carbonic anhydrase genes for CA VII (Car7) and CA-RP VIII (Car8) in mouse brain.** *J Histochem Cytochem* 1997, **45(5):**657-662.
30. Junji Hirota HA, Kozo Hamada, Katsuhiko Mikoshiba: **Carbonic anhydrase-related protein is a novel binding protein for inositol 1,4,5-trisphosphate receptor type 1.** *Biochem J* 2003, **372:**435-441.
31. Kleiderlein JJ, Nisson PE, Jessee J, Li WB, Becker KG, Derby ML, Ross CA, Margolis RL: **CCG repeats in cDNAs from human brain.** *Hum Genet* 1998, **103(6):**666-673.
32. **Ensembl genome database** [http://www.ensembl.org/]
33. **Universal Protein Resource** [http://www.uniprot.org/]
34. **Non-redundant database of DNA, RNA, and protein sequences** [http://www.ncbi.nlm.nih.gov/RefSeq/]
35. Altschul SF, Gish W, Miller W, Myers EW, Lipman DJ: **Basic local alignment search tool.** *J Mol Biol* 1990, **215(3):**403-410.
36. **UCSC Genome Browser** [http://genome.ucsc.edu/]
37. Larkin MA, Blackshields G, Brown NP, Chenna R, McGettigan PA, McWilliam H, Valentin F, Wallace IM, Wilm A, Lopez R, *et al.*: **Clustal W and Clustal X version 2.0.** *Bioinformatics* 2007, **23(21):**2947-2948.
38. Birney E, Clamp M, Durbin R: **GeneWise and Genomewise.** *Genome Res* 2004, **14(5):**988-995.
39. **Align Sequences using Clustal W2 EBI** [http://www.ebi.ac.uk/Tools/clustalw2/]
40. Nicholas KB, Nicholas HB Jr, Deerfield DW II: **GeneDoc: Analysis and Visualization of Genetic Variation.** *EMBNEWNEWS* 1997, **4:**14.
41. Tamura K, Dudley J, Nei M, Kumar S: **MEGA4: Molecular Evolutionary Genetics Analysis (MEGA) software version 4.0.** *Mol Biol Evol* 2007, **24(8):**1596-1599.
42. Pfaffl MW: **A new mathematical model for relative quantification in real-time RT-PCR.** *Nucleic Acids Res* 2001, **29(9):**e45.

doi: 10.1186/1471-2199-11-25
**Cite this article as:** Aspatwar *et al.*, Phylogeny and expression of carbonic anhydrase-related proteins *BMC Molecular Biology* 2010, **11**:25

*Human Molecular Genetics, 2013, Vol. 22, No. 3* ***417–432***
*doi:10.1093/hmg/dds438*
*Advance Access published on October 18, 2012*

# Abnormal cerebellar development and ataxia in CARP VIII morphant zebrafish

**Ashok Aspatwar[1,*], Martti E.E. Tolvanen[2], Eija Jokitalo[3], Mataleena Parikka[2], Csaba Ortutay[2], Sanna-Kaisa E. Harjula[2], Mika Rämet[2], Mauno Vihinen[2,4,5] and Seppo Parkkila[1,4]**

[1]Institute of Biomedical Technology and School of Medicine, [2]Institute of Biomedical Technology, University of Tampere and BioMediTech, Tampere 33014, Finland, [3]Electron Microscopy Unit, Institute of Biotechnology, University of Helsinki, Helsinki 00014, Finland, [4]Fimlab Laboratories, University of Tampere Hospital, Tampere 33014, Finland and [5]Department of Experimental Medical Science, Lund University, Lund, Sweden

Received September 19, 2012; Revised September 19, 2012; Accepted October 11, 2012

**Congenital ataxia and mental retardation are mainly caused by variations in the genes that affect brain development. Recent reports have shown that mutations in the *CA8* gene are associated with mental retardation and ataxia in humans and ataxia in mice. The gene product, carbonic anhydrase-related protein VIII (CARP VIII), is predominantly present in cerebellar Purkinje cells, where it interacts with the inositol 1,4,5-trisphosphate receptor type 1, a calcium channel. In this study, we investigated the effects of the loss of function of CARP VIII during embryonic development in zebrafish using antisense morpholino oligonucleotides against the *CA8* gene. Knockdown of *CA8* in zebrafish larvae resulted in a curved body axis, pericardial edema and abnormal movement patterns. Histologic examination revealed gross morphologic defects in the cerebellar region and in the muscle. Electron microscopy studies showed increased neuronal cell death in developing larvae injected with *CA8* antisense morpholinos. These data suggest a pivotal role for CARP VIII during embryonic development. Furthermore, suppression of *CA8* expression leads to defects in motor and coordination functions, mimicking the ataxic human phenotype. This work reveals an evolutionarily conserved function of CARP VIII in brain development and introduces a novel zebrafish model in which to investigate the mechanisms of CARP VIII-related ataxia and mental retardation in humans.**

## INTRODUCTION

Neurodegenerative disorders are a complex group of diseases caused mainly by genetic factors leading to motor disturbance, cognitive loss and psychiatric manifestations. Several genes have reported involvement in the development of neurologic disorders in humans, mostly due to mutations. In many instances, the genetic causes may involve as yet unknown genes. Recent studies in humans have shown that mutations in the *CA8* gene lead to mental retardation, ataxia and, in some instances, a quadrupedal gait (1,2). Similarly, a spontaneously occurring mutation in the *Car8* gene in waddle (*wdl*) mice leads to ataxia and a lifelong gait disorder (3). These studies demonstrate that novel genes with poorly characterized functions may be involved in the development of neurodegenerative disorders in humans.

The members of the mammalian α-carbonic anhydrase (α-CA) gene family are zinc-containing metalloenzymes that catalyze the reversible hydration of carbon dioxide (4–6). There are typically 16 isoforms in α-CA gene family in most mammals, of which 13 isozymes (CA I, II, III, IV, VA, VB, VI, VII, IX, XII, XIII, XIV and XV) are catalytically active. Three of the isoforms, namely, carbonic anhydrase-related proteins (CARPs) VIII, X and XI, represent catalytically inactive isoforms due to the lack of one or more of the three histidine residues required for CA catalytic activity (7).

Previous studies (8), including our recent investigations (9), showed predominant expression of all the CARPs in the brain. Expression analysis using both reverse transcriptase-quantitative PCR (RT-qPCR) and immunohistochemistry showed that carbonic anhydrase-related protein VIII (CARP

*To whom correspondence should be addressed. Tel: +358-503186251; Fax: +358-3-3641-482; Email: ashok.aspatwar@uta.fi

VIII) is highly expressed in the Purkinje cells of the cerebellum, whereas CARP X and XI show a more widespread distribution throughout the central nervous system (CNS). Although the wide distribution patterns suggest important roles for CARPs in the CNS, their precise functions are still unclear.

Phylogenetic analysis revealed that a highly conserved ortholog of human CARP VIII is present in zebrafish, with 79% protein sequence identity compared with human CARP VIII (9,10). Expression analysis showed that the *CA8* gene is expressed in both the zebrafish larvae and adult fish. This prompted us to use zebrafish as a model organism to knockdown the *CA8* gene to study the role of CARP VIII during embryonic development.

Many of the genes involved in neurodegenerative disorders play important roles in brain development during embryogenesis. Although the structure of the brain exhibits considerable differences among the vertebrate species, the molecular basis of brain development is relatively conserved (11). The zebrafish has recently emerged as an attractive model organism for studying vertebrate development, as it uniquely combines the advantages of genetic tractability with biologic relevance (12,13).

Thus far, there are neither studies on the role of CARP VIII during embryonic development in vertebrates, nor are there any targeted gene knockout or knockdown studies on CARP VIII to evaluate its function. Here, we investigate the role of CARP VIII in the zebrafish model during embryogenesis.

## RESULTS

### Bioinformatic analysis of zebrafish CARP VIII suggests an interaction with inositol 1,4,5-trisphosphate receptor type 1 (ITPR1)

Similar to mice and humans, zebrafish have an ortholog of the *CA8* gene, as reported previously (9). We obtained the zebrafish *CA8* transcript and protein sequences from Ensembl (transcript ID: ENSDART00000057098, protein ID: ENSDARP00000057097). The zebrafish transcript is encoded by a 23.49 kb gene located on the forward strand of chromosome 2. The gene contains 9 exons that code for 281 amino acids, whereas the mouse and human transcripts are encoded by genes of more than 90 kb in length, which are located on the reverse strand of chromosomes 4 and 8, respectively. A major portion of exon 1, a small part of exon 8, and all of exon 9 are non-coding, similar to mouse and human transcripts (Fig. 1A). The organization of coding exons in *CA8* of zebrafish is the same as in all orthologs we have studied. Figure 1B shows a representation of aligned protein sequences, which highlights the fact that all exon boundaries in *CA8* have been maintained in the same locations through deuterostome evolution.

Comparisons of the deduced amino acid sequence of the zebrafish CARP VIII (Ensembl protein ID: ENSDARP 00000057097) with the human and mouse CARP VIII sequences displayed a 79% overall amino acid identity, and the amino acid identity within the CA domain (amino acids 40–290 in the human sequence) was 84% (Fig. 2A). The deduced amino acid sequence of zebrafish CARP VIII is slightly shorter (281 amino acids) than the mouse and human CARP VIII proteins (291 and 290 amino acids, respectively). The difference is mainly due to the absence of seven glutamic acid (E) residues at the N-terminus of zebrafish CARP VIII.

Sequencing of the *CA8* cDNA revealed nucleotide variations at three places, but the amino acid sequence deduced from the nucleotide sequence did not show any change in the amino acid sequence, when compared with the sequence from the database (Supplementary Material, Figure S1).

The high degree of homology between the CARP VIII sequences suggests a conserved and essential function. CARP VIII interacts with the inositol 1,4,5-trisphosphate receptor type 1 (ITPR1), an ion channel protein that regulates internal $Ca^{2+}$ ion release (14). A schematic of the primary structure of ITPR1 is shown in Supplementary Material, Figure S2. It contains major domains for binding calmodulin and inositol trisphosphate (IP3), a channel domain and a modulatory domain. Deletion mutants have been used to map the binding of CARP VIII to the region of amino acids 1387–1647 within the modulatory domain (14). The binding of CARP VIII to ITPR1 is believed to reduce the sensitivity of ITPR1 to inositol trisphosphate (IP3) and control the release of $Ca^{2+}$ ions from the internal stores of the endoplasmic reticulum (15). Deletion mutagenesis experiments in a yeast two-hybrid system showed that almost the entire CA domain of CARP VIII is required for ITPR1 binding. Only one of the truncated constructs, which was missing the first 44 residues, showed binding, and even then, the reaction was slower (14).

To assess the functional association between ITPR1 and CARP VIII throughout the vertebrate evolution, we performed two coevolution analyses of genes coding for CARP VIII and ITPR1 in 31 species. In one analysis, the ITPR1 sequences included the 6 fish orthologs for *itpr1a* of *Danio rerio* together with 25 tetrapod sequences. In another analysis, the six fish orthologs for *itpr1b* of *D. rerio* were used instead. All ITPR1 sequences were restricted to the region of approximately 270 amino acids corresponding to the CARP VIII binding region in ITPR1 (14). Our results from the *itpr1a* orthologs show that the two protein sequences have several coevolving sites that are significant (chi-squared test, $P < 0.001$). The analysis with the fish *itpr1b* orthologs also suggested coevolution, but with a lower *P*-value ($P < 0.05$). This indicates that the gene product of *itpr1a* is more likely to have retained the interaction with CARP VIII in fish.

When the results of the coevolution analyses are projected on the 3D structure of human CARP VIII, we can observe a cluster of surface residues in which variations correlate strongly with variations in ITPR1 binding (Fig. 2B). Within residues 150–157, five residues show correlation coefficients of 0.95 or higher. They are localized in a single loop region, and both known human disease-causing *CA8* mutations are near this region. The G162R mutation (1) is found in the end of this loop. Any non-glycine residue in this position would cause a large change in the conformation and/or localization of the loop. Regarding this location, the researchers who first reported this location actually depicted G193 instead of G162 in their figure (1). The mutation S100P (2) is in the adjacent loop (Fig. 2B). This mutation is likely to change the conformation of the entire loop 100–109, which would also interfere with the loop 147–162.

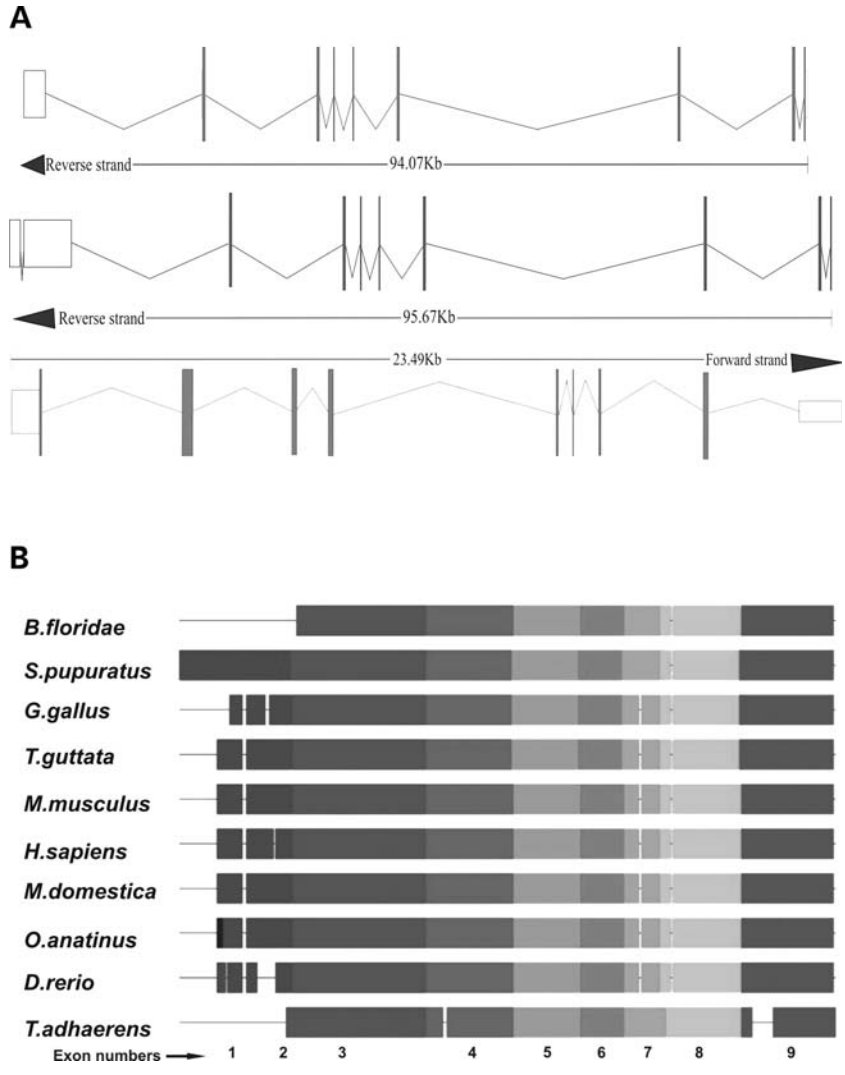


**Figure 1.** Exon structures: (**A**) A comparison of the *CA8* transcripts of human, mouse and zebrafish. A schematic representation of transcripts of human (ID: ENST00000317995), mouse (ID: ENSMUST00000066674) and zebrafish (ID: ENSDART00000057098). The exons are represented by vertical bars. The closed bars represent the coding exons, and the open bars are the non-coding exons. The introns are shown as horizontal bars. (**B**) The organization of coding exons in different organisms when compared with that of zebrafish, derived from a protein alignment. The gaps correspond to the alignment, and consecutive exons are shown in different shades. The exon boundaries have been retained in the same locations throughout the deuterostome evolution.

The coevolution results and the examination of mutation sites lead us to suggest that the region that contains residues 150–157 interacts with ITPR1. The coevolving and possibly interacting residues in ITPR1 are 15 residues in the range 1437–1630 (numbering by human ITPR1, isoform 1).

### Zebrafish *CA8* is strongly expressed in the nervous system

To confirm the presence of the *CA8* gene in zebrafish, we first designed primers to amplify genomic DNA (Table 1) and performed PCR analysis of genomic DNA from six different AB strains of zebrafish. We analyzed the expression of the *CA8* gene from total mRNA of 0 day post fertilization (dpf) to 5 dpf larvae and confirmed the presence of *CA8* gene in all developing larvae (Fig. 3A).

Next, we studied the expression pattern of *CA8* mRNA in 12 different tissues of adult zebrafish by RT-qPCR. *CA8* mRNA was expressed in almost all of the tissues analyzed (Fig. 3B). The expression was high in the brain, heart, kidney, eye and skin. Low levels of expression were observed in the male and female gonads, bowel, liver and gills, and very low levels were seen in the muscle. The expression studies using polyclonal antibodies against human CARP VIII showed strong expression of CARP VIII protein in the Purkinje cells of the zebrafish cerebellum but failed to detect any expression in the cerebrum (Fig. 3C and E).

### Zebrafish *CA8* mRNA is expressed during early development

To knockdown the *CA8* gene using antisense morpholino oligonucleotides (MOs), we first checked the expression pattern of the *CA8* gene in 1–5 dpf larvae. After isolating total mRNA, we pooled the RNA at each time point from

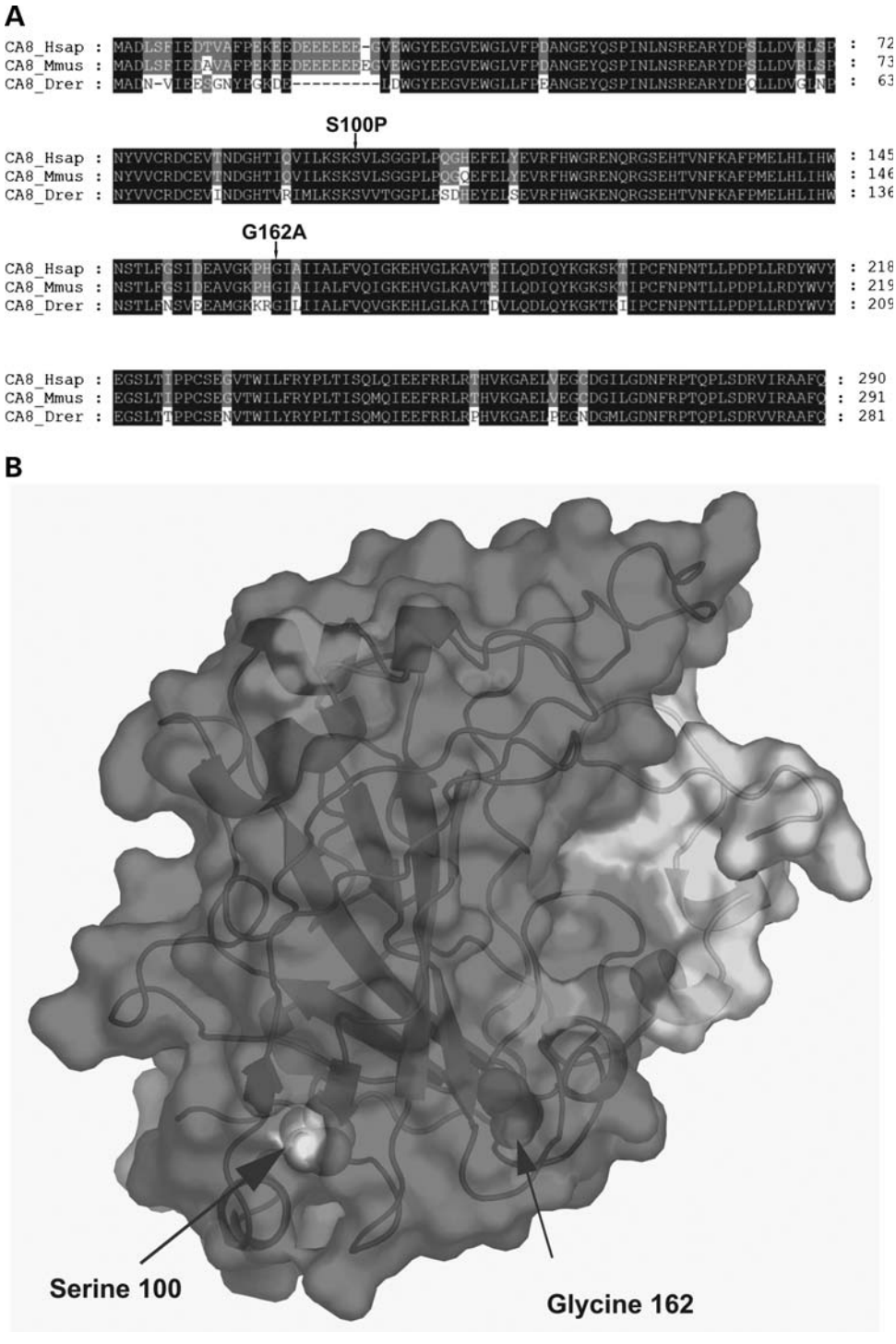


**Figure 2.** Alignment of human, mouse and zebrafish CARP VIII sequences. (**A**) The alignment of the amino acid sequences of CARP VIII. The zebrafish sequence lacks seven glutamic acid (E) residues at N-terminal region. The region responsible for binding to IP3R1 (amino acids 45–290) is highly conserved. The amino acids substituted in homozygous recessive human patients are indicated with arrows. (**B**) The 3D structure of CARP VIII and coevolution analysis. The crystallographic structure of human CARP VIII (2W2J) (26) was retrieved from PDB (27) and visualized with the PyMOL Molecular Graphics System (Version 1.3.1, Schrödinger, LLC). Arrows indicate two human disease-causing variation sites: G162 in red, S100 in white. Residues 23–44 in gray are not included in the minimal ITPR1-binding region. Residues 1–22 are missing from the structure. The other colors identify residues that correlate strongly with at least one residue in the CARP VIII binding region of ITPR1 (1368–1649 in human ITPR1 isoform 1), with different colors for various ranges of correlation coefficient: cyan (0.92 . . . 0.97), yellow (0.97 . . . 0.980) and magenta (0.98 . . . 1).

**Table 1.** Primer sequences for PCR, RT-PCR, RT-qPCR and sequences for antisense morpholinos

| Primer name | Forward primer | Reverse primer | Morpholino sequence name | MO sequence |
|---|---|---|---|---|
| CA8 G-DNA PCR | 5′GTATTGTGATACATCAGTTT3′ | 5′TTAAGCCAAACTGAGACAGG3′ | *CA8* antisense MO1 | 5′CGTGGAGAGAAGATTGAGTTGCCAT 3′ |
| CA8 RT-PCR | 5′TTCACTGGGGCAAAGAAAAC3′ | 5′ATGGCCTTCAGACCAAGATG 3′ | *CA8* antisense MO2 | 5′ AGGATCATGCTGAAATCCAAATCTG3′ |
| CA8 RT-qPCR | 5′CCCATGTTAAAGGAGCAGAGCTT3′ | 5′GGTTGGGTCGGTCTAAAGTTGT3′ | RC MO | 5′CCTCTTACCTCAGTTACAATTTATA3′ |
| ITPR1- RT-qPCR | 5′CCTGGGAGCTTTCAATGTTTG3′ | 5′CGATAACCCCGGGTGAATG3′ | p53 MO sequence | 5′ GCGCCATTGCTTTGCAAGAATTG 3′ |

1–5 dpf of zebrafish larvae. Next, we performed reverse transcriptase-PCR (RT-PCR) to synthesize the cDNA using the primers designed based on the *D. rerio* ortholog found in the Ensembl database, targeting a 100 bp region of *CA8* gene (Table 1). The expression of *CA8* mRNA was observed in all five time points in 1–5 dpf larvae (Fig. 3A).

To determine if the *CA8* gene product is required for embryonic development, we first checked its mRNA expression during development. The relative expression levels of *CA8* mRNA from 0 h post fertilization (hpf) to 168 hpf are shown in Supplementary Material, Figure S3A. The high level of *CA8* mRNA at 0 hpf suggested that it is important during early development and that the *CA8* transcript is of maternal origin. The expression of *CA8* mRNA throughout the analysis suggests that the *CA8* gene is required for embryonic development in zebrafish.

## Developmental expression of *itpr1a* mRNA is similar to *CA8* mRNA expression

Based on the expression analysis of *CA8* mRNA using RT-qPCR, *CA8* mRNA was of maternal origin and was present in zebrafish larvae at the beginning of development. It has been suggested that CARP VIII interacts with ITPR1 and functions as a cytosolic calcium signaling modulator by reducing the sensitivity of IP3 to ITPR1 (15). If this function is relevant during embryogenesis, we hypothesized that ITPR1 should also be expressed early in development, similar to *CA8* mRNA. Out of the two ITPR1 paralogs, *itpr1a* and *itpr1b*, our coevolution analyses suggested that the *itpr1a* gene product is more likely to interact with CARP VIII. We, therefore, analyzed the expression of *itpr1a* mRNA at different time points during early embryonic development. After isolating total mRNA, we synthesized cDNA and then analyzed the expression of *itpr1a* mRNA using RT-qPCR with primers designed according to the zebrafish sequence ENSDART00000149019 from the Ensembl database.

The relative expression pattern of *itpr1a* mRNA from 0 hpf to 168 hpf is shown in Supplementary Material, Figure S3B. A high level of *itpr1a* mRNA at 0 hpf suggested that *itpr1a* mRNA is of maternal origin, similar to *CA8* mRNA, and it is most likely required during embryonic development along with *CA8*. As shown in Supplementary Material, Figure S3A and B, both *itpr1a* and *CA8* mRNA levels show parallel changes during the initial phase of zebrafish embryogenesis, perhaps due to a functional interplay between these proteins in the developmental processes.

## Knockdown of *CA8* causes developmental defects in zebrafish larvae

Gene-specific antisense MOs have been widely used to suppress the expression of genes in zebrafish larvae. We designed two MOs (MO1 and MO2) (see ‘Materials and Methods’), MO1 was expected to block the translation of the *CA8* gene and MO2 was designed to block the splice junction at intron 3 and exon 4, as shown in Figure 4A. The *CA8* antisense MO1 targets a sequence that includes the ATG start codon (from −15 to +10 relative to ATG) that inhibits the translation of *CA8* mRNA. The MO2 targets exon 4 resulting in

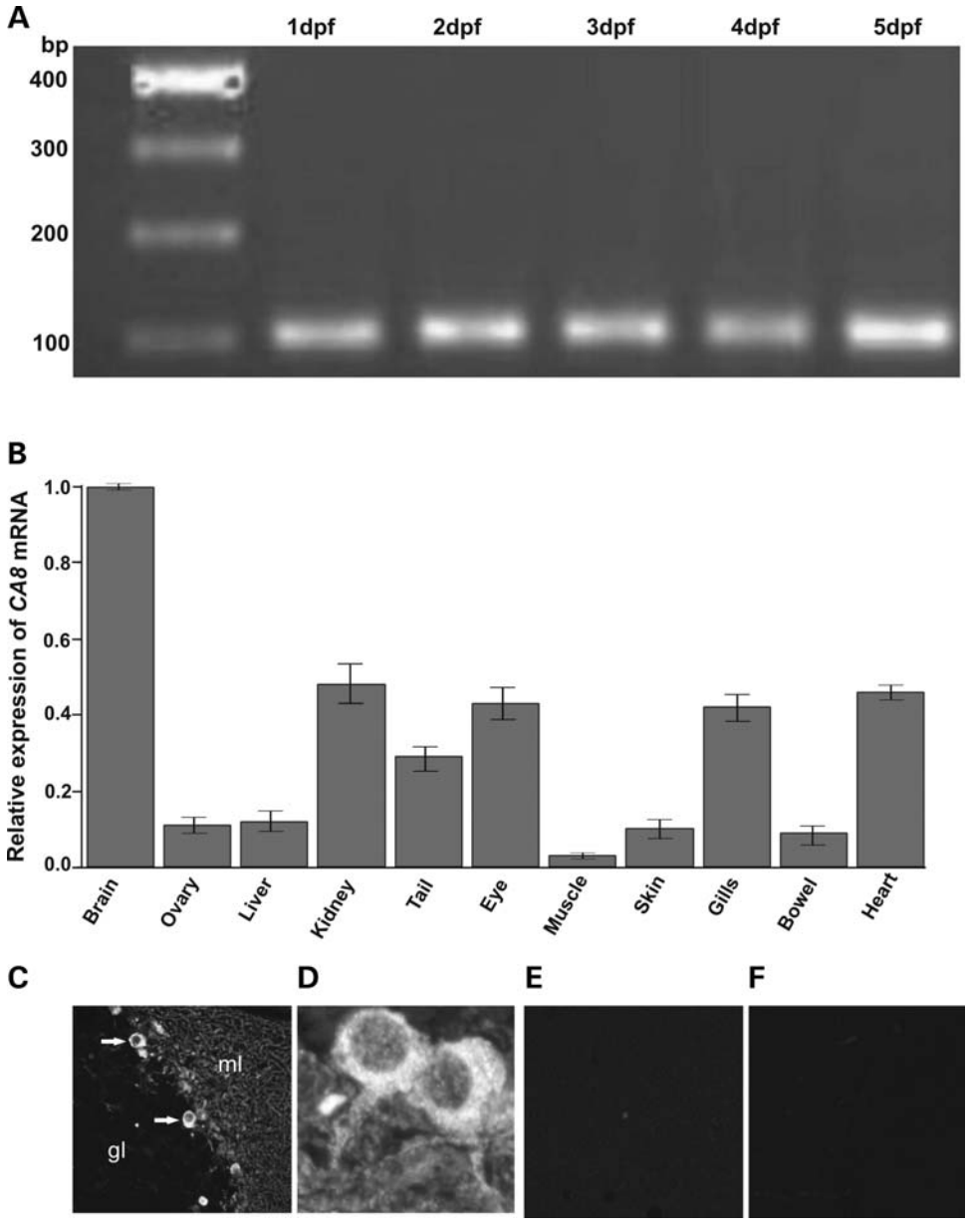


**Figure 3.** Expression analysis of *CA8* mRNA and the CARP VIII protein. (**A**) *CA8* mRNA is expressed throughout the development of zebrafish larvae. RT-PCR amplification of total mRNA from 1 to 5 dpf zebrafish larvae is shown. (**B**) The expression of CARP VIII mRNA (NM_001017571.1) in different tissues in adult zebrafish as determined using RT-qPCR. All values are expressed relative to the expression of mRNA in the brain, which was assigned a relative value of 1, and the values were normalized by inclusion of an internal control gene beta actin according to the pfuffl (24). (**C** and **D**) CARP VIII is expressed in the Purkinje cells of cerebellum. Immunohistochemical analysis was carried out using polyclonal antibodies raised against human CARP VIII. (**E**) CARP VIII is not detected in the cerebrum by immunostaining. (**F**) A negative staining control using rabbit non-specific IgG antibody instead of the CARP VIII antibody (C, E and F, magnification 20× and D 40×).

expression of shorter length *CA8* gene. These antisense MOs were used to analyze the role of *CA8* in zebrafish embryonic development. Uninjected larvae and those injected with random control (RC) morpholinos were used as controls for the phenotypic analysis of 1–5 dpf larvae.

We used western blot analysis to determine the expression of CARP VIII and RT-PCR analysis of *CA8* mRNA to ensure the effectiveness of the *CA8* antisense MO1 and MO2. As shown in the Figure 4B and C, western blotting of the 3 dpf uninjected (wild type) zebrafish lysates using polyclonal antibodies raised against 100 amino acids of the N-terminal domain of human CARP VIII detected a 32 kDa band. In contrast, lysates from the larvae injected with 125 μM *CA8*-MO1 did not show any band after 3 dpf (Fig. 4B). After 5 dpf, the lysates from larvae injected with 125 μM *CA8*-MO1 showed a lower intensity 32 kDa band, when compared with the wild-type embryo lysates (Fig. 4C). This indicates that the *CA8* antisense MO1 suppresses CARP VIII expression in 3 dpf zebrafish larvae. Similarly, analysis of mRNA from 5 dpf morphant embryos injected

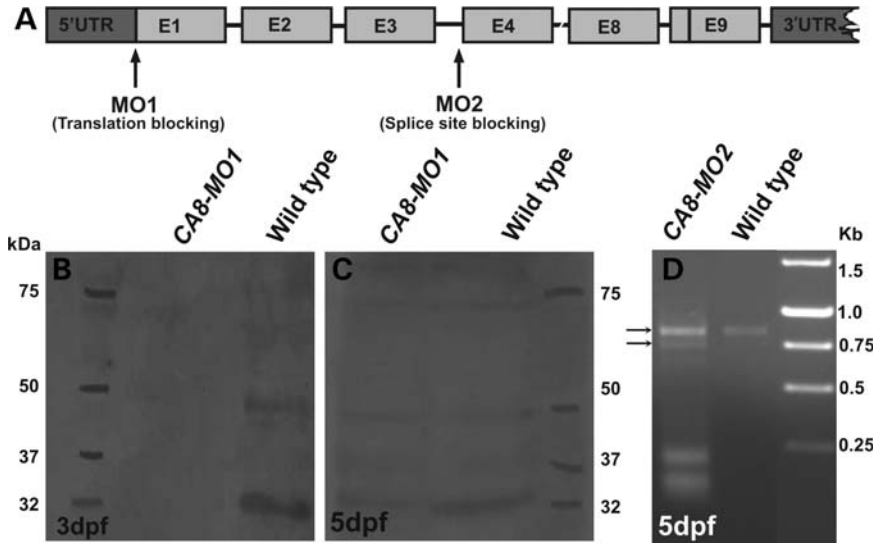


**Figure 4.** Western blotting and mRNA analysis of wild-type and *CA8* morphant larvae. (**A**) Schematic presentation of *CA8* mRNA showing the sites of translational blocking at the beginning of exon one (arrow) and splice site blocking at the junction of intron 3 and exon 4 as indicated by an arrow. (**B**) Western blotting analysis of lysates from 3 dpf zebrafish larvae microinjected with 125 μM *CA8*-MO1 indicates efficient suppression of CARP VIII protein expression. (**C**) The western blot of samples extracted from 5 dpf morphant larvae microinjected with 125 μM *CA8*-MO1 morpholinos shows the reappearance of the CARP VIII protein at the end of 5 dpf. (**D**) RT-PCR analysis of mRNA from morphant and control larvae analyzing the changes in the mRNA length of *CA8* gene caused by MO2.

with 250 μM *CA8*-MO2 showed a shorter length mRNA as a lower intensity band in addition to normal length mRNA, suggesting a partial knockdown of *CA8* with MO2, as shown in Figure 4D.

Larvae injected with 125 μM *CA8*-MO1 showed abnormal changes in the head as early as 9 hpf (data not shown). The 1 dpf zebrafish larvae injected with 125 μM *CA8*-MO1 showed defects in the head with a fragile and more easily breakable body, curved tail, small eye size and pericardial edema (Fig. 5A). As development progressed, the abnormalities became more prominent; shortened tail, curved body axis, absence of swim bladder and otolith vesicles were observed, when compared with the control larvae (Fig. 5A). Interestingly, embryos injected with MO2 showed a less severe phenotype, when compared to the phenotype produced by MO1 (Fig. 4B). In dose–response analysis with the *CA8*-MO1, larvae showed no apparent phenotypic changes at low concentrations of *CA8*-MO1, whereas the increased concentrations of *CA8*-MO1 led to severe phenotypic defects with increased mortality (Supplementary Material, Figure S2A–G, and Table 2). The injection of 2 μM *CA8*-MO1 per embryo did not produce any visible defects or changes in the mortality rate, when compared with the uninjected controls (Supplementary Material, Figure S4B, Table 2); however, the swimming pattern was abnormal, suggesting that 2 μM *CA8*-MO1 is the minimum dose required to produce the knockdown effect of *CA8* (Supplementary Material, Movie S2). The next higher concentration examined was 6 μM *CA8*-MO1, which showed a slightly visible functional defect during swimming (Supplementary Material, Figure S4C and S5B) and a mortality rate of 10.6% (Fig. 5C and Table 2). The larvae injected with concentrations of 10 μM, 75 μM, 125 μM, 250 μM and 500 μM *CA8*-MO1 showed moderate to severe phenotypic defects, and the mortality rate increased in larvae injected with 75 μM or higher *CA8*-MO1 (Fig. 5C, Table 2). There was no difference between the phenotype defects or mortality rates of larvae injected with *CA8*-MO1 alone or together with *p53*-MOs (Fig. 5C and Table 2). The western blot results (Fig. 4B and C) suggested that the concentration required for the complete knockdown of *CA8* gene was 125 μM, at which level the morphant larvae showed severe phenotypic defects. Therefore, 125 μM MO1 was the optimal effective concentration used for the most of the experiments in this study. However, the phenotype of 5 dpf larvae injected with 125 μM concentration of MO2 was similar to the phenotype of 6 μM MO1-injected larvae and showed an abnormal swim pattern (Supplementary Material, Movie S5).

### *CA8* morphant zebrafish have increased neuronal cell death in the cerebellum

Expression analyses of the *CA8* gene in zebrafish tissues showed a widespread distribution of *CA8* mRNA (Fig. 3B). The highest expression was observed in the brain, with lower levels of expression in other organs, suggesting an important function in several tissues. We studied morphologic changes in larvae injected with 125 μM *CA8*-MO1 and compared the findings with control larvae injected with RC MOs and *p53* MOs. We made semithin (10 μm) sections of 5 dpf control larvae and larvae injected with 125 μM *CA8*-MO1 and stained them with hematoxylin and eosin. The 125 μM *CA8*-MO1-injected larvae showed gross morphologic changes in the cerebellar region with a reduction in the size of the cerebellum (Fig. 6H). Similarly, there was a clear difference between the somites of control larvae and those of the *CA8*-MO-injected morphant larvae. The *CA8*-MO1-injected zebrafish showed abnormal muscle development, when compared with the control zebrafish larvae (data not shown).

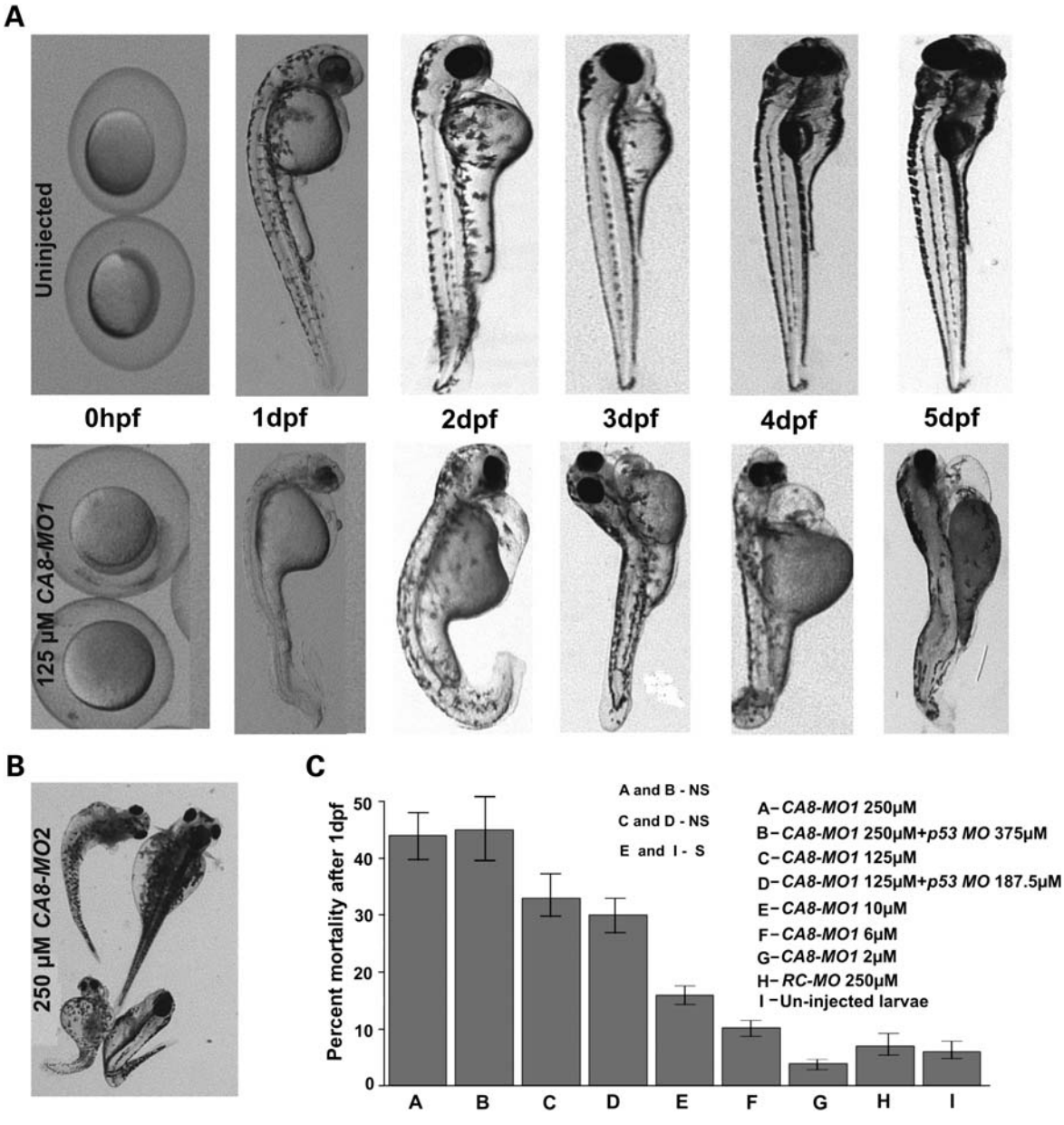


**Figure 5.** The *CA8* gene product is essential for the normal embryogenesis of zebrafish. Developmental images are shown over the period of 0–5 dpf of zebrafish larvae injected with 125 μM translational blocking antisense morpholinos (MO1) for the *CA8* gene when compared with normal (uninjected) larvae. (**A**) The top row of images show lateral views of 0–5 dpf uninjected zebrafish larvae with the gradual, normal development of organs, the disappearance of yolk sac and the appearance of swim bladder at the end of 5 dpf. The bottom row of images show lateral views of *CA8* morphants embryo from 0 to 5 dpf showing morphologic changes at 24 hpf with abnormal shaped head, tail and yolk sac and the beginning of dilation of the pericardium. (**B**) The 5 dpf larvae injected with 250 μM of *CA8*-MO2 (splice site blocking) showing a defective phenotype. (**C**) The percent mortality in *CA8* morphant larvae at 24 hpf. The histogram shows the percentage of dead larvae in each group injected with different concentrations of *CA8*-MO1 when compared with the RC-injected and uninjected zebrafish larvae. The mortality rate was significantly higher ($P < 0.001$) in the larvae injected with greater than 10 μM *CA8*-MO1. There was no difference in mortality rates of the larvae injected with *p53*-MOs along with *CA8*-MOs and larvae injected with *CA8*-MO1 alone.

The TdT-UTP nick end labeling (TUNEL) assay showed cells undergoing apoptosis in the head region and periphery of tail region in the larvae injected with 125 μM *CA8*-MO1, whereas there was no detectable signal for apoptosis in the wild-type larvae (Fig. 6A–D).

After finding the morphologic changes in the cerebellum by histologic staining and light microscopy and cell death in the head region by the TUNEL assay, we analyzed the cerebellar region of the zebrafish injected with 125 μM *CA8*-MO1 using transmission electron microscopy to detect any ultrastructural changes occurring as a consequence of knockdown of the *CA8* gene. The only significant change at the ultrastructural level was the increased neuronal cell death (the apoptotic changes included a condensed nucleus, fragmented mitochondrial profiles and debris of dead cells) that was observed in samples from the MO1-injected zebrafish, when compared with the

**Table 2.** Phenotypes of 24 hpf zebrafish larvae knocked down with different concentrations of *CA8* antisense morpholinos

| Morpholino (μM) | Normal | Mild | Moderate | Severe | Dead | Total |
|---|---|---|---|---|---|---|
| *CA8* MO 250[a] | 0 (0) | 0 (0) | 15 (10) | 69 (46) | 66 (44) | 150 |
| *CA8* MO 250 + p53 375[a] | 0 (0) | 0 (0) | 14 (9.3) | 71 (47.3) | 68 (45.3) | 150 |
| *CA8* MO 125[b] | 11 (2.2) | 0 (0) | 8 (1.6) | 311 (62.2) | 162 (32.4) | 500 |
| *CA8* MO 125 + p53187.5[b] | 13 (2.6) | 7 (1.4) | 9 (1.8) | 320 (64) | 151 (30.2) | 500 |
| *CA8* MO 10[c] | 8 (5.3) | 18 (12) | 93 (62) | 7 (4.6) | 24 (16) | 150 |
| *CA8* MO 6[c] | 20 (13.3) | 104 (69.3) | 11 (7.3) | 23 (15.3) | 16 (10.6) | 150 |
| *CA8* MO 2[c] | 132 (88) | 12 (8) | 0 (3.3) | 0 (15.3) | 6 (4.0) | 150 |
| RC MO[b]468 | (93.6) | 0 (0) | 0 (3.3) | 0 (15.3) | 32 (6.4) | 500 |
| Uninjected[b] | 472 (94.4) | 0 (0) | 5 (1.0) | 23 (4.6) | 28 (5.6) | 500 |

The phenotypic data were obtained from total of 3[a], 10[b] and 2[c] independent sets of morpholino injections with a minimum of 50 zebrafish larvae per group. The total number of larvae examined for each phenotypic class is shown as percentage of total number of larvae studied for each concentration of morpholinos. RC morpholino injections were made with either RC-MO alone or RC-MOs together with p53 MOs (one-and-a-half times the RC-MO concentration). Larvae injected with 2 μM concentrations of MOs had a phenotype similar to uninjected larvae but showed abnormal swim patterns (Supplementary Material, Figure S2, and Movie S2).

wild-type larvae (Fig. 6E and F). There was no difference between the morphant larvae injected with *CA8*-MO1s alone or in combination with *p53*-MOs.

### *CA8* morphant zebrafish larvae have altered movement patterns

Because of the ataxia and lifelong gait disorder in *wdl* mice and ataxia and quadrupedal gait in human patients (1–3) due to spontaneously occurring mutations in the *CA8* gene, we analyzed whether the *CA8* knockdown changed the swimming behavior of 5 dpf zebrafish larvae. We compared spontaneous swimming behavior of 5 dpf control larvae (uninjected), larvae injected with RC morpholinos and larvae injected with different concentrations of antisense *CA8*-MO1. We expected that the larvae with body and tail abnormalities, induced by *CA8* antisense morpholinos with concentrations above 6 μM, would show abnormal swimming behavior. To test this hypothesis, we injected the larvae with minimum concentrations of 2 and 6 μM *CA8*-MO1. With these concentrations, the 5 dpf larvae showed normal body and tail development, similar to RC-injected and uninjected larvae (Supplementary Material, Figure S4A, B, and C). For each experiment, five different groups (uninjected and injected with *CA8*-MO1 concentrations of 2 μM, 6 μM, 10 and 100 μM) were analyzed for movement patterns.

We tracked the movement patterns of the 5 dpf larvae under the microscope in a 35 mm × 15 mm transparent polypropylene Petri dish filled with embryo medium containing a minimum of five zebrafish larvae. After placing the Petri dish under the microscope (Carl Zeiss Lumar V.12MicroImaging GmbH and software AxioVision versions 4.7 and 4.8.), the larvae were allowed to settle for at least 2 min, and the movement of larvae was observed for 10 min to trace the pattern of movement (shown schematically in Fig. 7A). The percentage of movement in *CA8*-MO1-injected larvae when compared with the control larvae was analyzed for each group (Fig. 7B). A 30 s movie of the movement patterns was also recorded and can be seen in Supplementary data (Supplementary Material, Movies S1–S4). The larvae injected with 2 μM *CA8*-MO1 had a slightly abnormal pattern of swimming, when compared with the wild-type larvae. When compared with the uninjected larvae, larvae injected with 6 μM concentrations of *CA8*-MO1s moved considerably slower, showed an increased turning angle and mostly swam along the periphery of the Petri dish. Additionally, the larvae injected with 6 μM *CA8*-MO1s showed a pronounced difficulty in balancing the body while swimming, when compared with the wild-type larvae (Supplementary Material, Figure S5A and B and Movies S1 and S2). Moreover, the larvae injected with 10 μM *CA8*-MO1s had severely restricted movement and showed occasional displacement at the corners of the Petri dish with great difficulty in balancing themselves (Supplementary Material, Figure S4 right and Movie S4). The larvae injected with 125 μM *CA8*-MO1s, which had severe phenotypic defects, exhibited occasional sideways turning and did not show any displacement. The larvae injected with 125 μM *CA8*-MO2, which had phenotypically normal appearance of the body, showed an abnormal swim pattern similar to the 6 μM *CA8*-MO1-injected larvae (Supplementary Material, Movie S5).

## DISCUSSION

Here, we show that the knockdown of the *CA8* gene, which is responsible for ataxia, gait disorder and mental retardation in human patients and mice, results in an abnormal movement pattern in zebrafish, mimicking the movement disorder in humans and mice. Our observations suggest that the suppression of *CA8* expression is responsible for the abnormal movement pattern in zebrafish larvae: (i) injection of *CA8* antisense MO1s at 2 μM concentration shows abnormal movement without any morphologic phenotypic defects, (ii) RC MOs do not show any change in the behavior or morphology even at very high (125 μM) concentrations and (iii) the abnormal movement and structural changes in the larvae were dependent on the concentration of the *CA8*-antisense morpholinos injected.

Evolutionarily conserved genes generally have important biologic functions, manifested through high selection pressure. The high conservation of CARP VIII across the species, exceeding even the conservation of enzymatically active CAs, and the very specific expression pattern in the brain

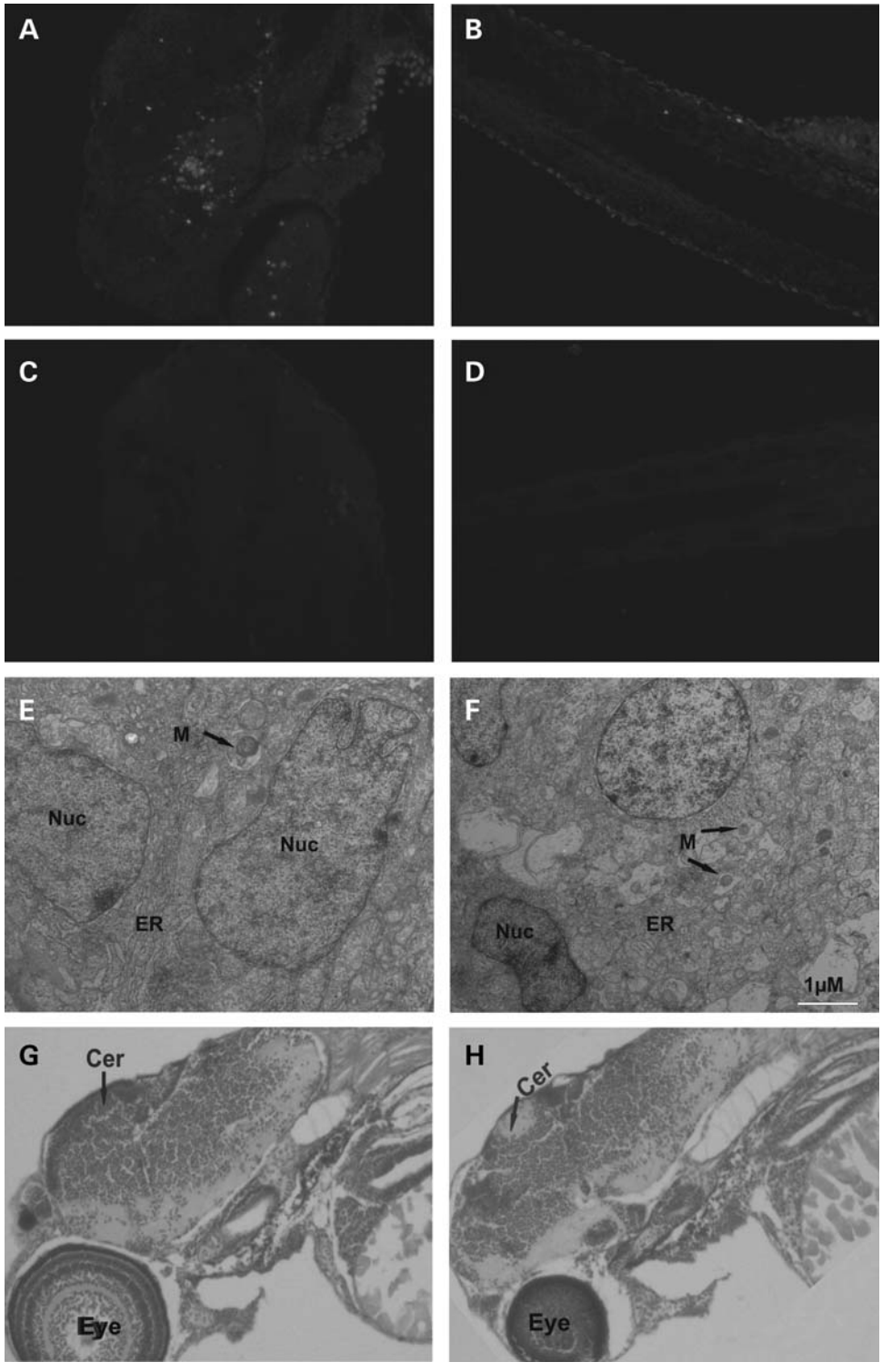


**Figure 6.** TUNEL assay, electron microscopy and histochemical staining. (**A**) At 5 dpf, prominent apoptosis was observed in head region of zebrafish larvae with the *CA8* gene knocked down. (**B**) Apoptosis was also observed at the periphery of the tail region in larvae knocked down for *CA8* gene. (**C** and **D**) There was no apoptosis in control larvae in either the head region C or tail region D. (**E**) A micrograph of control (uninjected) 5 dpf zebrafish larvae inside a normal neuronal cell in the cerebellum. (**F**) A micrograph of a 5 dpf zebrafish embryo injected with 125 μM *CA8*-MO1 showing inside of a neuronal cell undergoing apoptosis in the cerebellum. Abbreviations: M, mitochondria; ER, endoplasmic reticulum and Nuc, nucleus. (**G**) A sagittal section of the head region showing normal morphology of the cerebellar region, 20×. (**H**) A sagittal section of the head region showing abnormal morphology of the cerebellar region, 20×.

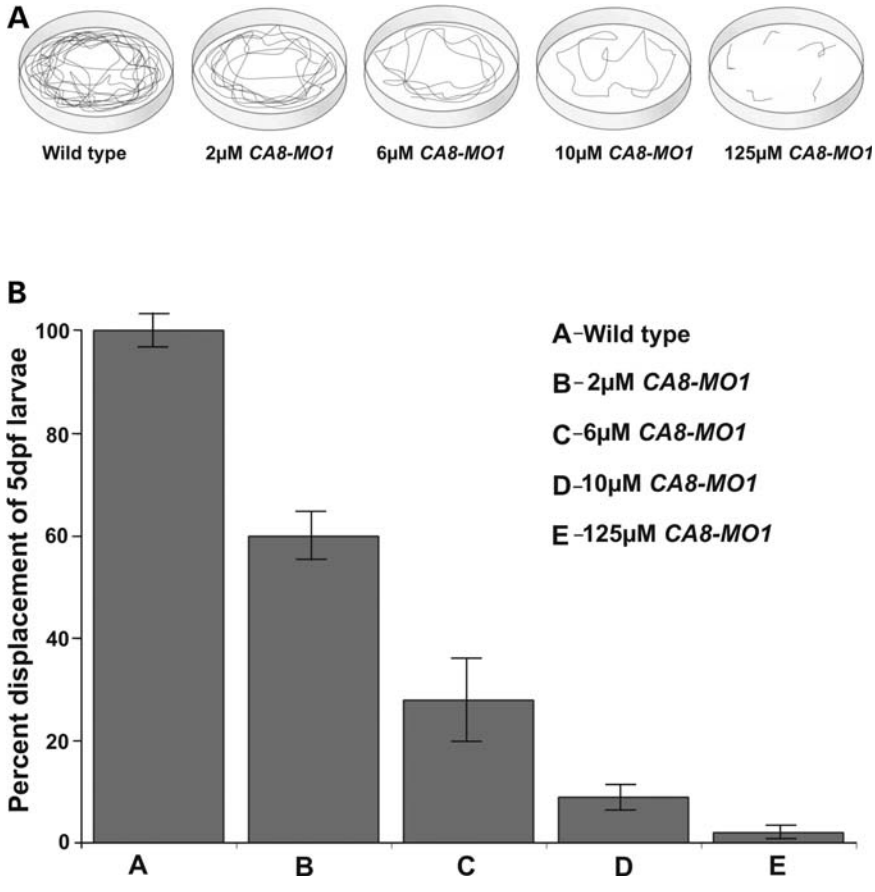


**Figure 7.** Swim patterns of control and *CA8* morphant larvae. The trajectories of the 5 dpf larvae injected with different concentrations of *CA8*-MO1 when compared with uninjected 5 dpf larvae. Zebrafish larvae at 5 dpf show a concentration-dependent increase in abnormal swimming patterns when compared with the uninjected 5 dpf larvae. The swimming trajectories of a minimum of five larvae were observed for 10 min in a 15 × 30 mm sterile petri dish in embryo medium under a Zeiss microscope. The larvae were initially allowed to rest for 2 min after the transfer of larvae to the petri dish and the swim pattern was studied for 10 min. The comparison of swimming trajectories of uninjected larvae with larvae injected with different concentration of *CA8*-MO1 (**A**). The displacement of the larvae was traced for 10 min using Zeiss microscope. The percent displacement of the morphant larvae injected with different concentrations of *CA8*-MOs compared with uninjected larvae (**B**). Half-minute sample movies of swim patterns of uninjected larvae and those injected with three different concentrations of *CA8* antisense MOs (2, 6 and 10 μM) can be seen in additional Supplementary movie files.

indicate that CARP VIII has a very important biologic function (9).

CARP VIII is an enzymatically inactive member of α-CA gene family, similar to CARP X and CARP XI, and its exact physiologic role is only starting to emerge. Previous reports suggest that CARP VIII is abundantly expressed in human and mouse brain, especially in cerebellar Purkinje cells, and it controls intracellular calcium signaling by binding to ITPR1 (14). A report on *wdl* mice, which have a 19 bp deletion in the *Car8* gene, demonstrated clear ataxia and dystonia with a lifelong gait disorder (3). Recent studies have also shown that spontaneously occurring mutations in the *CA8* gene lead to similar defects in coordination and mental retardation in human patients (1,2). Apart from these reports, there are neither studies on the role of CARP VIII, nor do any knockout or knockdown vertebrate models exist for studying its physiologic role in the embryonic development of vertebrates.

The objective of this study was to determine in a zebrafish knockdown model whether the *CA8* gene product is required for normal embryonic development, especially in brain development. We focused on the developmental and behavioral consequences of the knockdown of the *CA8* gene and on brain ultrastructure in the embryonic development of zebrafish.

The RT-qPCR analysis of the relative expression of *CA8* mRNA in 0 hpf–168 hpf showed the expression pattern throughout the developmental period, with peaks at 0, 24 and 120 hpf. The presence of a high level of maternal *CA8* mRNA at 0 hpf shows that it is required early in embryonic development.

In a previous mouse study (16), the expression of *Car8* mRNA was determined by *in situ* hybridization during embryonic development. At 9.5 days of gestation, *Car8* mRNA is expressed in a variety of organs, such as liver, bronchial arches, neuroepithelium and developing myocardium. As development progressed, the expression became restricted to brain, liver, lung, heart, gut, thymus and the epithelium covering the head and the oronasal cavity. Unfortunately, there were no results prior to 9.5 days of gestation. In another mouse study (15), the expression was analyzed in different tissues at four different gestational days by RT-PCR and northern

blot analysis (7–17 days after fertilization). Expression of *Car8* mRNA was found at 11 days of gestation by RT-PCR but only at 15 days of gestation by northern blot analysis. The developmental expression analysis in human brain suggested that the *CA8* gene and CARP VIII protein are expressed at 84 days of gestation in the brain with discrepant findings between the results of northern blot and immunohistochemical analysis (8). *CA8*/*Car8* expression during development would need to be reinvestigated in a mammalian model by a more sensitive method, such as RT-qPCR.

Similar to our previous study on the expression of *Car8* mRNA in a panel of mouse tissues, we analyzed the expression pattern of *CA8* mRNA by RT-qPCR in 12 different zebrafish tissues. The expression analysis showed predominant expression of *CA8* mRNA in the brain (Fig. 3B) similar to the mouse *Car8* and human *CA8* expression patterns. This expression pattern suggests that it is required in the early development and function in the zebrafish brain. High expression levels were also found in zebrafish kidneys, heart, eyes, tail and skin. Low expression levels were observed in male and female gonads, liver, gills and bowel, and a weak signal was found in the muscle in this study. The expression patterns of *CA8* in these other tissues were different from mouse, with a high level of expression in kidneys, eyes and heart and male and female gonads in the zebrafish; we have currently no explanation for this unique pattern of expression in zebrafish. Similar to the predominant expression of the CARP VIII protein in cerebellar Purkinje cells in human and mice by immunohistochemistry (8,9), our immunohistochemistry results showed an intense signal for the CARP VIII protein in Purkinje cells of cerebellum. This localization agrees with the motor coordination defects observed in the phenotypes, both in our study and in previous examples from mice and men (1–3).

The zebrafish CARP VIII protein has an unusually high level of sequence identity with human CARP VIII (10), yet the functional significance of CARP VIII in vertebrate development is not known. We hypothesized that zebrafish CARP VIII might play a critical role during embryogenesis because (i) CARP VIII is highly conserved, (ii) it is expressed within the Purkinje cells of cerebellum similar to humans and mice and (iii) a high amount of its mRNA of maternal origin is present during the earliest stages of embryogenesis. Therefore, we further hypothesized that knockdown of the *CA8* gene using antisense morpholinos might result in an abnormal phenotype in zebrafish larvae.

We knocked the *CA8* gene down by injection of translation-blocking and splice site-blocking antisense MOs at the 1–2 cell stage in zebrafish larvae. The larvae revealed phenotypes from very mild (without apparent morphologic defects with 2 μM *CA8*-MO1) to a severe phenotype (500 μM *CA8*-MO1) with morphologic defects such as a short curved tail, abnormal head shape, small eyes, pericardial edema, abnormal otolith sacs, absence of swim bladder, fragile body and defects in somites. The abnormal head shape was observed as early as 9 hpf during development (data not shown). The specificity of the *CA8*-MOs was indirectly confirmed by repeatedly reproducible phenotypes obtained by injection of translation-blocking and splice site-blocking morpholinos specific for *CA8* gene. The specificity of the knockdown effect by *CA8*-MOs was further confirmed by western blotting with polyclonal antibodies against the CARP VIII protein and analysis of mRNA length from *CA8*-MO2 morphant embryos.

The possible off-target effects due to antisense MOs were excluded by injecting RC morpholinos that produced normal larvae, similar to uninjected ones, which again supported the specificity of *CA8*-MOs. The off-target effects of antisense morpholinos occasionally lead to apoptosis. To suppress the possible off-target effects of *CA8*-MOs, if any, we also injected *p53*-MOs, which excluded the disruption of myotomes and pericardial edema as non-specific effects of morpholino studies (17).

The specificity of the morpholinos was confirmed by western blotting of lysates from 3 dpf larvae injected with 125 μM *CA8*-MO1s and the analysis of mRNA length from MO2 morphant larvae. Although these samples showed no 32 kDa polypeptide band corresponding to CARP VIII, the analysis of lysates after 5 dpf (injected with 125 μM MOs) showed a faint band at 32 kDa, suggesting that the effect of *CA8*-MO1 was diminishing. However, the presence of CARP VIII protein after 5 dpf did not rescue the phenotypic defects that occurred early in the development. In a previous study, knockdown of the huntingtin protein produced defective phenotypes in 3 dpf larvae, but contrary to our results with CARP VIII, the huntingtin phenotypes were reversed after 5 dpf when the MOs could no longer completely suppress the translation (18).

Our study suggests that CARP VIII protein is required for normal development during early embryogenesis and that changes occurring early in development resulting from insufficient CARP VIII protein are not reversible, even if the protein reappears later in the development.

CARP VIII is known to interact with ITPR1 and to modulate the calcium ion release from intracellular reserves. Both CARP VIII and ITPR1 are expressed abundantly in the Purkinje cells of mice cerebellum (14). Because the *ITPR1* gene has been duplicated during the evolution of fish, we performed a coevolution test (analysis of correlated mutations in two genes) to evaluate which of the fish orthologs would more likely have retained the interaction with CARP VIII. We analyzed the correlations in sequence variation between the *CA8* and *ITPR1* gene products in 31 vertebrate species, using either *itpr1a* or *itpr1b* sequences from six fish species in two parallel analyses. The correlations were stronger for *itpr1a*, which indicates that *itpr1a* is more likely to have coevolved with *CA8* in fishes. Coevolution means that changes in one gene product are reflected as changes in the other to retain a functional interaction; therefore, we suggest that *itpr1a* is the main binding partner of CARP VIII in fishes, whereas the *itpr1b* gene product diverges to perform other functions.

We studied the coevolution of residues in CARP VIII in the 3D structure and noticed a cluster of residues (150–157) in the vicinity of the known human disease-causing variation sites. We suggest that the binding site to ITPR1 would be at or near this region. The coevolution analysis also narrows down our estimate of the CARP VIII binding region in ITPR1 to amino acids 1437 to 1630 in human isoform 1, corresponding to 1451 to 1644 in mouse isoform 1.

We measured *itpr1a* mRNA levels during zebrafish embryonic development from 0 hpf to 168 hpf. Our results show that

the temporal expression pattern of *itpr1a* is very similar to that of *CA8*, which further supports their functional association.

The phenotype in the morphant larvae is most likely due to the improper modulation of ITPR1 function for calcium signaling in the brain in the absence of CARP VIII. It has been hypothesized that the binding of CARP VIII to ITPR1 in the regulatory region (Supplementary Material, Figure S2) reduces the sensitivity of IP3 to its receptor ITPR1, and hence, the controlled calcium release from intracellular reserves. In the absence of CARP VIII, the sensitivity of ITPR1 to IP3 increases and excessive calcium is released from intracellular reserves (15,19).

The ataxia and mental retardation observed in human patients with *CA8* variations are also likely due to disruption of the ITPR1 interaction. Interestingly, mutations in ITPR1 lead to ataxia in mice, and mutations in ITPR1 have been identified in spinocerebellar ataxia 15 in humans (20,21). Thus, the involvement of *CA8* should be considered in the diagnosis of unknown forms of ataxia and mental retardation in humans.

Because many CAs facilitate ion transport and bind to ion transporters (22) and CARP VIII is involved in ion channel regulation, we have arrived at a hypothesis for the unknown functions of other highly conserved CARPs. We propose that CARP X and CARP XI would be modulators of ion transport similar to CARP VIII. Our search for CARP X targets is underway.

Studies on the cerebellum in *wdl* mice, with a 19 bp deletion in *Car8* gene, suggest a critical role for CARP VIII in synaptogenesis and/or maintenance of proper synaptic morphology and function in the cerebellum (20). Previous reports on a *CA8* mutation in members of an Iraqi family did not provide any data on possible morphologic changes of the cerebellum (2). However, another report on a human *CA8* mutation revealed a significant loss in the volume of cerebellum proportional to the age of the patients with ataxia and mental retardation (1).

In this zebrafish study, we noted obvious external malformations and a lack of proper head development at the time point of neuronal differentiation (1 dpf). In addition, we detected increased neuronal apoptosis in the cerebellum of the 5 dpf *CA8* knockdown larvae. Histologic examination of semithin sections of the 5 dpf larvae revealed gross morphologic change in the cerebellar region with a reduction in the size of cerebellum in the brain and alterations in somite structures and muscle fibers. Moreover, electron microscopy studies showed increased neuronal cell death in the cerebellum in 5 dpf zebrafish larvae, mimicking the phenotype found in human patients.

We showed that the phenotypic changes became more prominent as the concentration of *CA8* antisense MOs was increased. Our data also indicate that the loss of the *CA8* gene leads to a swim pattern abnormality similar to the ataxia and gait disorder in *wdl* mice and ataxia in human patients with *CA8* mutations (1–3). The severe phenotype observed with the 125 μM concentration of *CA8*-MO1 is because this concentration of MOs targets both zygotic and maternal *CA8* mRNA and completely suppresses *CA8* mRNA in zebrafish larvae. The zebrafish knockdown model with a high concentration of MOs resembles a null mutant phenotype, in contrast to the mutations found in the two reports of human disease-causing *CA8* mutations (1,2) It remains to be seen if more severe mutations in *CA8* in humans lead to viable individuals. By allowing partial knockdown with lower concentrations of MOs, the model presented in this study helps us to understand the phenotypic spectrum we may see in human patients with defects in the *CA8* gene.

In summary, we describe a zebrafish model with an abnormal movement pattern resulting from the knockdown of the *CA8* gene. This is similar to defects in CARP VIII, which lead to ataxia, mental retardation and quadrupedal gait in human patients and ataxia and lifelong gait disorder in *wdl* mice. In addition, we provide evidence that the *CA8* gene product is indispensable in early embryonic development in zebrafish, particularly in the brain and eye. Our study also suggests that this phenomenon is conserved across vertebrate species. This novel zebrafish model is available for further investigations of the mechanisms of CARP VIII-related ataxia and mental retardation in humans.

## MATERIALS AND METHODS

### Bioinformatic analysis of the *CA8* gene and CARP VIII protein

The zebrafish (ID: ENSDARP00000057097), mouse (ID: ENSMUSP00000095891) and human (ENSP00000314407) CARP VIII protein sequences were obtained from the Ensembl database. Multiple sequence alignments and the counting of percent identity of amino acids were conducted for all the three CARP VIII sequences using the ClustalW program *CA8* transcripts for zebrafish (ID: ENSDART00000057098), mouse (ID: ENSMUST00000098290) and human (transcript ID: ENST00000317995) were from Ensembl, and the organization of the exon structure and comparative analysis of all the three transcripts was performed.

### Coevolution analysis

The vertebrate ortholog protein sequences of human CARP VIII and ITPR1 proteins were obtained from Ensembl. The ITPR1 sequences were edited to contain only the region mapped for CARP VIII binding (12), plus four residues on the N-terminal and seven residues on the C-terminal side (corresponding to 1368–1649 in human ITPR1 isoform 1). Likewise, the CARP VIII sequences were shortened to the minimal ITPR1-binding fragment 45–291 (human numbering). Only complete sequences were retained, and the sequence sets were reduced so that we had an identical list of species for both proteins. The CARP VIII alignment consisted of 31 sequences, whereas the ITPR1 alignment included 37 sequences, due to an early duplication in the fish lineages, which has led to two paralogs for ITPR1 genes in fish genomes. A phylogenetic tree was reconstructed using the CARP VIII alignment with the neighbor-joining method, rooting by using the fish sequences as the outgroup.

Two alignments were built from the ITPR1 sequences so that the 25 tetrapod species were present in both, whereas the 12 sequences from 6 fish species were divided. The orthologs of *D. rerio itpr1a* were included in one alignment (‘clade1’) and the orthologs of *itpr1b* in another alignment

('clade2'). The two alignments of ITPR1 from the 31 species were analyzed separately for coevolution with the CARP VIII sequences.

The CAPS program (21) (PMID: 17 005 535) was used with the sequence alignments and the phylogenetic tree to identify the likelihood of coevolution between sites of CARP VIII and ITPR1 proteins.

### Zebrafish husbandry for experiments

Wild-type zebrafish of the AB strain were maintained at 28.5°C under standard conditions (23). Larvae were collected from the breeder tanks with a sieve, rinsed with embryonic medium (Sarsted, Nümbrecht, Germany) and placed into Petri dishes (24). The larvae were kept in Petri dishes in embryonic medium supplemented with 1-phenyl 2-thiourea (Sigma-Aldrich) at 28.5°C until they were used in experiments. The maximum number of larvae on a 9 cm diameter Petri dish was 50. The embryonic medium contained 5 mM NaCl, 0.17 mM KCl, 0.33 mM $CaCl_2$, 0.33 mM $MgSO_4$ and 10–15% Methylene Blue (Sigma-Aldrich). The embryonic medium in Petri dishes was replaced every day with Pasteur pipette and larvae were kept at 28.5°C.

### RNA extraction

Total RNA was isolated from 0 to 168 hpf whole larvae at different stages of development and from different organs of the adult zebrafish. The samples used for mRNA isolation were stabilized in RNA later (Ambion, Austin, TX, USA) immediately following collection, and the total RNA was isolated from 30 mg sample using an RNAeasy® Mini kit (Qiagen, Hilden, Germany) by following the manufacturer's instructions. The concentration and purity of total RNA were determined using a Nanodrop Spectrophotometer at 260 and 280 nm.

### Synthesis of cDNA, PCR amplification, cloning and sequencing

Total RNA was isolated from brain tissue using an RNAeasy® Lipid Tissue extraction kit from Qiagen according to the instructions. RT-PCR was performed using 0.1–5 μg of total RNA to synthesize the first strand of cDNA using a First Strand cDNA Synthesis kit (High-Capacity cDNA Reverse Transcription Kits, Applied Biosystems, Foster City, CA, USA) with random primers and M-MuLV reverse transcriptase according to the protocol recommended by the manufacturer.

PCR amplification was carried out using the forward and reverse primers designed for *CA8* gene in Ensembl (Table 1). The resulting PCR product was ligated into a plasmid vector (pcDNA3.1). The plasmid/*CA8* construct was then transformed into One Shot® TOP10 competent cells (Invitrogen, Espoo, Finland), and the cells were plated on LB/ampicillin plates. The colonies were screened by colony PCR for the presence of the correct insert. DNA sequencing of four different clones was carried out. The sequences were aligned with ClustalW and compared with cDNA obtained from Ensembl (ENSDART00000057097) database (Supplementary Material, Figure S1).

### Real-time quantitative PCR

RT-PCR was performed using 0.1–5 μg of total RNA to synthesize the first strand cDNA using a First Strand cDNA Synthesis kit (High-Capacity cDNA Reverse Transcription Kits, Applied Biosystems, Foster City, CA, USA) with random primers and M-MuLV Reverse transcriptase according to the protocol recommended by the manufacturer. Real-time qPCR primers were designed based on the complete cDNA sequence taken from Ensembl (ENSDART00000057097), using the program Primer Express® Software v2.0 (Applied Biosystems) (Table 1).

Real-time qPCR was performed using a SYBR Green PCR Master Mix Kit in an ABI PRISM 7000 Detection System™, according to the manufacturer's instructions (Applied Biosystems). The PCR conditions consisted of an initial denaturation step at 95°C for 10 min followed by 40 cycles at 95°C for 15 s (denaturation) and 60°C for 1 min (elongation). The data were analyzed using the ABI PRISM 7000 SDS™ software (Applied Biosystems). Each PCR reaction was performed in a total reaction volume of 15 μl containing 2 μl of first strand cDNA (20 ng cDNA), 1 × Power SYBR green PCR Master Mix™ (Applied Biosystems, Foster City, CA, USA) and 0.5 μM of each primer. The final results, expressed as the N-fold relative difference (ratio) in gene expression between the studied samples, internal control gene β-actin and the relative expressions were calculated according to Pfaffl's equation with appropriate modifications (25).

### Immunolocalization of the CARP VIII protein in the adult zebrafish brain

Wild-type adult zebrafish heads were fixed in 4% paraformaldehyde (PFA) in phosphate-buffered saline (PBS) and embedded in paraffin. Fluorescent immunohistochemistry was carried out on rehydrated sections (5 μm) of normal adult zebrafish heads. The specimens were rinsed with PBS and subjected to immunofluorescence staining that consisted of the following steps: (i) pretreatment with 0.1% BSA in PBS (BSA-PBS) for 30 min, (ii) incubation for 1 h with rabbit anti-human CARP VIII antibody (Santa Cruz Biotechnology, Inc., Bergheimer Heidelberg, Germany) (diluted 1:20) or normal rabbit serum (diluted 1:20) in 0.1% BSA-PBS, (iii) rinsing three times for 5 min with BSA-PBS, (iv) incubation for 1 h with 1:100 diluted Alexa Fluor 488 goat anti-rabbit IgG antibodies (Molecular Probes, Eugene, Oregon, USA) in 0.1% BSA-PBS and (v) rinsing twice for 5 min with BSA-PBS and once with PBS. Immunostained sections were then analyzed and photographed using a Zeiss LSM 700 Confocal laser scanning microscope.

### Analysis of genomic DNA from adult zebrafish and expression of *CA8* in 1–5 dpf larvae

Before designing antisense MOs for translation and splice site blocking of *CA8* mRNA, we checked the expression pattern during developmental stages 1–5 dpf in the larvae for the

knockdown study. Total RNA from 1 to 5 dpf larvae was used to synthesize the first-strand cDNA using reverse transcriptase (Superscript II kit; Invitrogen). The resulting cDNA was then amplified using primers for a 100 bp region of *CA8* cDNA (Table 1). To check for possible polymorphisms at the morpholino target sequence in AB strain of zebrafish in our laboratory (Table 1), we amplified PCR products for the target region and sequenced the PCR product from the six different zebrafish individuals.

### Morpholino injections

Two independent (one translation blocking and second splice junction blocking) antisense MOs (GeneTools LLC, Philomath, OR, USA) were designed by GeneTools to target the *CA8* translation initiation site. The random MOs that were used as a control and *p53*-MOs used to suppress the expression of *p53* mRNA were also obtained from Gene Tools (Table 1). The supplied MOs were resuspended in sterile water at a 1 mM stock concentration. Immediately prior to injection, the *CA8*-MOs were diluted to the intended concentration (500, 250, 125, 75, 10, 6 and 2 μM), and 1% phenol red (Sigma, Poole, UK) was added to the solution to monitor injection efficiency. We injected 1 nl of antisense MOs into the yolk of one- to two-cell stage larvae. When *p53*-MOs were included for injections, the concentration of *p53*-MOs was one-and-a-half times the concentration of antisense *CA8*-MOs.

### Western blotting and mRNA analysis of *CA8*-MO-injected zebrafish larvae

For immunoblotting, 3 dpf wild-type and *CA8* antisense-MO-injected larvae were homogenized with a hand-held pestle in a microcentrifuge tube in 50 μl of lysis buffer (50 mM Tris–HCl pH 7.4, 150 mM NaCl, 5 mM EDTA, 1% NP40) on ice. The lysate was centrifuged at 10 000*g* for 5 min, 10 μl of the lysate was used per lane on a 10% SDS polyacrylamide gel and the separated proteins were transferred onto a polyvinylidene difluoride membrane (Immobilon, Millipore). The CARP VIII protein was detected by incubating the membrane with primary rabbit anti-human CARP VIII antibodies (Santa Cruz Biotechnology) raised against amino acids 1 to 100 (human CARP VIII) and horseradish peroxidase-conjugated goat anti-rabbit IgG (H + L) antibody. The signals were visualized using a chemiluminescence system (Western Lightning; Perkin Elmer Life Science). For mRNA analysis of the MO2-injected 5 dpf morphant, larvae were homogenized along with wild type in trizol reagent, and mRNA was isolated according to the instructions in RNAeasy® Mini kit (Qiagen, Hilden, Germany). The cDNA was prepared according to the procedure described previously, and PCR-amplified products were electrophoresed on a 0.8% agarose gel, visualized and photographed.

### Live image analysis of zebrafish phenotypes

Gross morphology was analyzed by light-field microscopy. Typically, 10–20 *CA8*-MOs injected larvae were screened per MO experiment, with a similar number of matched controls tested. Larvae were first anesthetized using 5% Tricaine in embryo medium and embedded in 17% high molecular weight methyl cellulose in 15 × 30 mm transparent polypropylene Petri dish [for taking images of the developing larvae starting from Day 1 to Day 5 using a Lumar V1.12 fluorescence stereomicroscope attached with a camera and with 1.5× lens (Carl Zeiss MicroImaging GmbH, Göttingen, Germany)]. The images were analyzed with AxioVision software versions 4.7 and 4.8.

### Behavioral analysis of 5 dpf *CA8* knockdown zebrafish larvae

Larvae were tested for behavioral consequences due to the *CA8* knockdown by measuring the swimming pattern at 5 dpf. Control (uninjected) and *CA8* knockdown larvae were raised in embryo medium and, after 5 dpf, screened for swimming patterns. Fully developed larvae were arrayed (5 per well) in a 15 × 30 mm one-well Petri dish containing embryo medium and placed on a light stage with a transmitted light source. The larvae were allowed to acclimate to the dish for 2 min, and the movement patterns were observed for 10 min, while simultaneously tracing the movements of the fish. Similarly a 30 s movie was recorded for each group using a Lumar V1.12 fluorescence stereomicroscope (Carl Zeiss MicroImaging GmbH) and AxioVision software versions 4.7 and 4.8. Each experiment was repeated a minimum of three times.

### Histochemical analysis of 5 dpf uninjected and *CA8* knockdown larvae

For histochemical analysis, 5 dpf zebrafish larvae were washed with PBS, fixed with 4% PFA in PBS for 3 h at room temperature, transferred to 70% ethanol and stored at 4°C before being embedded in paraffin. The paraffin-embedded samples were cut into 5 μm slices.

The fixed sections were deparaffinized in xylene, rehydrated in an alcohol series and histologically stained with Mayer's hematoxylin and Eosin Y (both from Sigma-Aldrich). After dehydration, the slides were mounted with Entellan Neu™ (Merck, Darmstadt, Germany), examined and photographed using a Nikon Microphot microscope (Nikon Microphot-FXA, Japan). All of these procedures were carried out at room temperature.

### TUNEL assay on whole mount larvae

The whole mount morphant and control larvae were sectioned, and TUNEL assays were performed using a QIA39 FragEL™ DNA Fragmentation Detection Kit, Fluorescent—TdT Enzyme (Merck Chemicals Ltd., Nottingham, UK). The zebrafish larvae were fixed with 4% PFA in PBS for 3 h and transferred to 70% ethanol before being embedded in paraffin and sectioned. Proteinase K-treated whole larvae or deparaffinized sections (5 μm) of larvae were incubated with the TdT enzyme followed by incubation with anti-digoxigenin. The fluorescein, generated as intense signal, was detected by fluorescence microscopy.

### Electron microscopic analysis

Five-day-old zebrafish larvae were fixed overnight with 2% glutaraldehyde, 2% formaldehyde in 0.1 M sodium cacodylate buffer, pH 7.4 at +4°C and post fixed with 1% reduced, buffered osmium tetroxide for 1 h at room temperature. After dehydration with a graded ethanol series, the specimens were epon-embedded into TAAB embedding resin (TAAB Ltd., UK). Semithin sections were cut and stained with Toluidine Blue for light microscopy analysis (Axiophot, Zeiss Lumar V.12, Thornwood, NY, USA equipped with an Olympus DP70 digital camera). A suitable area was then selected for ultrathin sectioning, and sections were collected on pioloform-coated single-slot copper grids and post stained with uranyl acetate and lead citrate. The resulting sections were analyzed using a transmission electron microscope (Tecnai 12, FEI, Hilsboro, OR, USA) operated at 80 kV, and images were acquired with a MultiScan 794 1K × 1K CCD camera (Gatan, Pleasanton, CA, USA). In all comparisons, at least six larvae for each category were examined.

## SUPPLEMENTARY MATERIAL

Supplementary material is available at *HMG* online.

## ACKNOWLEDGEMENTS

We thank Marianne Kuuslahti and Aulikki Lehmus for their skillful technical assistance with the experiments. We greatly appreciate the help by Leena Mäkinen and Matilda Martikainen in morpholino injections. We are grateful to Annemari Uusimäki for providing cDNA samples from different adult zebrafish tissues.

*Conflict of Interest statement*. None declared.

## FUNDING

This work was supported by the competitive Research Funding of the Tampere University Hospital (Grant 9L071, Grant 9M093, Grant 9L070) and grants from the Academy of Finland (S.P., M.R., M.P.), Sigrid Juselius Foundation (S.P., M.R.) and Tampere Tuberculosis Foundation (M.R. and M.P.). The zebrafish work was carried out at the Tampere Zebrafish Core Facility funded by the Biocenter Finland, Tampere Tuberculosis Foundation and Emil Aaltonen Foundation.

## REFERENCES

1. Kaya, N., Aldhalaan, H., Al-Younes, B., Colak, D., Shuaib, T., Al-Mohaileb, F., Al-Sugair, A., Nester, M., Al-Yamani, S., Al-Bakheet, A. *et al.* (2011) Phenotypical spectrum of cerebellar ataxia associated with a novel mutation in the CA8 gene, encoding carbonic anhydrase (CA) VIII. *Am. J. Med. Genet. B. Neuropsychiatr. Genet.*, **156**, 826–834.
2. Turkmen, S., Guo, G., Garshasbi, M., Hoffmann, K., Alshalah, A.J., Mischung, C., Kuss, A., Humphrey, N., Mundlos, S. and Robinson, P.N. (2009) CA8 mutations cause a novel syndrome characterized by ataxia and mild mental retardation with predisposition to quadrupedal gait. *PLoS Genet.*, **5**, e1000487.
3. Jiao, Y., Yan, J., Zhao, Y., Donahue, L.R., Beamer, W.G., Li, X., Roe, B.A., Ledoux, M.S. and Gu, W. (2005) Carbonic anhydrase-related protein VIII deficiency is associated with a distinctive lifelong gait disorder in waddles mice. *Genetics*, **171**, 1239–1246.
4. Sly, W.S. and Hu, P.Y. (1995) Human carbonic anhydrases and carbonic anhydrase deficiencies. *Annu. Rev. Biochem.*, **64**, 375–401.
5. Pastorekova, S., Parkkila, S., Pastorek, J. and Supuran, C.T. (2004) Carbonic anhydrases: current state of the art, therapeutic applications and future prospects. *J. Enzyme Inhib. Med. Chem.*, **19**, 199–229.
6. Bellingham, J., Gregory-Evans, K. and Gregory-Evans, C.Y. (1998) Sequence and tissue expression of a novel human carbonic anhydrase-related protein, CARP-2, mapping to chromosome 19q13.3. *Biochem. Biophys. Res. Commun.*, **253**, 364–367.
7. Hewett-Emmett, D. and Tashian, R.E. (1996) Functional diversity, conservation, and convergence in the evolution of the α-, β-, and γ-carbonic anhydrase gene families. *Mol. Phylogenet. Evol.*, **5**, 50–77.
8. Taniuchi, K., Nishimori, I., Takeuchi, T., Fujikawa-Adachi, K., Ohtsuki, Y. and Onishi, S. (2002) Developmental expression of carbonic anhydrase-related proteins VIII, X, and XI in the human brain. *Neuroscience*, **112**, 93–99.
9. Aspatwar, A., Tolvanen, M.E. and Parkkila, S. (2010) Phylogeny and expression of carbonic anhydrase-related proteins. *BMC Mol. Biol.*, **11**, 25.
10. Aspatwar, A., Tolvanen, M.E., Ortutay, C. and Parkkila, S. (2010) Carbonic anhydrase related protein VIII and its role in neurodegeneration and cancer. *Curr. Pharm. Des.*, **16**, 3264–3276.
11. Zakon, H.H. (2002) Convergent evolution on the molecular level. *Brain Behav. Evol.*, **59**, 250–261.
12. Carradice, D. and Lieschke, G.J. (2008) Zebrafish in hematology: sushi or science? *Blood*, **111**, 3331–3342.
13. Lohi, O., Parikka, M. and Ramet, M. The zebrafish as a model for paediatric diseases. *Acta Paediatr*. [Epub ahead of print].
14. Hirota, J., Ando, H., Hamada, K. and Mikoshiba, K. (2003) Carbonic anhydrase-related protein is a novel binding protein for inositol 1,4,5-trisphosphate receptor type 1. *Biochem. J.*, **372**, 435–441.
15. Mikoshiba, K. (2007) IP3 receptor/Ca2+ channel: from discovery to new signaling concepts. *J. Neurochem.*, **102**, 1426–1446.
16. Lakkis, M.M., Bergenhem, N.C., O'Shea, K.S. and Tashian, R.E. (1997) Expression of the acatalytic carbonic anhydrase VIII gene, Car8, during mouse embryonic development. *Histochem. J.*, **29**, 135–141.
17. Ekker, S.C. and Larson, J.D. (2001) Morphant technology in model developmental systems. *Genesis*, **30**, 89–93.
18. Diekmann, H., Anichtchik, O., Fleming, A., Futter, M., Goldsmith, P., Roach, A. and Rubinsztein, D.C. (2009) Decreased BDNF levels are a major contributor to the embryonic phenotype of huntingtin knockdown zebrafish. *J. Neurosci.*, **29**, 1343–1349.
19. Yan, J., Jiao, Y., Jiao, F., Stuart, J., Donahue, L.R., Beamer, W.G., Li, X., Roe, B.A., LeDoux, M.S. and Gu, W. (2007) Effects of carbonic anhydrase VIII deficiency on cerebellar gene expression profiles in the wdl mouse. *Neurosci. Lett.*, **413**, 196–201.
20. Hirasawa, M., Xu, X., Trask, R.B., Maddatu, T.P., Johnson, B.A., Naggert, J.K., Nishina, P.M. and Ikeda, A. (2007) Carbonic anhydrase related protein 8 mutation results in aberrant synaptic morphology and excitatory synaptic function in the cerebellum. *Mol. Cell Neurosci.*, **35**, 161–170.
21. Fares, M.A. and McNally, D. (2006) CAPS: coevolution analysis using protein sequences. *Bioinformatics*, **22**, 2821–2822.
22. Sterling, D., Reithmeier, R.A. and Casey, J.R. (2001) A transport metabolon. Functional interaction of carbonic anhydrase II and chloride/bicarbonate exchangers. *J. Biol. Chem.*, **276**, 47886–47894.
23. Westerfield, M. (2000) The Zebrafish Book: A Guide for the Laboratory Use of Zebrafish *(*Danio Rerio*)*. University of Oregon, Eugene.
24. Kimmel, C.B., Ballard, B.W., Kimmel, S.R., Ullmann, B. and Schilling, T.F. (1995) Stages of embryonic development of the zebrafish. *Dev. Dyn.*, **203**, 253–310.
25. Pfaffl, M.W. (2001) A new mathematical model for relative quantification in real-time RT-PCR. *Nucleic Acids Res.*, **29**, e45.
26. Picaud, S.S., Muniz, J.R., Kramm, A., Pilka, E.S., Kochan, G., Oppermann, U. and Yue, W.W. (2009) Crystal structure of human carbonic anhydrase-related protein VIII reveals the basis for catalytic silencing. *Proteins*, **76**, 507–511.
27. Berman, H.M., Westbrook, J., Feng, Z., Gilliland, G., Bhat, T.N., Weissig, H., Shindyalov, I.N. and Bourne, P.E. (2000) The Protein Data Bank. *Nucleic Acids Res.*, **28**, 235–242.